Dislocations dans les minéraux: une affaire de cœur

Patrick Cordier

Université de Lille

Institut Universitaire de France

2-3 Sept 2021 Journée Thématique *Défauts dans les cristaux: Origines, caractérisation et conséquences*

Volterra's distorsions

Vito Volterra (1860-1940)
Italian mathematician and physicist

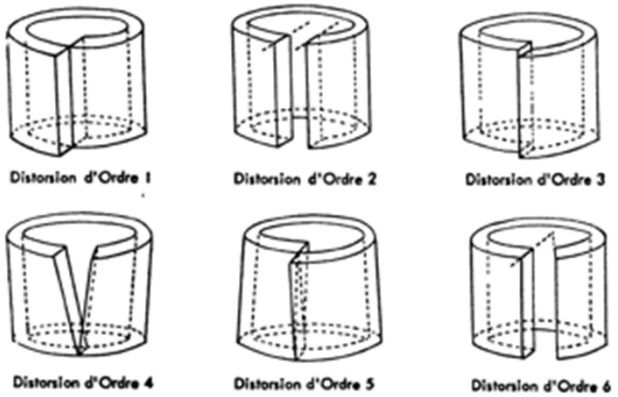

Vito Volterra, Sur l'équilibre des corps élastiques multiplement connexes, 1907

The concept of dislocations

Egon Orowan

Sir Geoffrey Ingram Taylor

Michael Polanyi

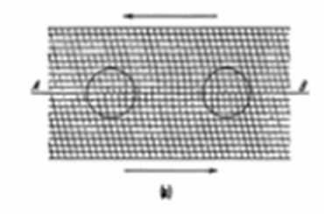

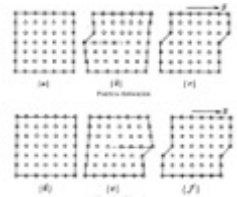

Fig. 1. Schema einer Gitterversetzung.

1934

Shearing crystals

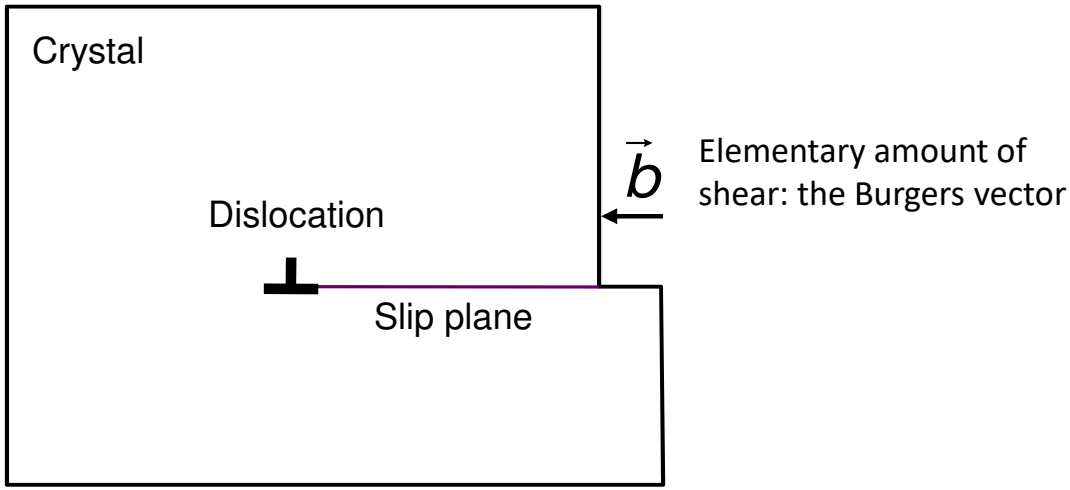

Dislocations: important parameters

- Elementary amount of shear: the Burgers vector
- Dislocation line orientation (local)
- Slip plane: contains *L* and *b*

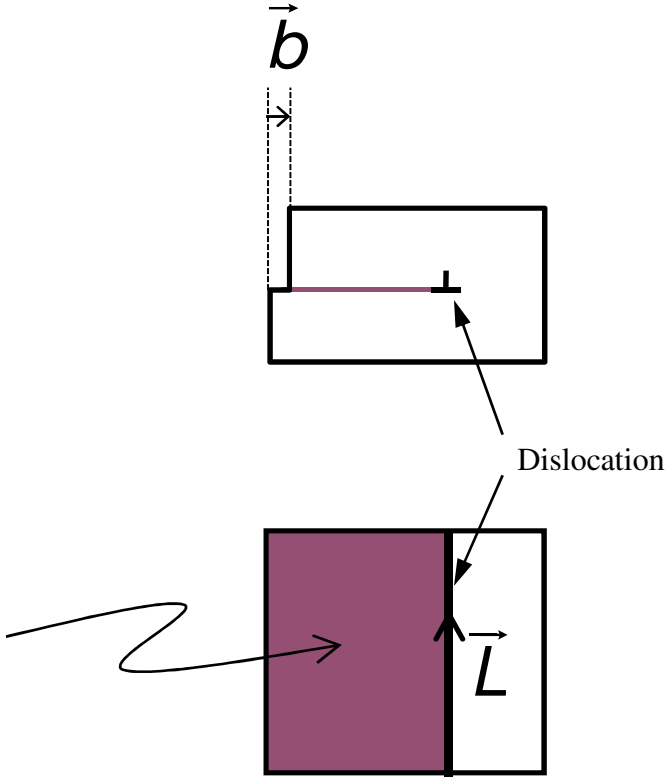

Dislocations: the far field

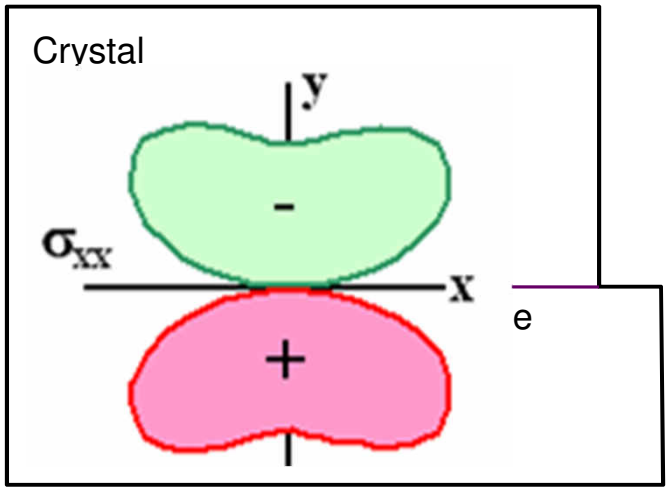

Volterra dislocation

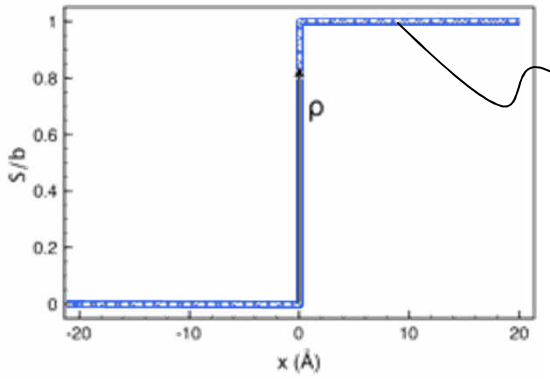

Shear profile

Dislocations: the far field

Elasticity theory

- *Screw dislocation*

$$\vec{R} = \frac{\vec{b}}{2\pi}\theta$$

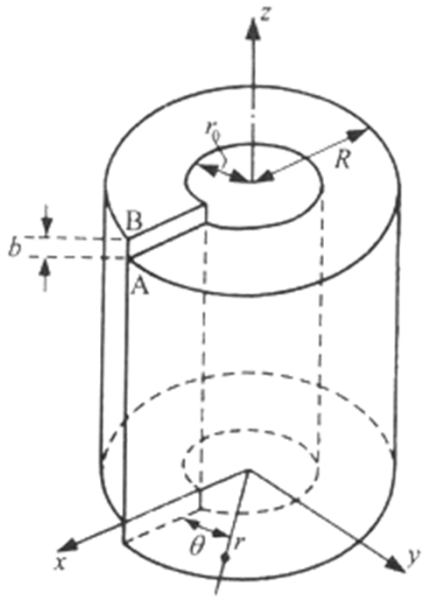

Strain:
$$\overline{\overline{\varepsilon}} = \frac{b}{4\pi r}\begin{pmatrix} 0 & 0 & 0 \\ 0 & 0 & 1 \\ 0 & 1 & 0 \end{pmatrix}$$

Stress:
$$\overline{\overline{\sigma}} = \frac{\mu b}{2\pi r}\begin{pmatrix} 0 & 0 & 0 \\ 0 & 0 & 1 \\ 0 & 1 & 0 \end{pmatrix}$$

Dislocations: the far field

- Elasticity theory
  - *Edge dislocation*

$$R_r = \frac{b}{2\pi}\left[-\frac{(1-2\nu)}{(2(1-\nu)}\sin\theta\ln r + \frac{\sin\theta}{4(1-\nu)} + \theta\cos\theta\right]$$

$$R_\theta = \frac{b}{2\pi}\left[-\frac{(1-2\nu)}{(2(1-\nu)}\cos\theta\ln r + \frac{\cos\theta}{4(1-\nu)} - \theta\sin\theta\right]$$

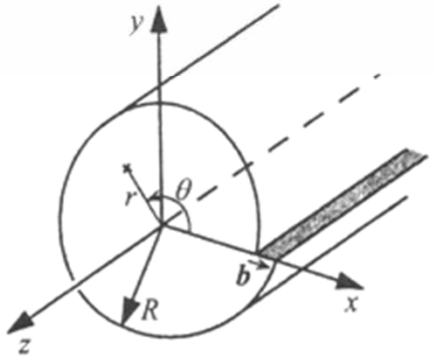

Dislocations: the far field

- Elasticity theory
  - *Edge dislocation*

$$\overline{\overline{\sigma}} = \frac{\mu b}{2\pi(1-\nu)} \begin{pmatrix} -\dfrac{y(3x^2+y^2)}{(x^2+y^2)^2} & \dfrac{x(x^2-y^2)}{(x^2+y^2)^2} & 0 \\ \dfrac{x(x^2-y^2)}{(x^2+y^2)^2} & \dfrac{y(x^2-y^2)}{(x^2+y^2)^2} & 0 \\ 0 & 0 & \dfrac{-2\nu y}{x^2+y^2} \end{pmatrix}$$

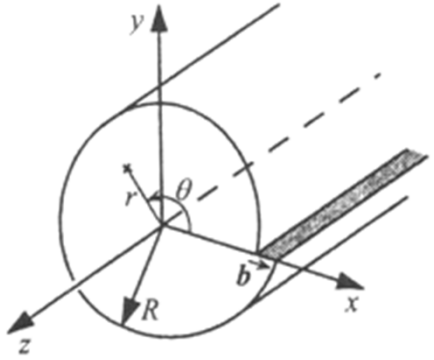

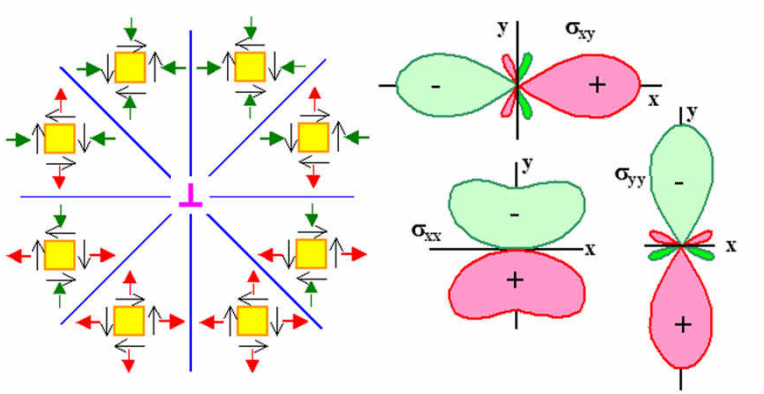

Volterra dislocations: the far field

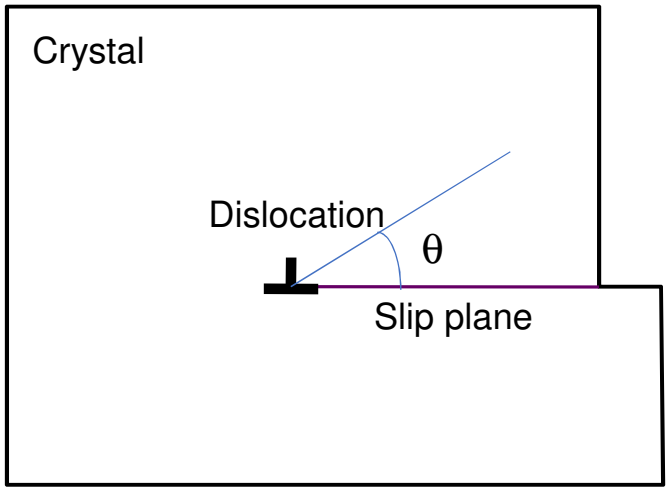

$$\sigma \propto \frac{\mu b}{2\pi} \frac{f(\theta)}{r}$$

Volterra dislocation

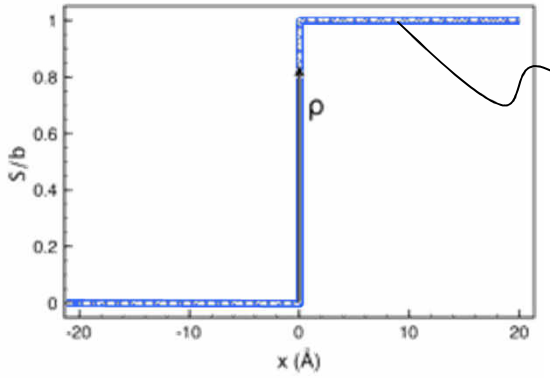

Shear profile

Dislocations: the displacement field

- *Mixed dislocation (general case)*

$$\vec{R} = \frac{1}{2\pi}\left[\vec{b}\theta + \vec{b}_e \frac{\sin 2\theta}{4(1-\nu)} + \left(\vec{b}\times\vec{L}\right).\left(\frac{(1-2\nu)}{2(1-\nu)}\ln r + \frac{\cos 2\theta}{4(1-\nu)}\right)\right]$$

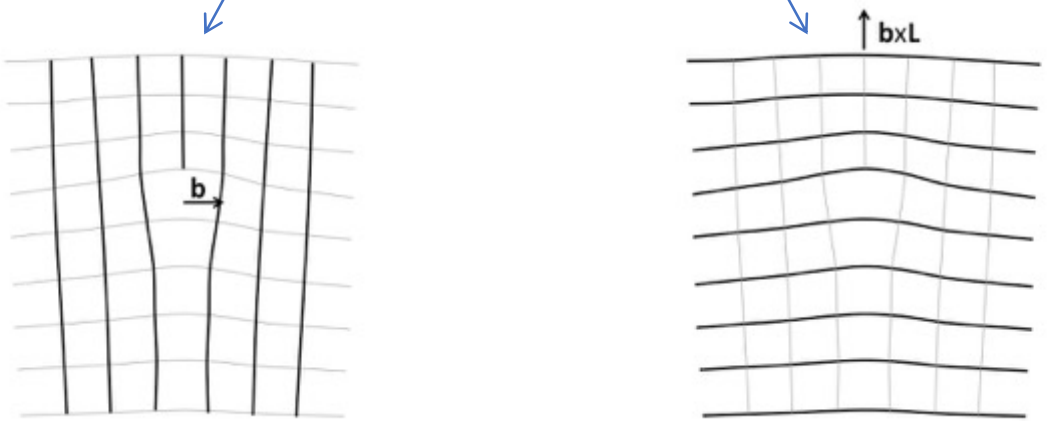

Dislocations: observations

- Transmission electron microscopy

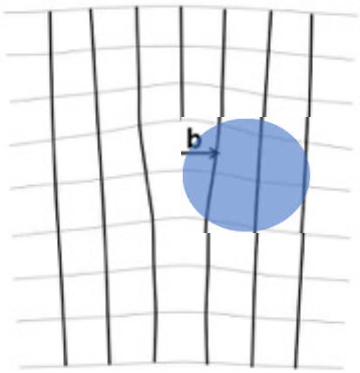

Dark Field

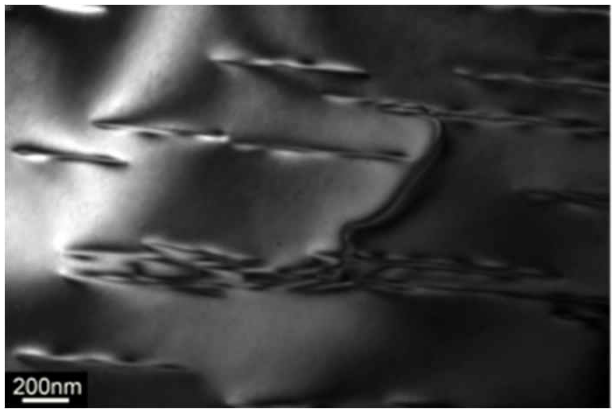

Dislocations: observations

- Transmission electron microscopy

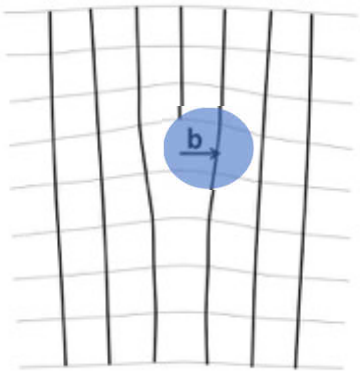

Weak-Beam Dark Field

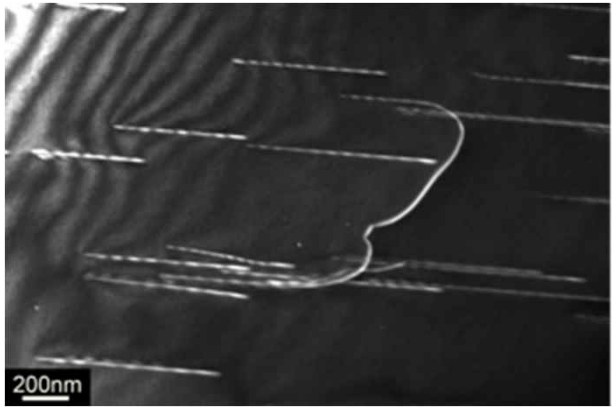

Dislocations: observations

- Transmission electron microscopy

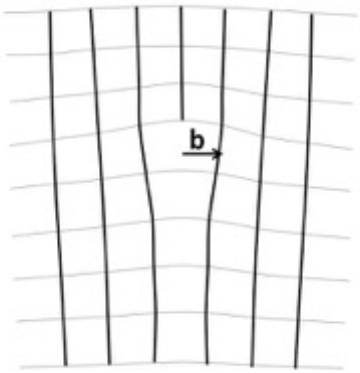

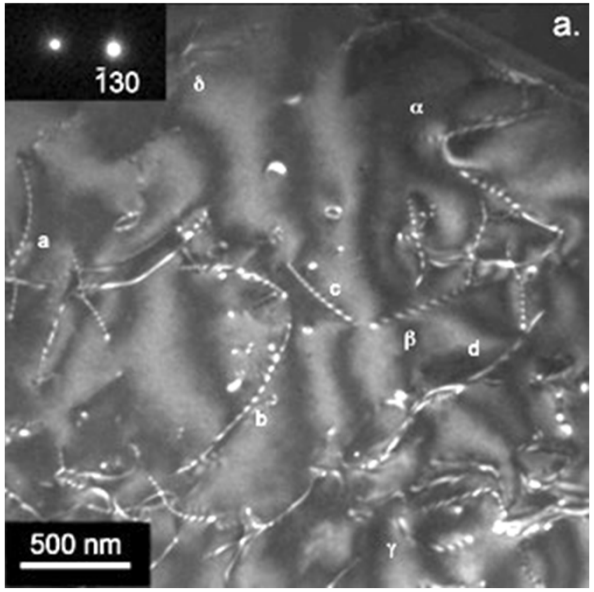

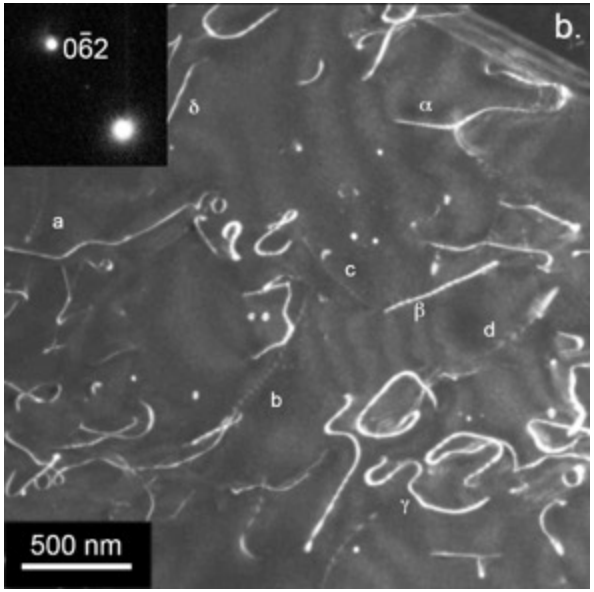

Olivine deformed at 900°C – Sample courtesy S. Demouchy

Dislocations: observations

- Electron Chanelling Contrast Imaging (ECCI) in the SEM

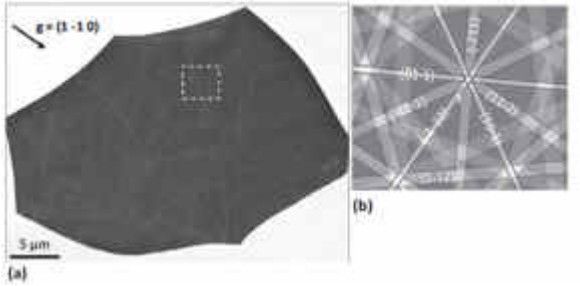

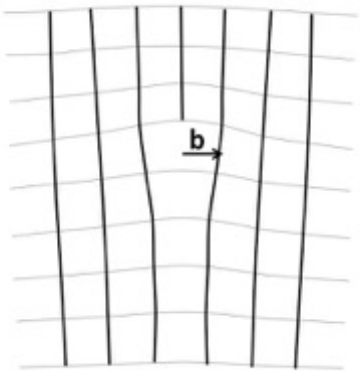

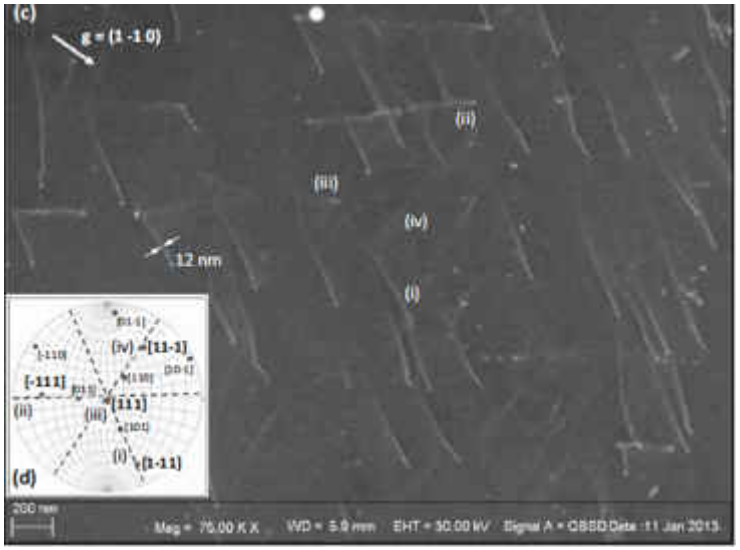

S. Zaefferer, N.-N. Elhami / Acta Materialia 75 (2014) 20–50

Dislocations: observations

- X-ray diffraction peak broadening analysis (strain anisotropy)

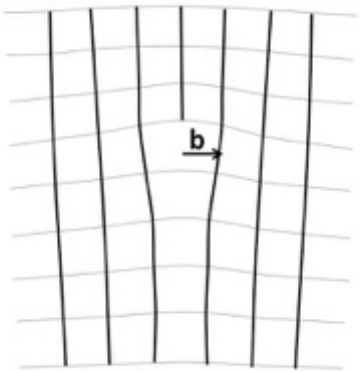

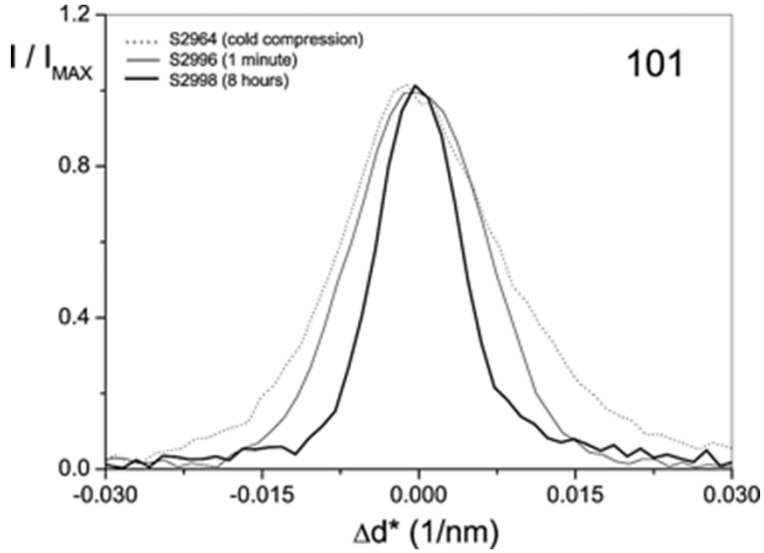

Shear deformation of forsterite – Couvy et al. (2004) Eur. J. Mineral.

Dislocations: observations

- X-ray diffraction peak broadening analysis (strain anisotropy)

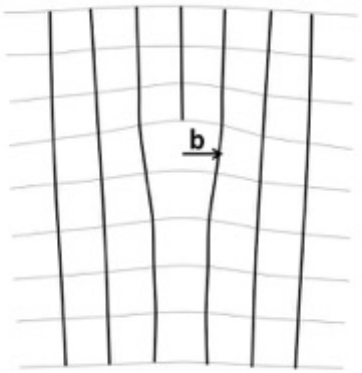

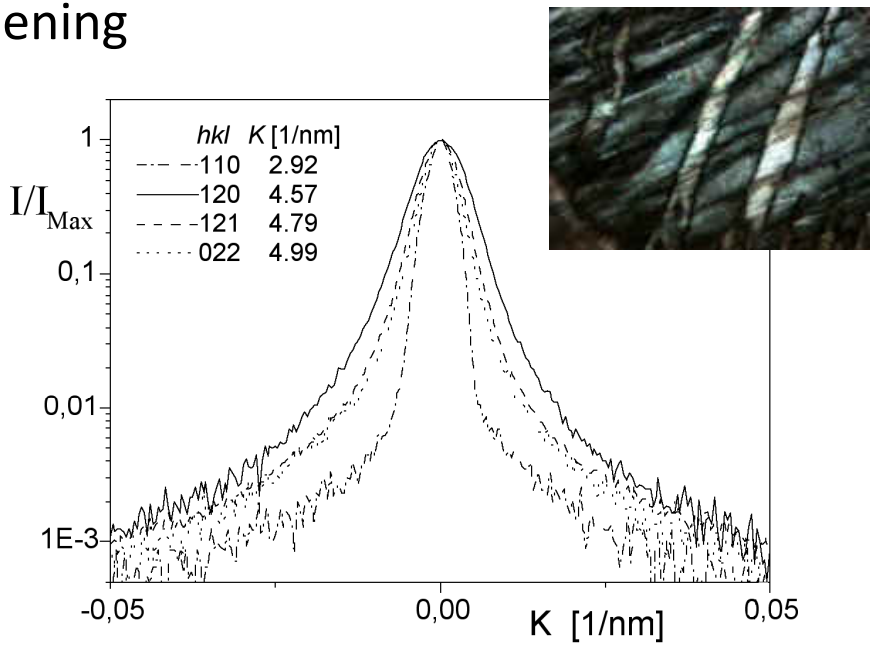

Cordier, Ungár, Zsoldos & Tichy (2004) Nature 428, 837-840

Volterra dislocations: the core

$$E_{el} = \frac{\mu b^2}{4\pi K} \ln\left(\frac{R}{r_0}\right)$$

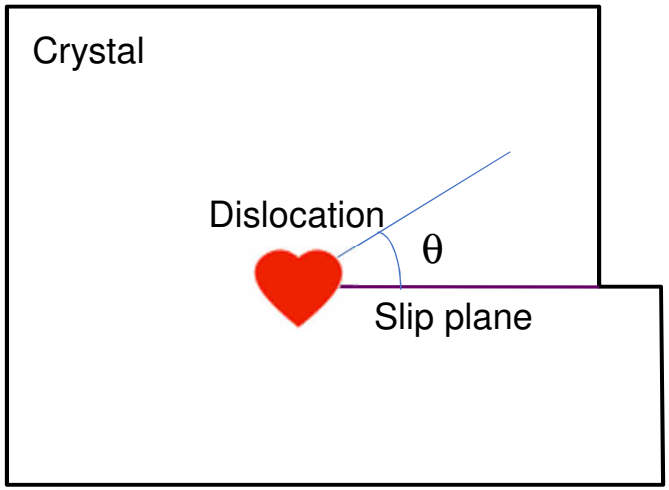

$$\sigma \propto \frac{\mu b}{2\pi} \frac{f(\theta)}{r}$$

Volterra dislocation

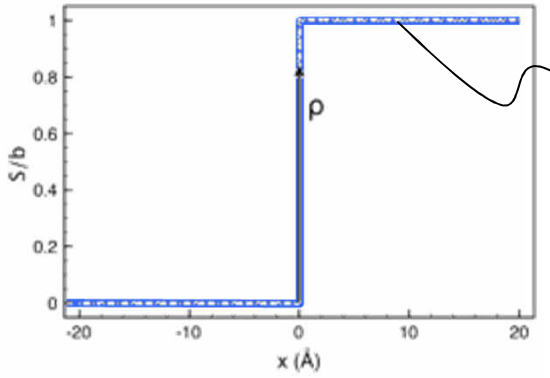

Shear profile

The Original Manuscript of the Peierls Dislocation Model*

(kindly made available by E. Orowan)

1940

THE SIZE OF A DISLOCATION

By R. PEIERLS, The University, Birmingham

ABSTRACT. Calculations are made of the size of a dislocation and of the critical shear stress for its motion.

It is generally supposed that the plastic deformation of crystals proceeds by means of the propagation of dislocations along the slip planes. Since a dislocation consists of a displacement of a great many atoms, it is obviously impossible to obtain a rigorous solution of the equilibrium conditions for all these atoms. Dr Orowan has shown me how to obtain an idealized model, which leads to equations that can be solved, of the forces in a dislocation, and in this note I shall report on the results.

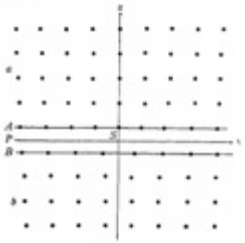

Figure 1.

The type of dislocation which I have investigated is sketched in figure 1. The slip plane $P(x=0)$ divides the crystal into an upper part a and a lower part b. These are symmetrical about the vertical plane $S(x=0)$. The central plane S lies in a net plane in the upper half-crystal a, and half way between two net planes in b.

The y axis at right angles to the plane of the figure (i.e. the line in which the plane S meets the slip plane P) is called the *dislocation line*. In the neighbourhood of this line the atoms of a are moved inwards and those of b are moved apart, so that at great distances from the dislocation line the two planes A and B which are immediately above and below the slip plane are again in correct alignment, A containing, however, one row of atoms more than B.

The atoms in the plane A are then subject to two forces: (i) The interaction

Modeling dislocations using the Peierls-Nabarro model

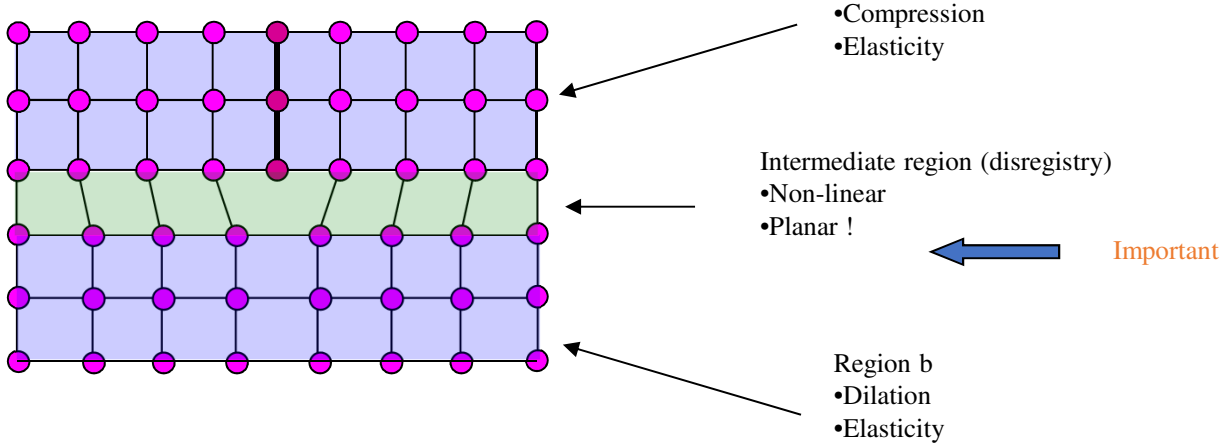

Modeling dislocations using the Peierls-Nabarro model

$$\frac{K}{2\pi}\int_{-\infty}^{+\infty}\frac{1}{x-x'}\left[\frac{dS(x')}{dx'}\right]dx' = \frac{K}{2\pi}\int_{-\infty}^{+\infty}\frac{\rho(x')}{x-x'}dx' = F(S(x))$$

Sinusoidal
(assumed !)

$$F(S(x)) = \tau^{max}\sin\left(\frac{2\pi S(x)}{b}\right)$$

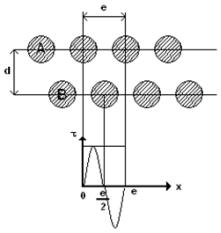

$$\sigma_p = \frac{Kb}{a'}\exp\left(-\frac{2\pi\zeta}{a'}\right)$$

Modeling dislocations using the Peierls-Nabarro model

$$\frac{K}{2\pi}\int_{-\infty}^{+\infty}\frac{1}{x-x'}\left[\frac{dS(x')}{dx'}\right]dx' = \frac{K}{2\pi}\int_{-\infty}^{+\infty}\frac{\rho(x')}{x-x'}dx' = F(S(x))$$

$$F(S) = -\frac{\partial\gamma}{\partial S}$$

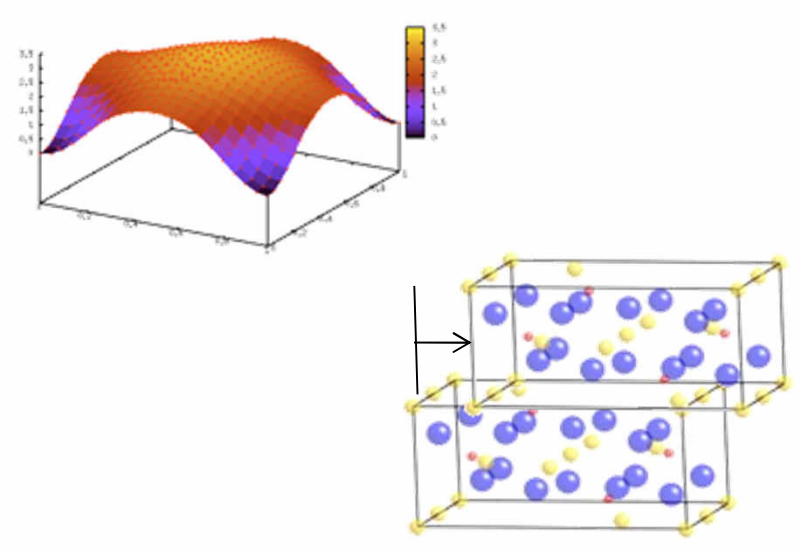

Generalised Stacking Faults (GSF)

Can be calculated *ab initio*

Modeling dislocations using the Peierls-Nabarro model

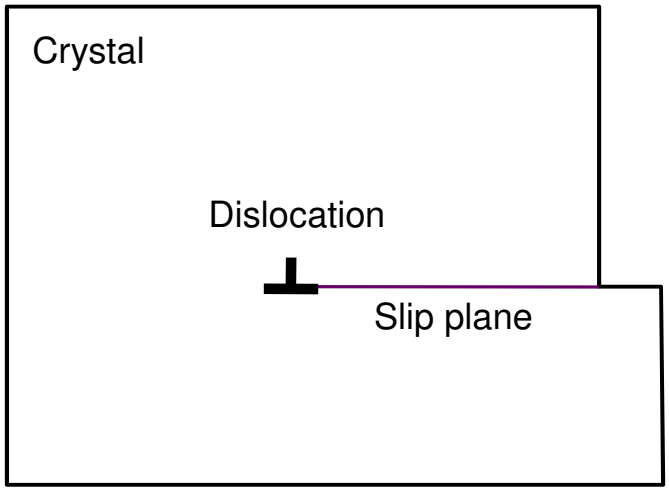

Peierls dislocation

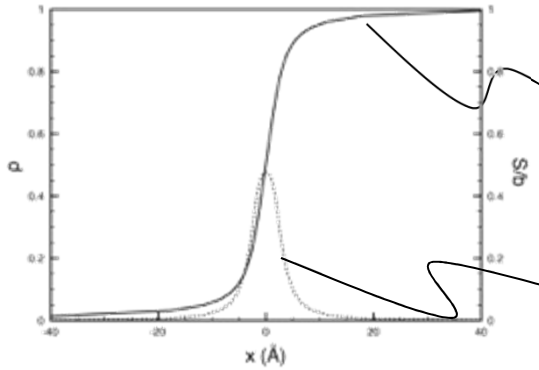

Shear profile

Dislocation core profile

Testing the Peierls-Nabarro model: $SrTiO_3$

$\langle 100 \rangle \{ 010 \}$ a = 3.905 Å

a = 5.52 Å $\langle 110 \rangle \{ 1\bar{1}0 \}$

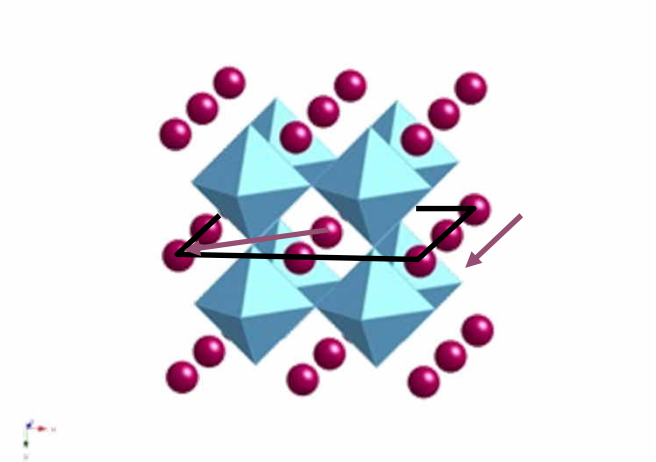

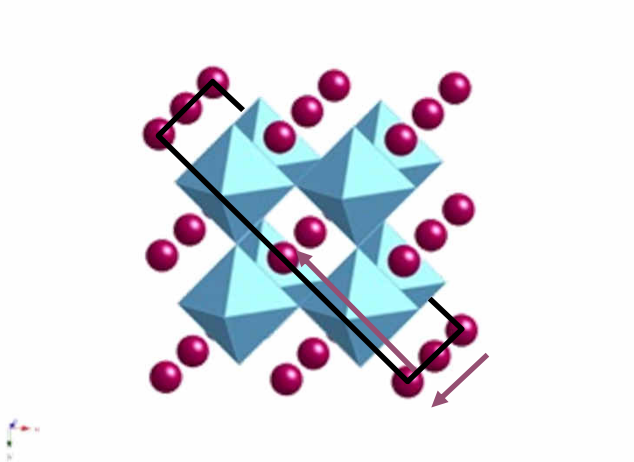

$SrTiO_3$: generalyzed stacking faults

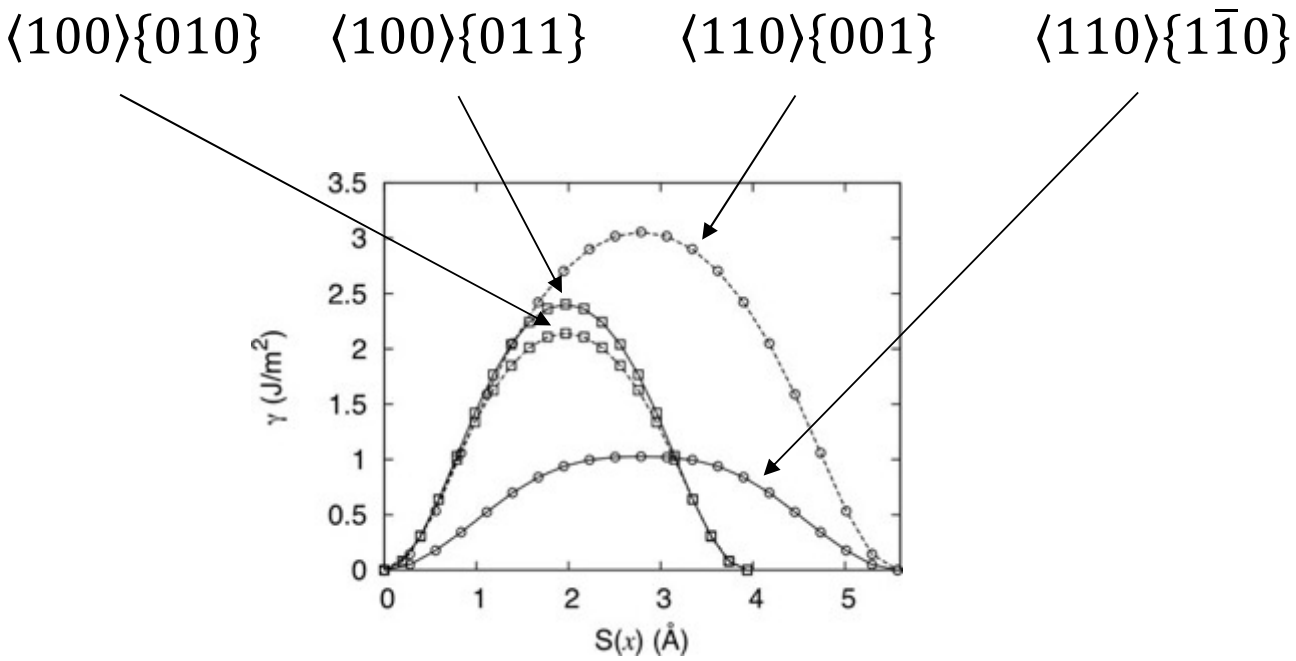

$SrTiO_3$: generalyzed stacking faults

$\langle 100 \rangle \{ 010 \}$ $\langle 100 \rangle \{ 011 \}$ $\langle 110 \rangle \{ 001 \}$ $\langle 110 \rangle \{ 1\bar{1}0 \}$

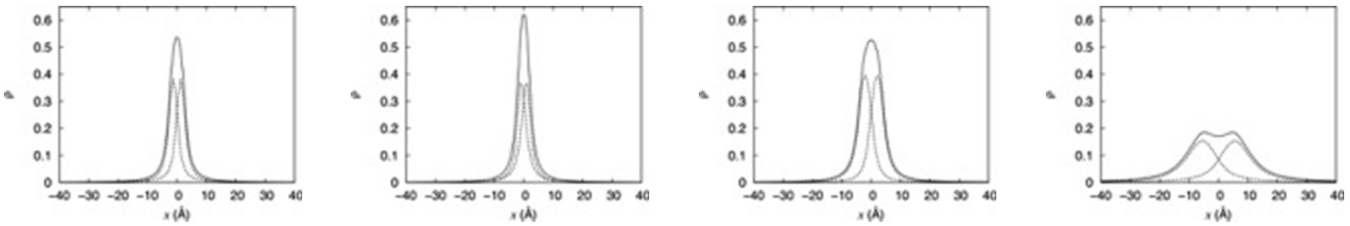

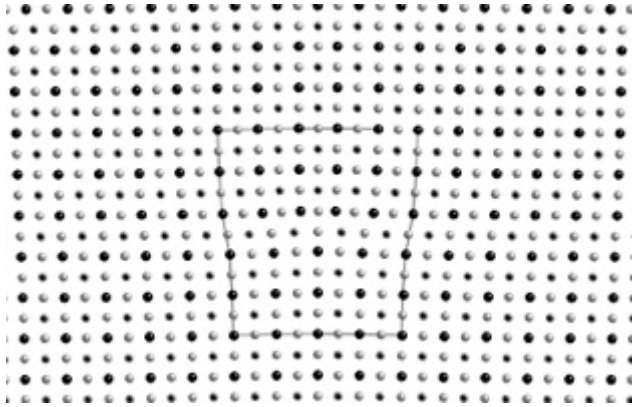

⟨100⟩{010}

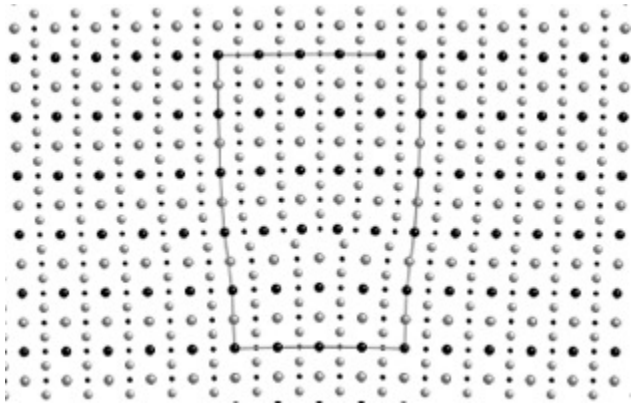

⟨100⟩{011}

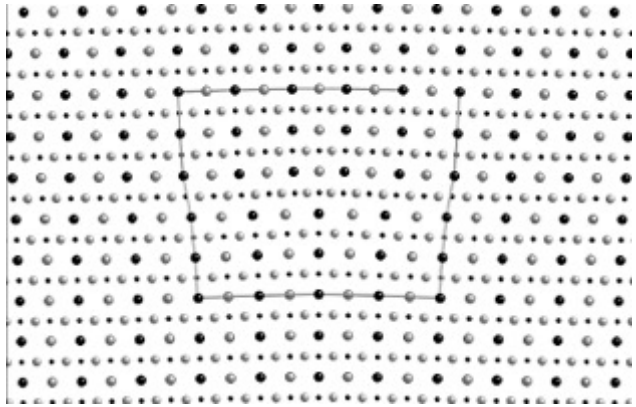

⟨110⟩{001}

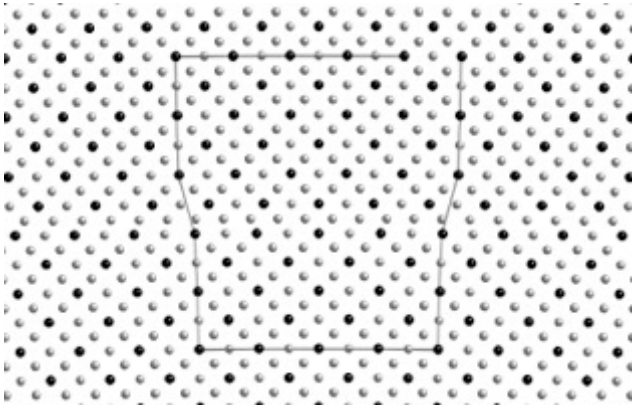

⟨110⟩{1$\bar{1}$0}

Testing the Peierls-Nabarro model: $SrTiO_3$

Comparison with HRTEM images

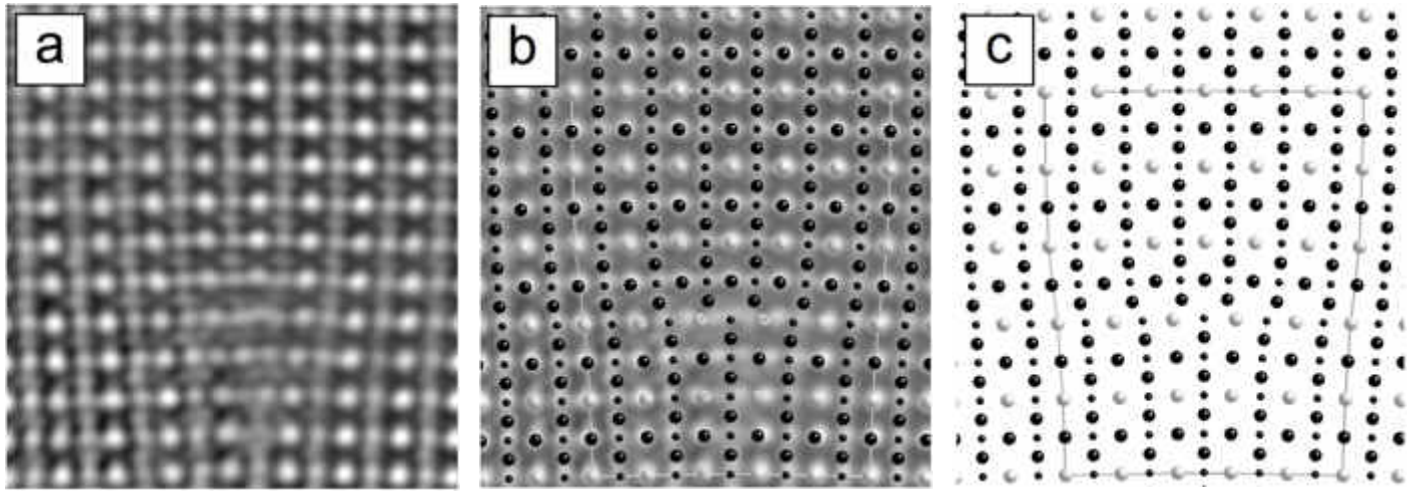

Atomic scale model
Peierls-Nabarro
Courtesy Ferré et al. (2008)

The Peierls-Nabarro model: lattice friction

Analytical model: Joos & Duesberry (1997)

Dimensionless parameter: $\Gamma = \zeta / a'$

Two cases:

- Narrow cores $\Gamma << 1$ $$\sigma_p(\Gamma \ll 1) = \frac{3\sqrt{3}}{8} \tau^{max} \frac{a'}{\pi \zeta}$$

- Wide cores $\Gamma >> 1$ $$\sigma_p(\Gamma \gg 1) = \frac{Kb}{a'} \exp\left(\frac{-2\pi\zeta}{a'}\right).$$

$SrTiO_3$: lattice friction

$\langle 100 \rangle \{ 010 \}$	$\langle 100 \rangle \{ 011 \}$	$\langle 110 \rangle \{ 001 \}$	$\langle 110 \rangle \{ 1\bar{1}0 \}$
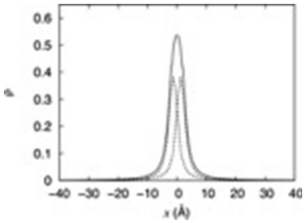	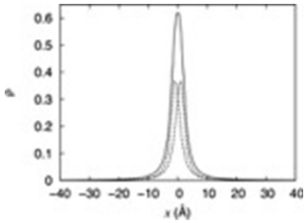	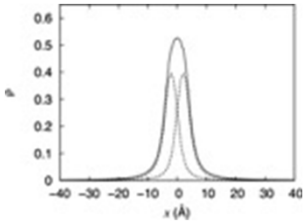	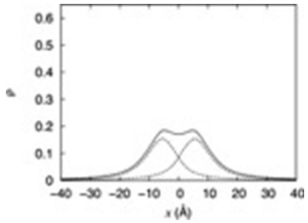
Edge (GPa)			
0.6	0.6	1.2	0.004
Screw (GPa)			
0.7	9.9	0.9	0.006

When the core structure determines the glide plane

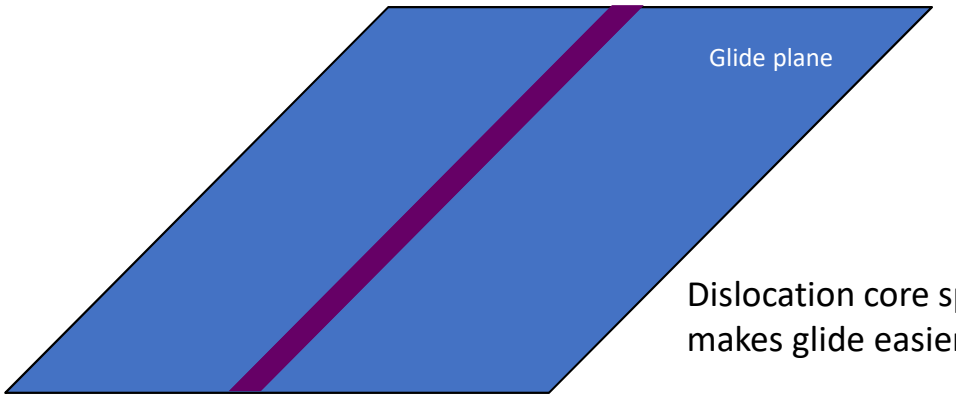

When the core structure determines the glide plane

But glide will be more difficult in another plane !

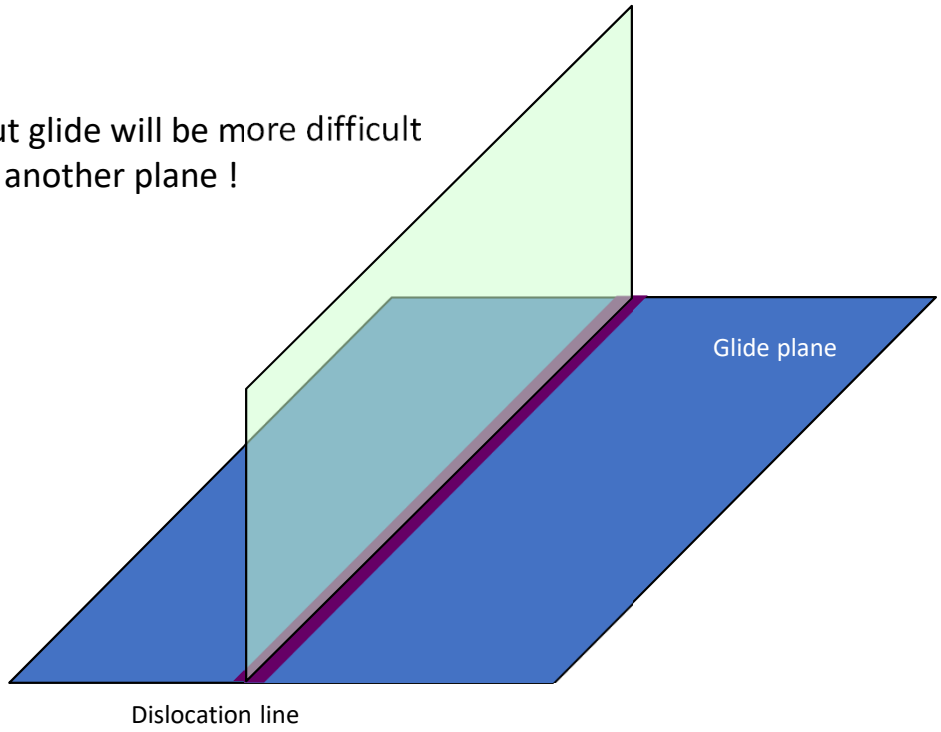

“Predicting” slip systems in MgO

B1 cubic crystal structure (space group $Fm\bar{3}m$)

Rock-salt (NaCl) structure.

Lattice parameter is about 4.21 Å

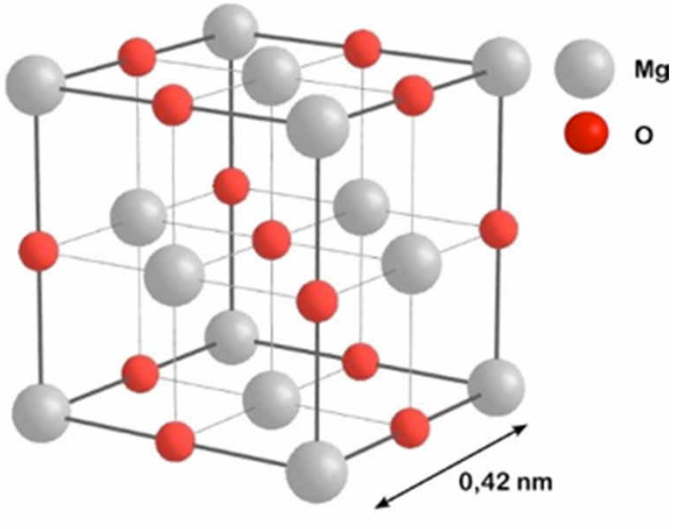

“Predicting” slip systems in MgO

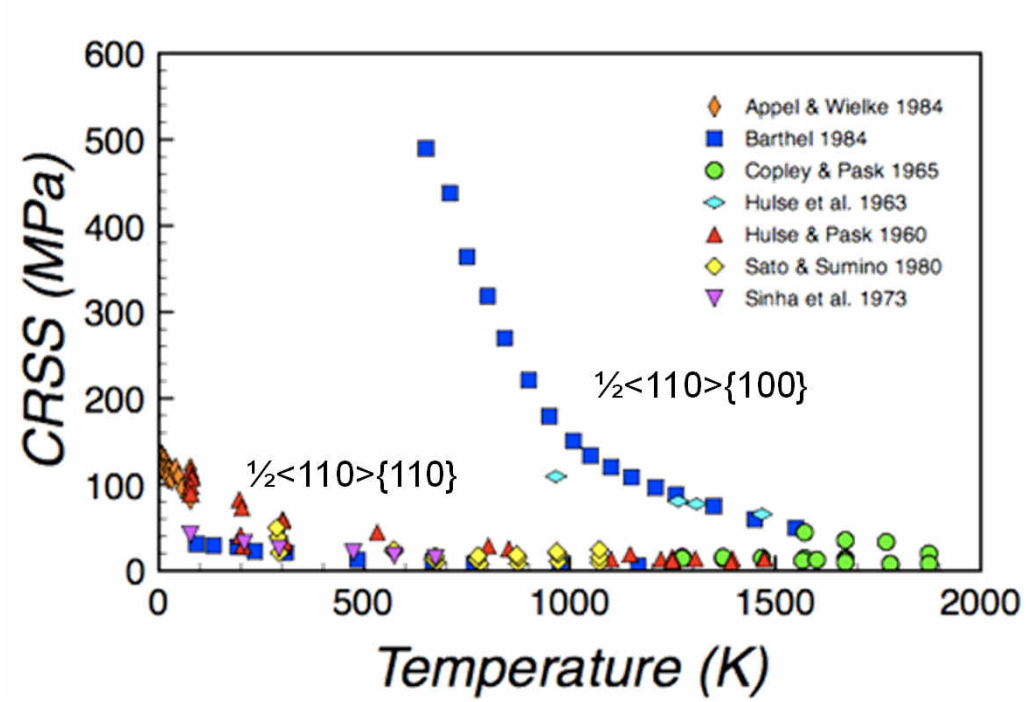

“Predicting” slip systems in MgO with the Peierls-Nabarro model

$$\frac{K}{2\pi}\int_{-\infty}^{+\infty}\frac{1}{x-x'}\left[\frac{dS(x')}{dx'}\right]dx' = \frac{K}{2\pi}\int_{-\infty}^{+\infty}\frac{\rho(x')}{x-x'}dx' = F\left(S(x)\right)$$

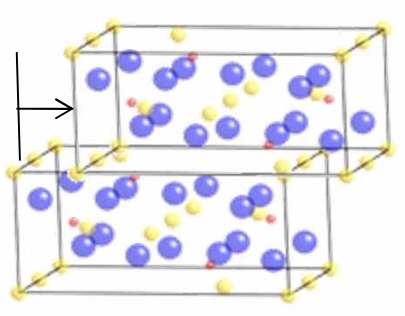

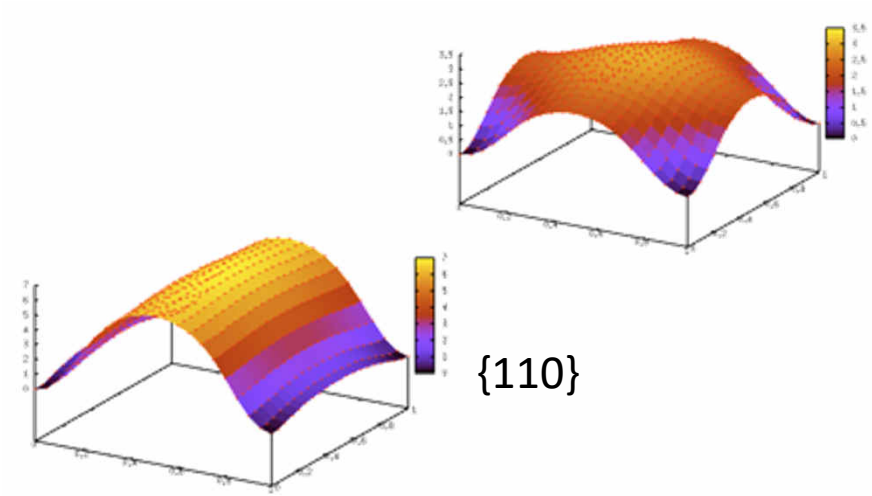

{100}

{110}

“Predicting” slip systems in MgO with the Peierls-Nabarro Galerkin model

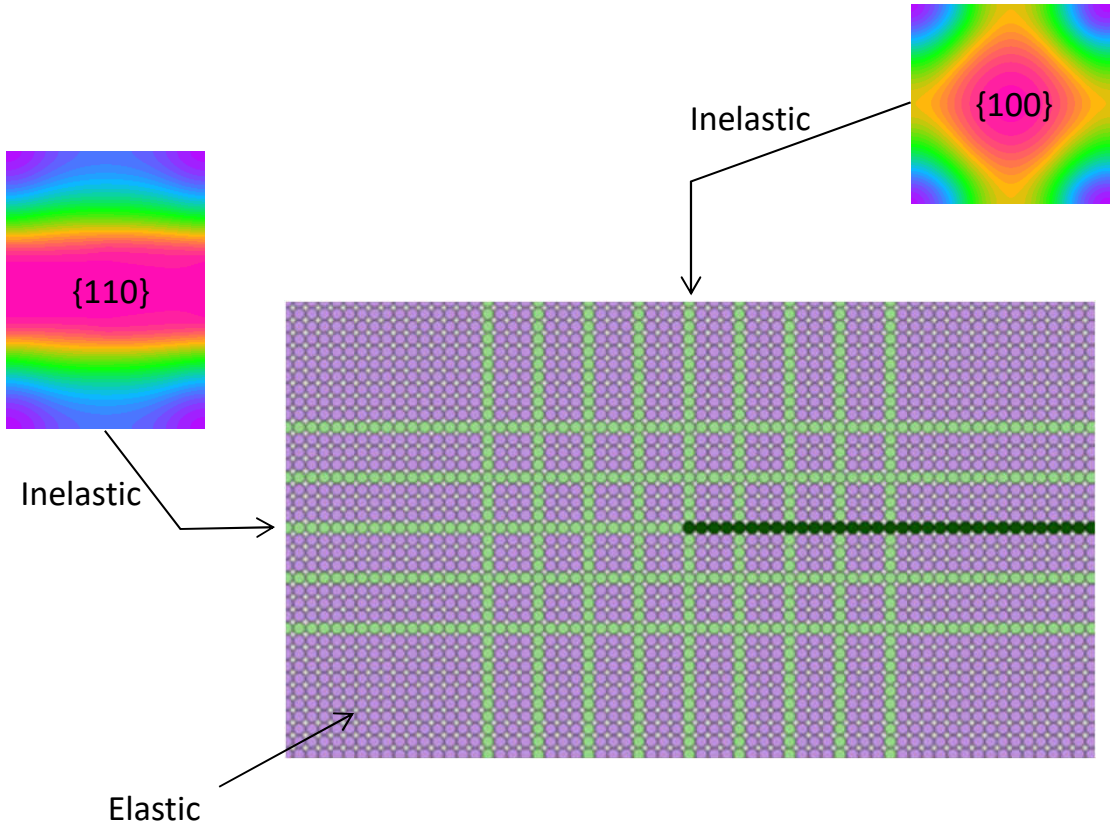

C. Denoual (CEA-DAM)

“Predicting” slip systems in MgO with the Peierls-Nabarro Galerkin model

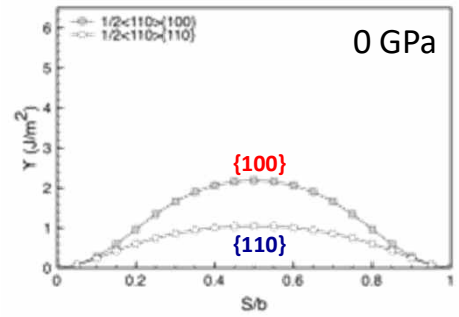

0 GPa

Glide in {110}

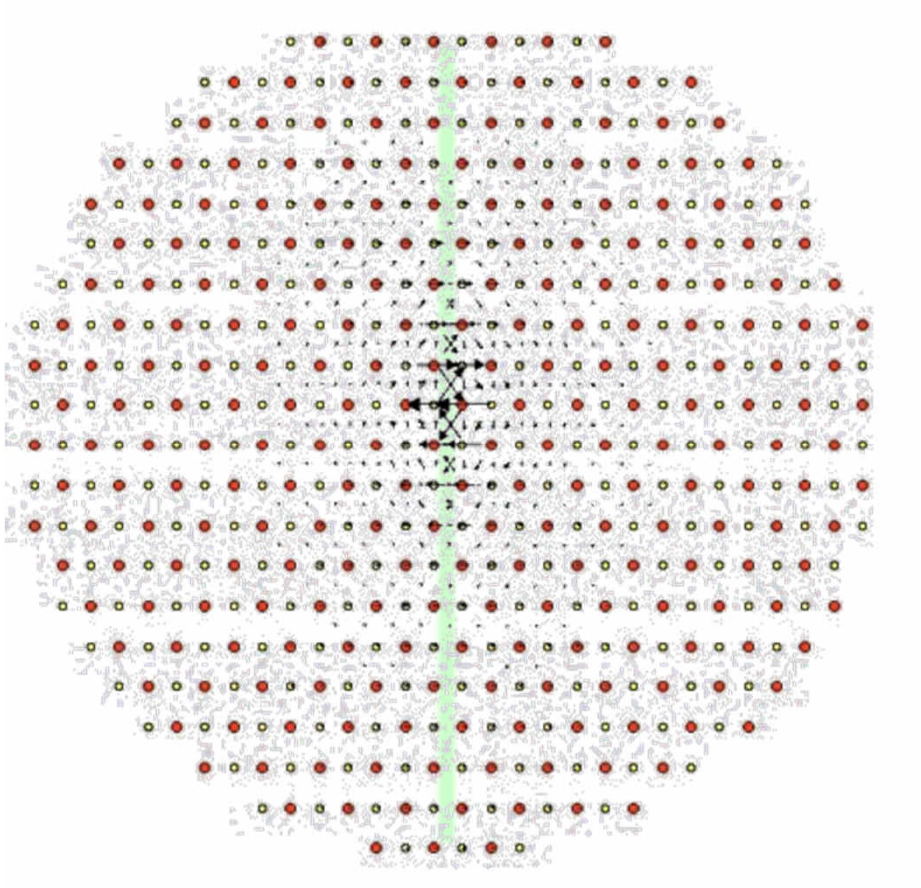

{110}

“Predicting” slip systems in MgO with the Peierls-Nabarro Galerkin model

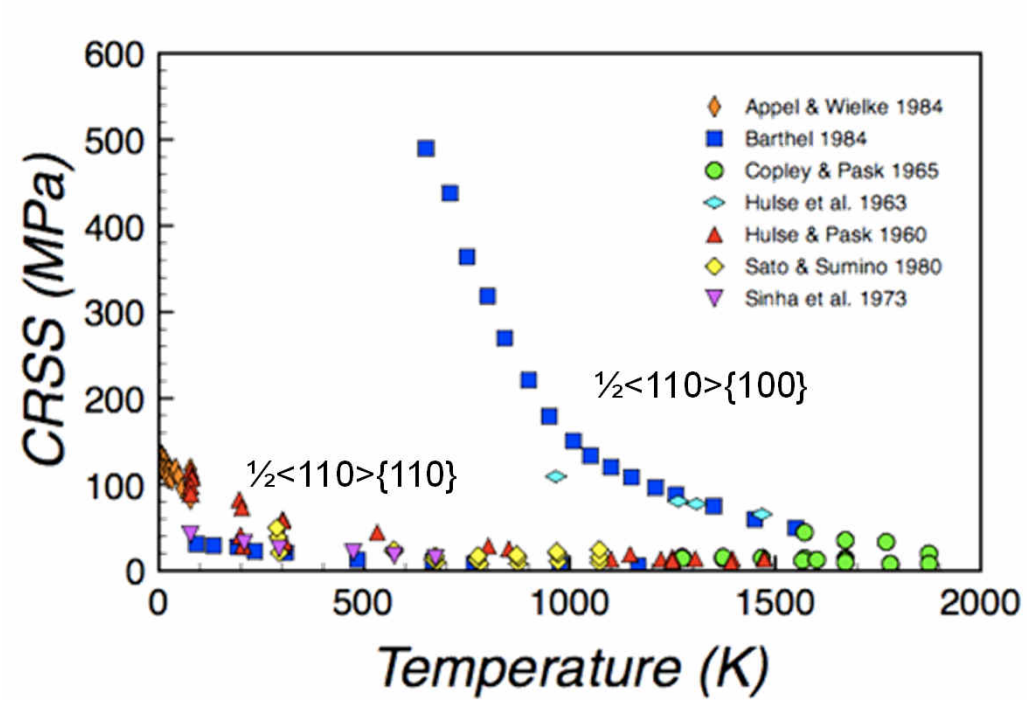

(Mg,Fe)O in the mantle

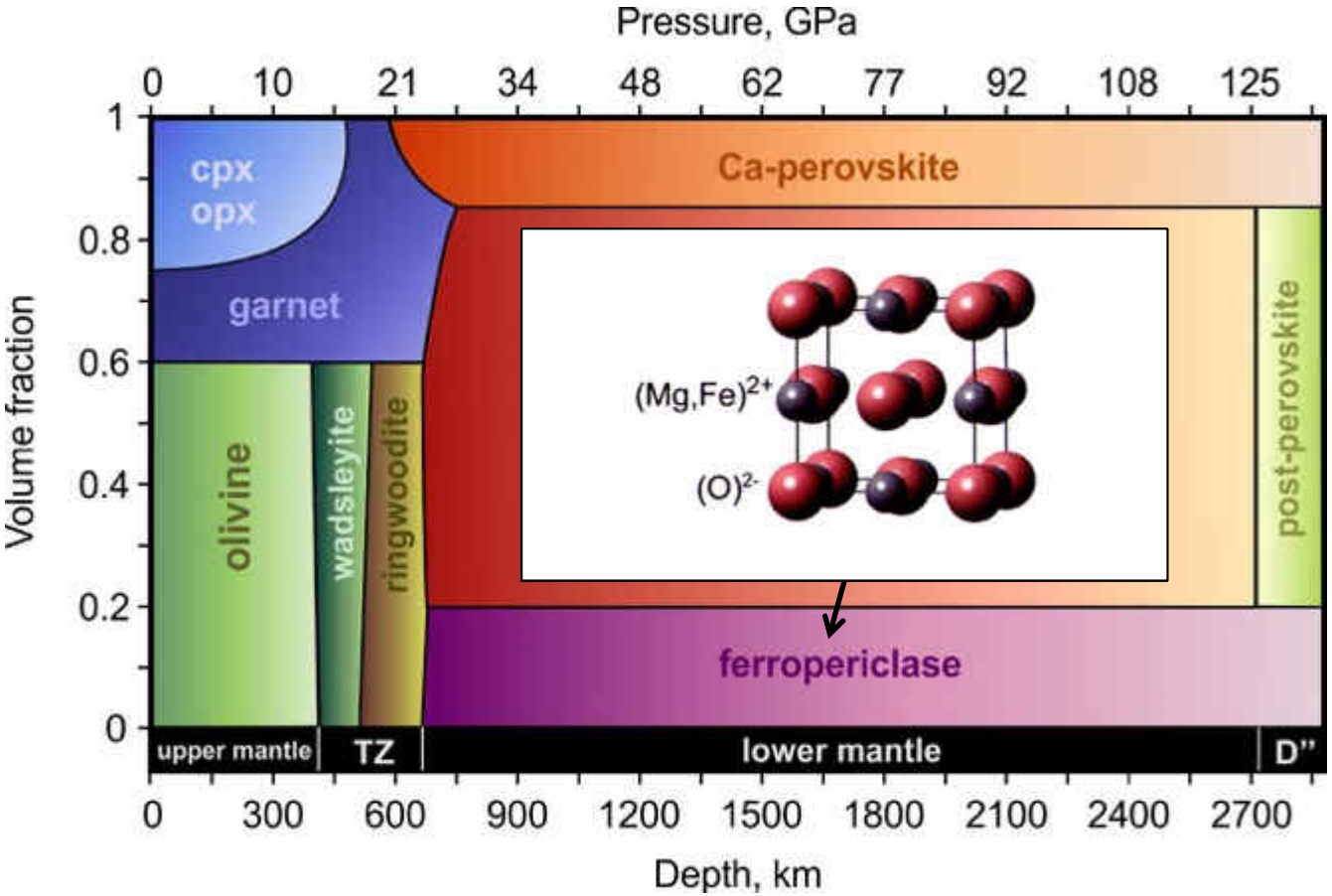

Predicting slip systems in MgO with the Peierls-Nabarro Galerkin model

0 GPa | 60 GPa | 100 GPa

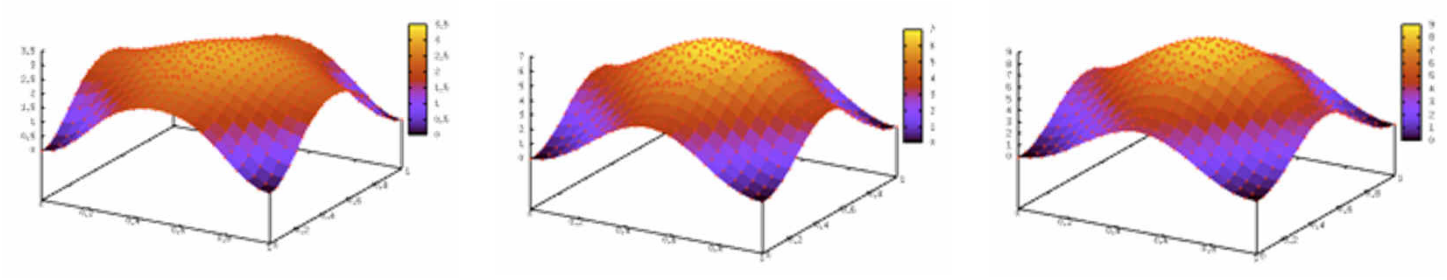

{100}

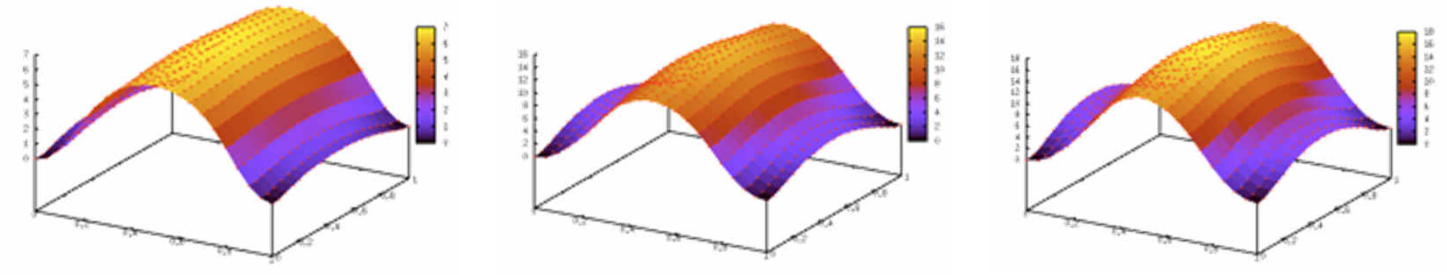

{110}

Predicting slip systems in MgO with the Peierls-Nabarro Galerkin model

{100}

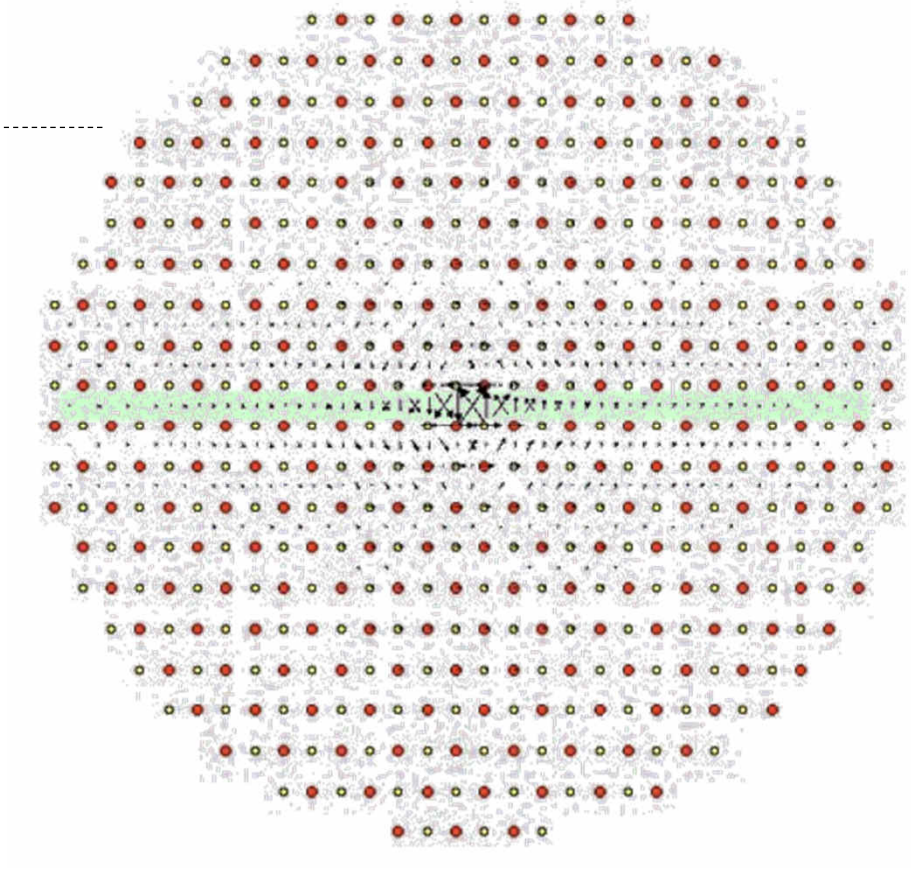

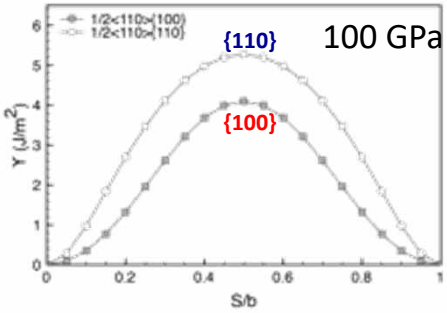

100 GPa

Glide in {100}

Predicting slip systems in MgO with the Peierls-Nabarro Galerkin model

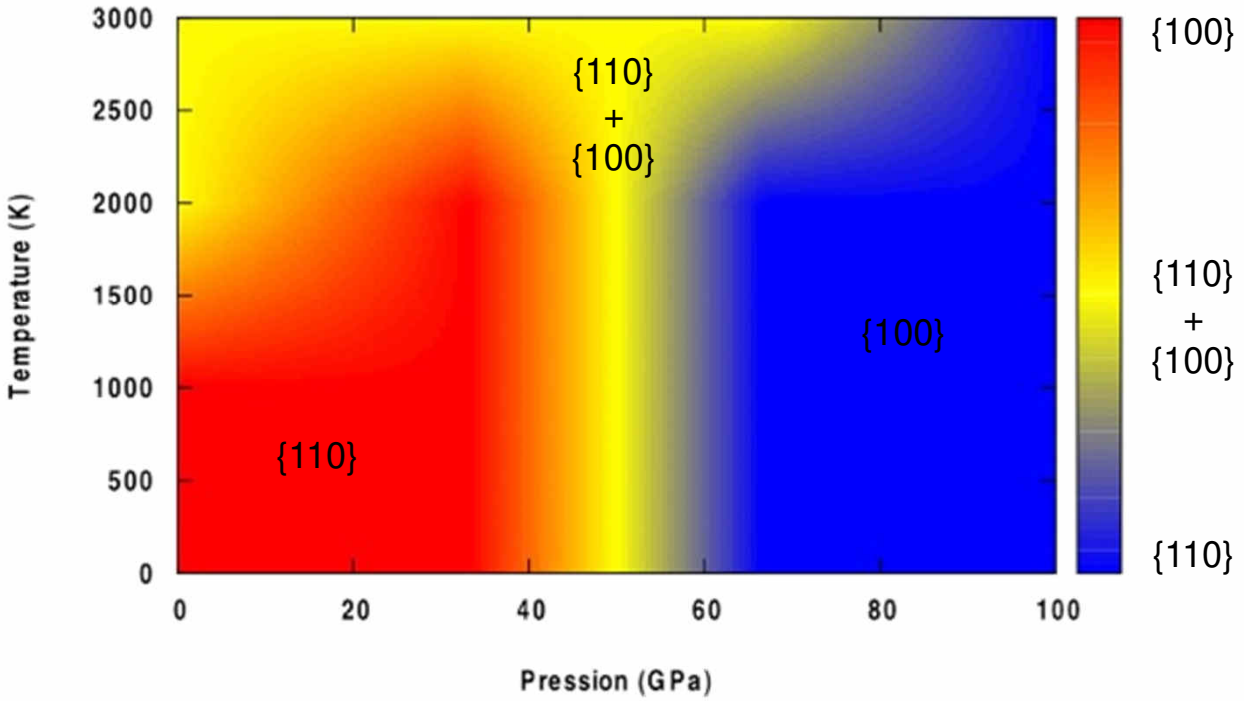

$\dot{\varepsilon} = 10^{-4}\ s^{-1};\ \rho = 10^{12}\ m^{-2}$

Experimental evidence

J. Immoor et al. / Earth and Planetary Science Letters 489 (2018) 251–257

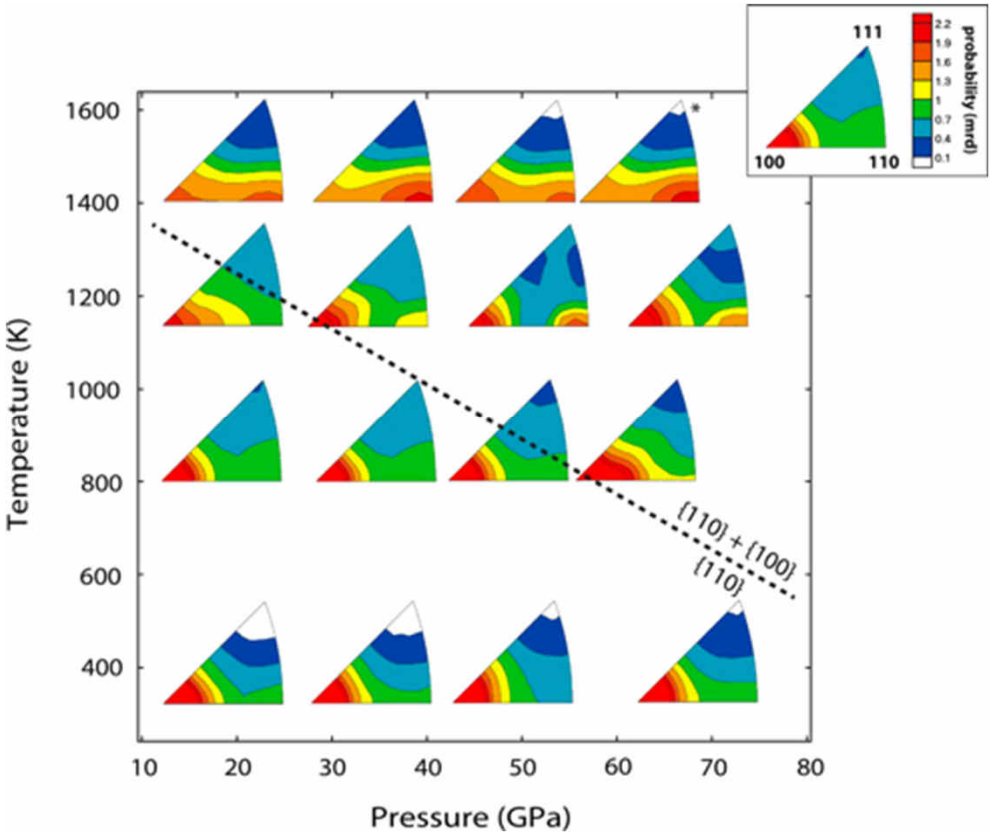

Beyond core spreading: dissociation

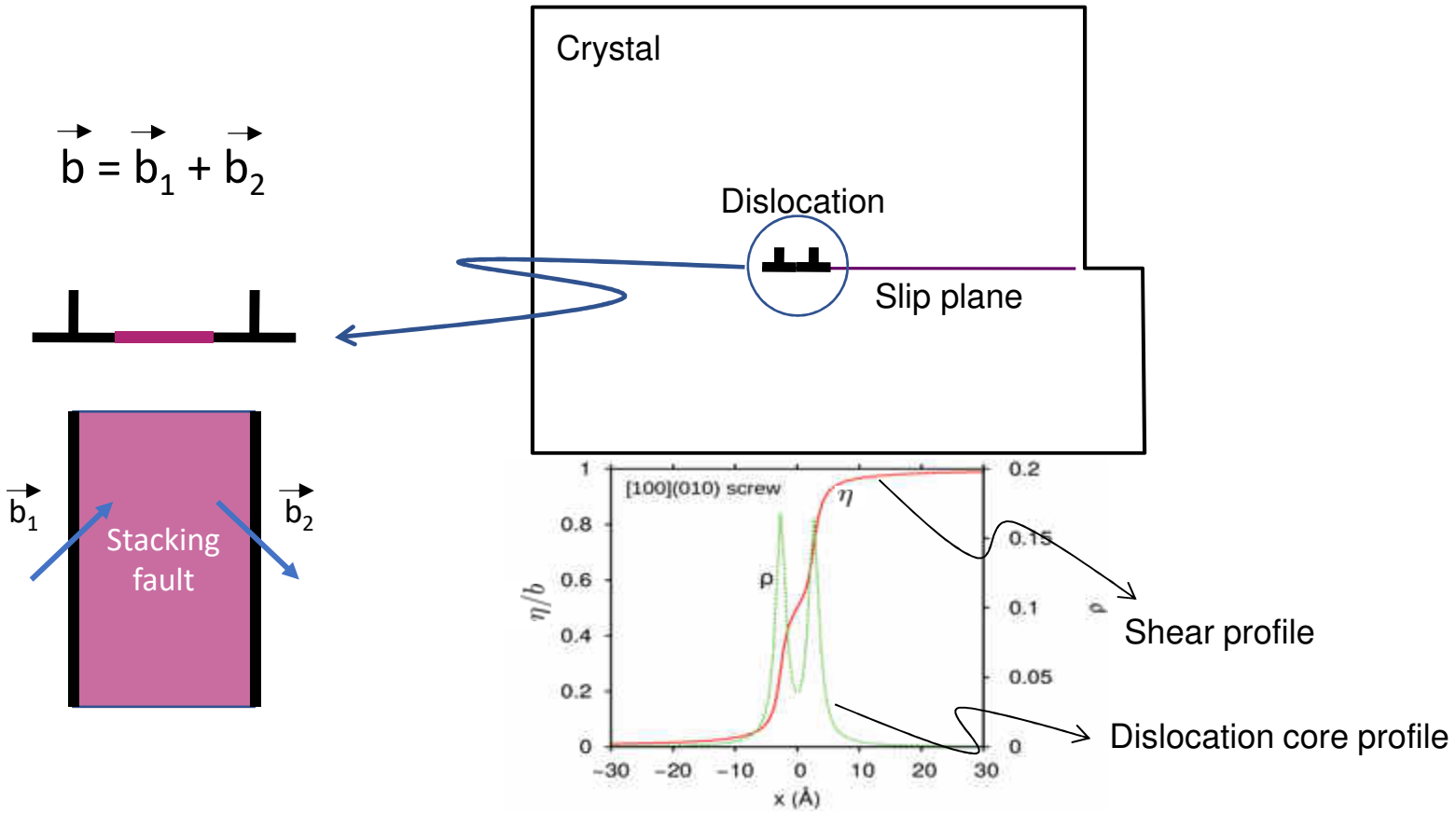

Ringwoodite (Mg_2SiO_4)

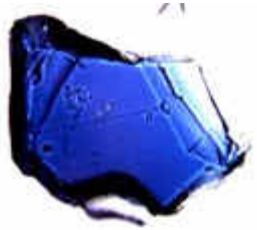

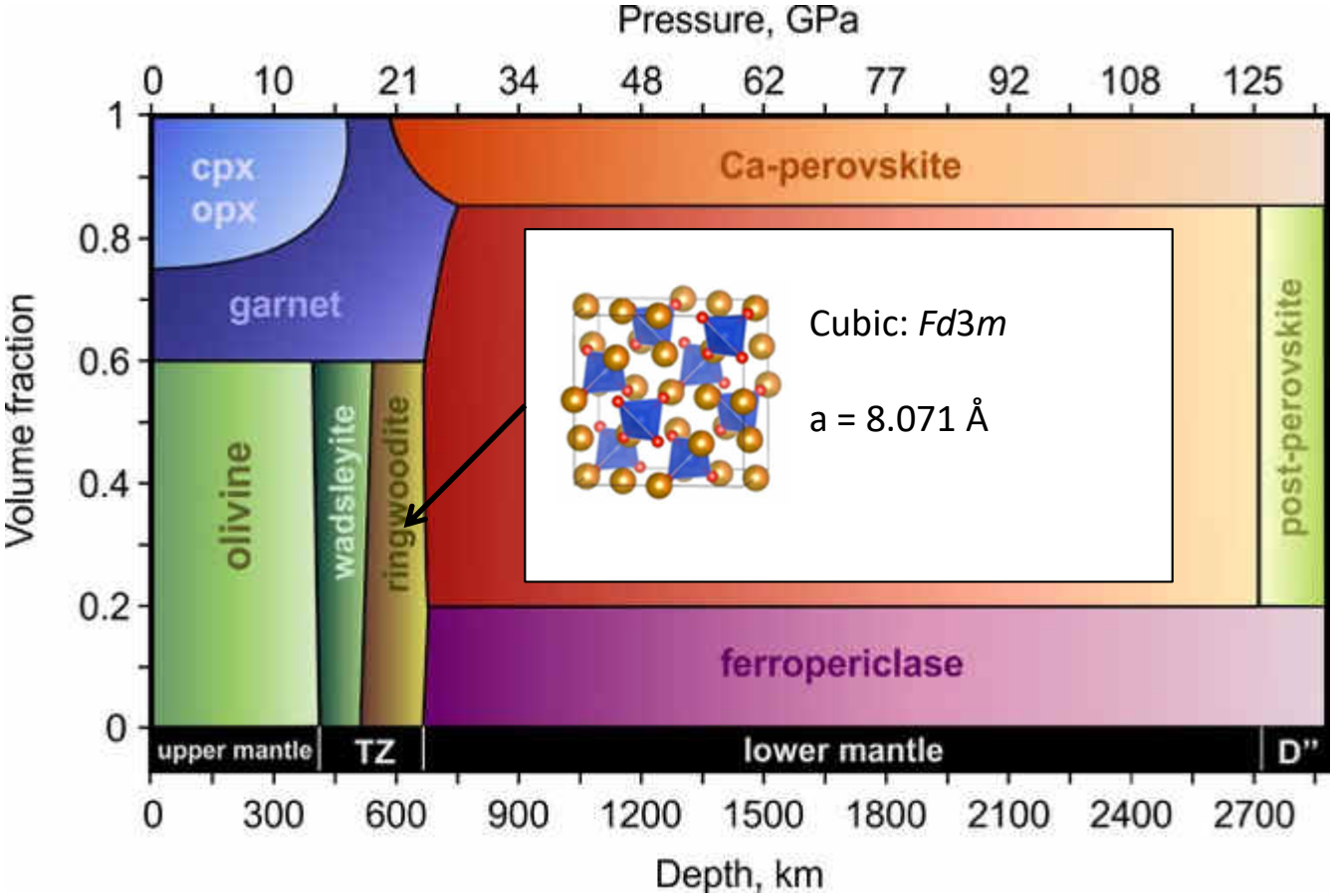

Ringwoodite: generalyzed stacking faults

Ringwoodite (20 GPa)
(110) plane

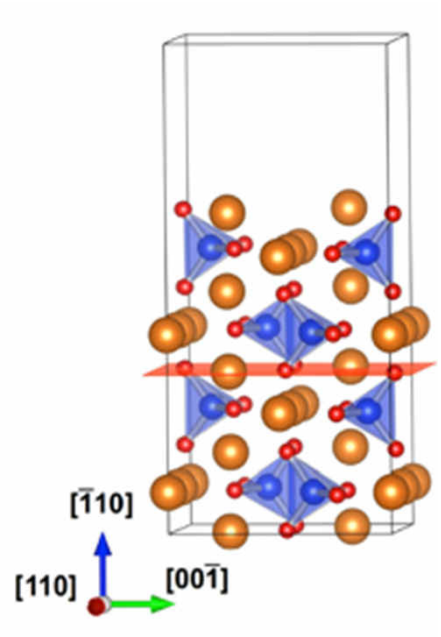

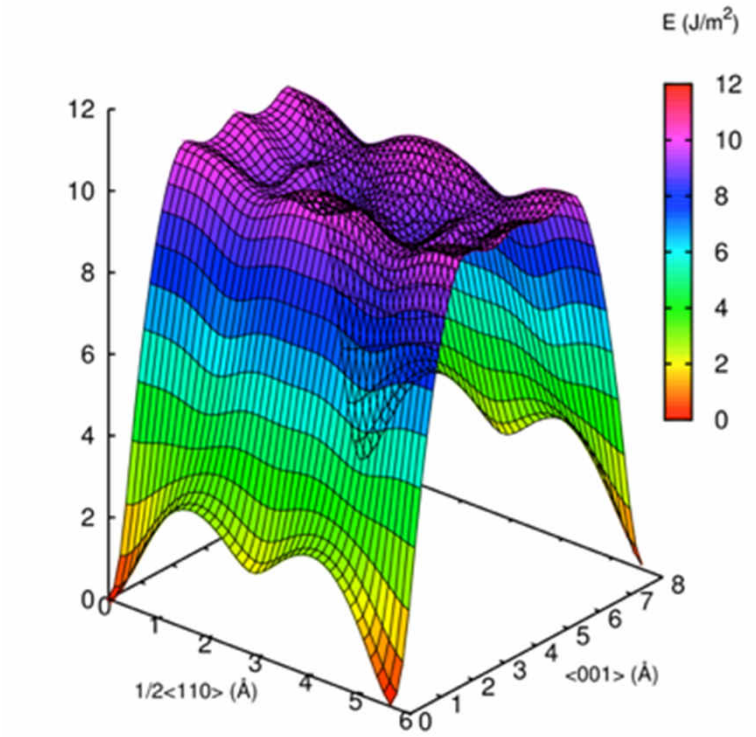

Easy shear path along the ½[-110] direction

Defines the **Burgers vector**

Ritterbex et al. (2015)

Ringwoodite: generalyzed stacking faults

Ringwoodite (20 GPa)

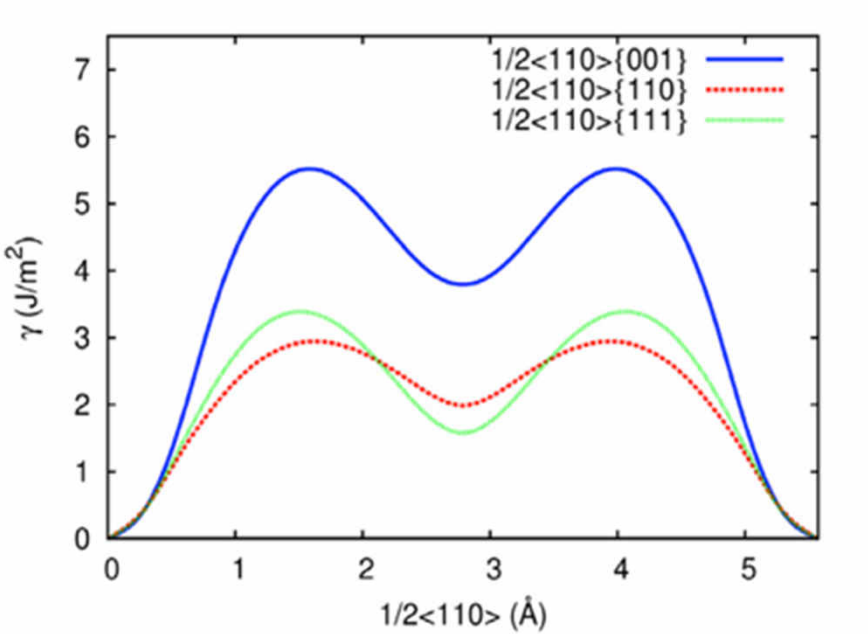

Easy shear path along the ½[-110] direction

Ritterbex et al. (2015)

Ringwoodite: dissociated dislocations

½ <110>{111}

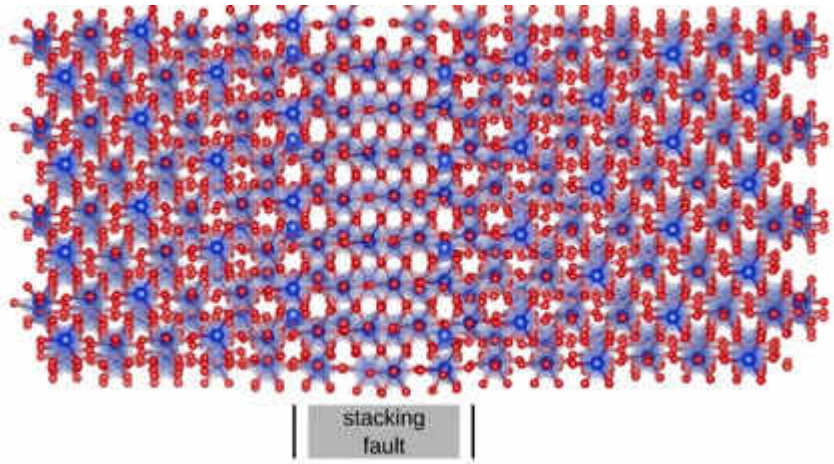

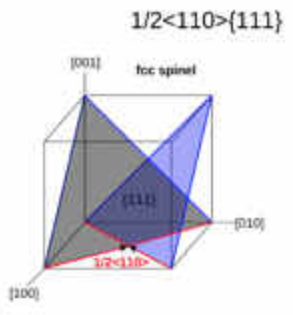

½ <110>{110}

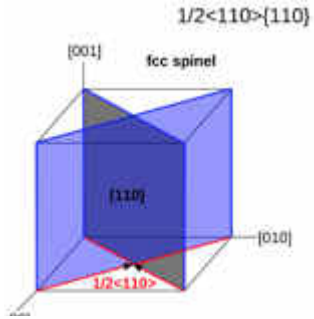

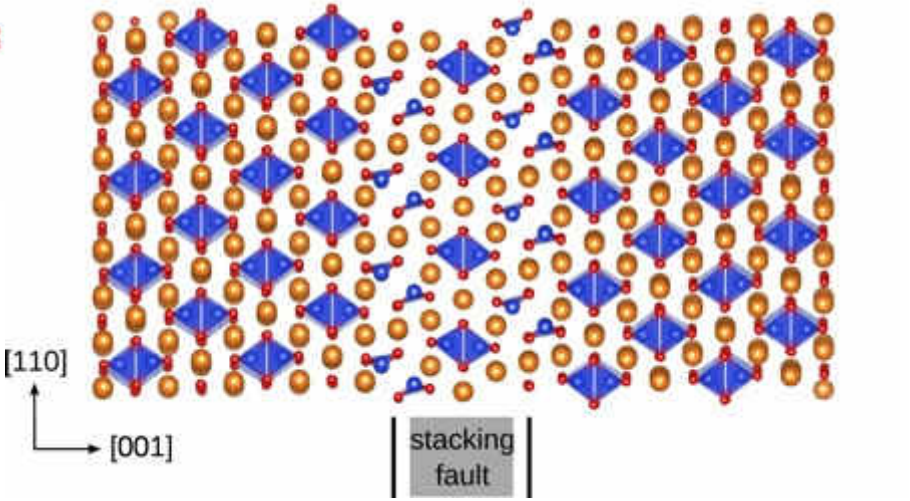

Wadsleyite (Mg_2SiO_4)

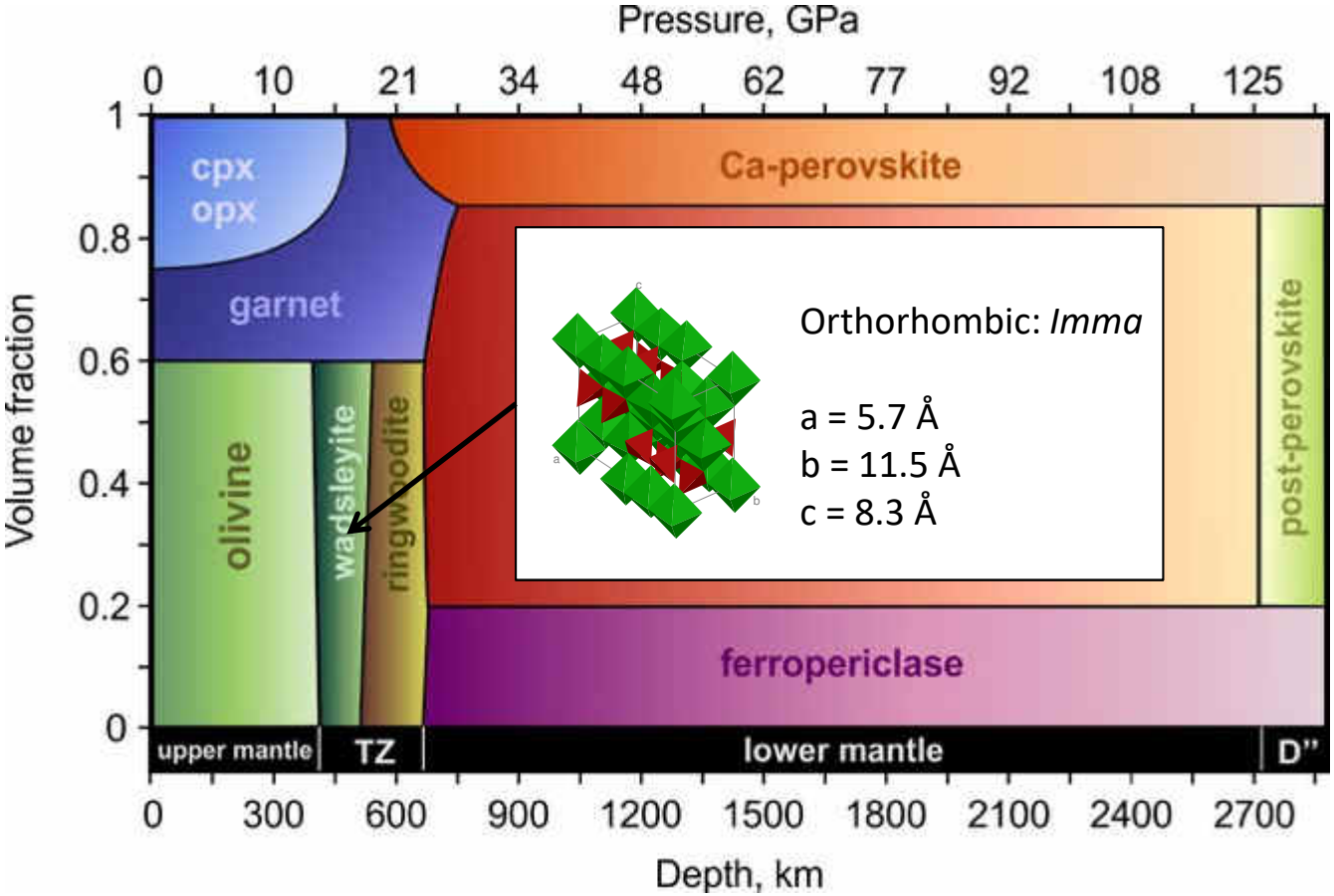

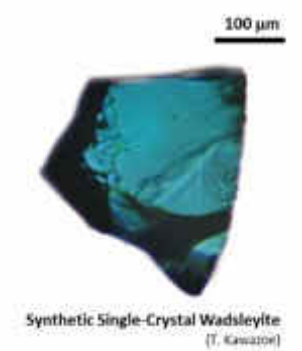

Wadsleyite (Mg_2SiO_4)

[100] glide: the shortest lattice repeat (5.5 Å)

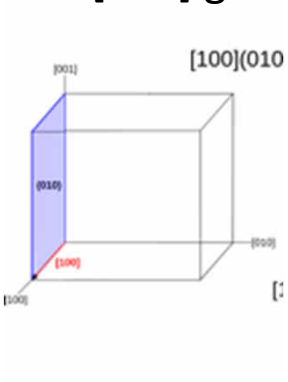

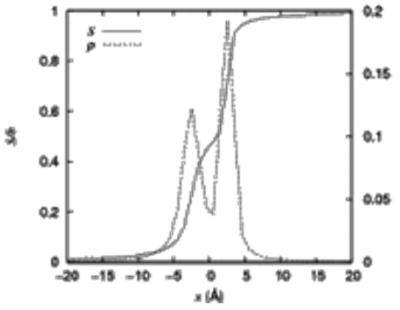

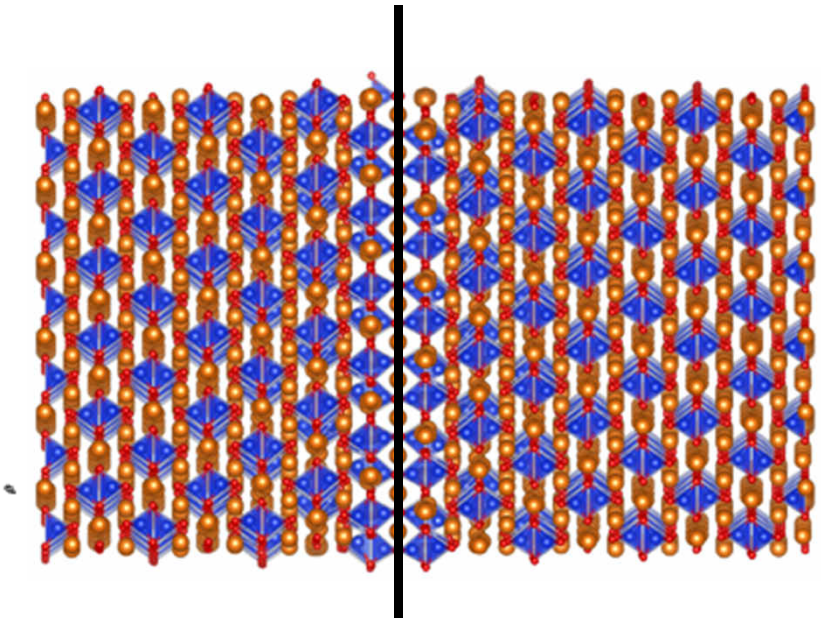

[100](010) screw

E. Thurel PhD thesis

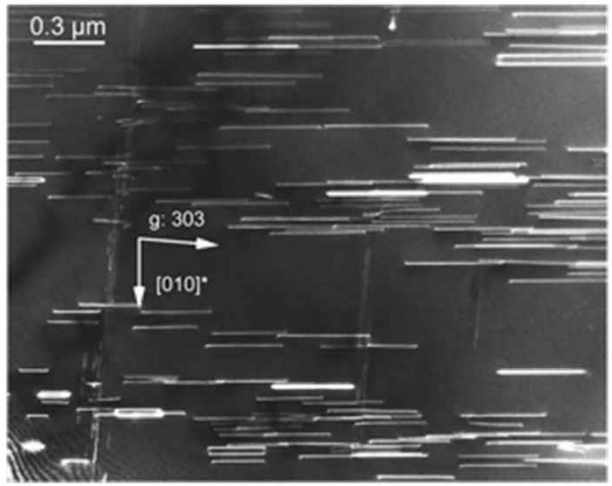

Fig. 13 [100] dislocations gliding in (010). Some [010] dislocations gliding in (101) can be seen through their residual contrast. Weak-beam dark field g: 303

Easiest slip system

Wadsleyite (Mg_2SiO_4)

½<111>{101} (7.5 Å)

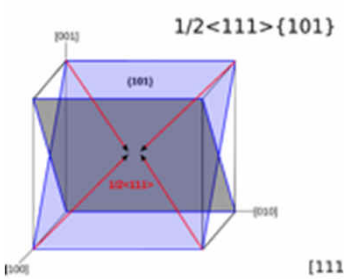

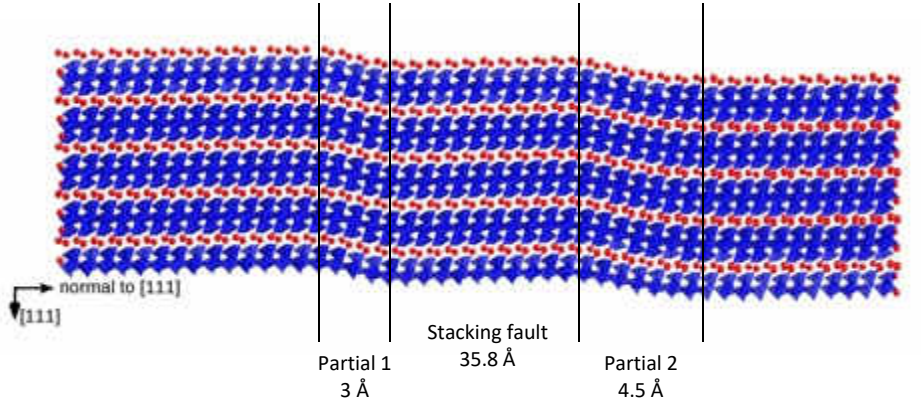

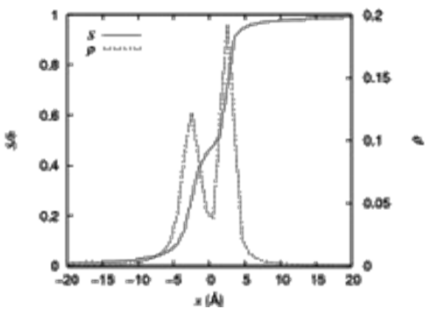

½ [111](101)

Second easiest slip system

weakest plane

+

Wide dissociation (5-8 b)

E. Thurel PhD thesis

Wadsleyite deformed at 18 GPa - 1600°C

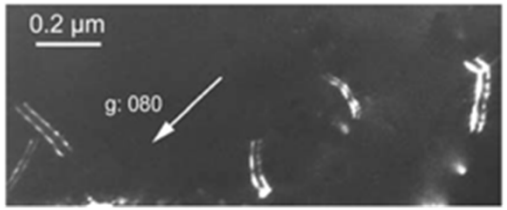

Dissociated 1/2<111> dislocations gliding in {101}

Wadsleyite (Mg_2SiO_4)

[010] dislocations: the largest lattice repeat (11.5 Å)

DISLOCATION CORES IN CRYSTALS WITH LARGE UNIT CELLS

F.R.N. Nabarro
Department of Physics, University of the Witwatersrand, Johannesburg, South Africa.

Résumé - Une maille cristalline peut être grande dans 0, 1, 2 ou 3 directions, et peut être définie comme petite, allongée, raccourci ou grande. Les proprietés mécaniques, et en particulier, la structure de coeur des dislocations dépendent des forces aussi bien que de la longueur des liaisons dans les trois directions principales. Si nous ne distinguons que les catégories courte/longue et forte/faible, nous trouvons 20 catégories cristallines plastiques. Des exemples de quelques-unes de ces catégories sont discutées et la largeur et les contraintes de Peierls de quelques-unes de leurs dislocations sont considérées. Les défauts d'empilement et les dislocations partielles compliquent l'analyse. L'influence des liaisons courte/longue et forte/faible sur la stabilité des dislocations creuses et sur les tubes de corrosion est examinée, et certains problèmes concernant les dislocations de croissance et les tubes de corrosion sont mentionnés.

Abstract - A crystal cell may be large in 0, 1, 2 or 3 directions, so that it may be described as small, prolate, oblate or large. The mechanical properties, and in particular the dislocation structure, depend on the strengths as well as the lengths of the bonds in the three principal directions. If we distinguish only the classes short/long and strong/weak, we find 20 plastic crystal classes. Examples of some of these classes are discussed, and the widths and Peierls stresses of some of their dislocations are considered. Stacking faults and partial dislocations complicate the analysis. The influence of short/long and strong/weak bonds on the stability of hollow dislocations and etch tubes is examined, and some problems concerning growth dislocations and etch tubes are mentioned.

Acta Cryst. (1951). **4**, 497

Capillary Equilibria of Dislocated Crystals

By F. C. Frank
H. H. Wills Physical Laboratory, University of Bristol, England

(*Received* 2 *November* 1950)

It is shown that a dislocation whose Burgers vector exceeds a critical value, of the order of magnitude 10 A., is only in equilibrium with an empty tube at its core. This is not the case in metals or other simple crystalline solids, but is likely to be the case in protein crystals, which therefore, unfortunately, do not provide good models of simple crystalline substances in respect of dislocations. The same causes generally give rise to a dimple or crater where a dislocation meets a free surface, and the shape of this crater is calculated. Though shallow in form, it is infinitely deep except at a habit face of a crystal, where it is of finite depth and may be totally absent.

1. The equilibrium of open-cored dislocations

It will be shown that for a dislocation of large Burgers vector* there exists a state of equilibrium in which the core of the dislocation is an empty tube. We shall find, however, that this is not the case for the elementary dislocations of a typical metal or simple ionic crystal; but it may be so for substances with large unit cells, of the order of 10 A. or more, e.g. some silicates. It will assuredly be the case in protein crystals.

For simplicity we consider the case of a screw dislocation in a material with isotropic elastic constants. Strain-energy densities are of similar magnitude at similar distances from dislocations of other orientation and in materials of naturally occurring degrees of anisotropy in their elastic behaviour. Let there be an empty cylinder of radius r, the dislocation line lying in the cylinder. Then the shear strain at the surface of the cylinder is $b/2\pi r$, where b is the modulus of the Burgers vector. There is consequently a strain-energy density here of $\mu b^2/8\pi^2 r^2$, where μ is the rigidity modulus.

Suppose that a shell of material of thickness dr evaporates from this cylinder and deposits elsewhere, on a surface of the material whose radius of curvature is negligibly large. The interior cylindrical surface is thus enlarged. If γ is the specific surface free energy of the substance, the total increase in free energy per unit length of cylinder is

$$dF = 2\pi\gamma\, dr - (\mu b^2/8\pi^2 r^2)\, 2\pi r\, dr. \qquad (1)$$

There is an equilibrium when dF/dr is zero, i.e. when

$$r = \mu b^2/8\pi^2\gamma. \qquad (2)$$

Now, empirically the rigidities and surface energies of substances tend to vary in a parallel manner so that γ/μ is very roughly a constant length (cf. Table 1), a typical value being say $\frac{1}{4}$ A. In consequence r is less than 1 A. unless b exceeds 4–5 A. The implied assumption of linear elasticity is then invalid. If b were as large as 100 A., as would be appropriate in protein crystals, this objection would disappear, and we may conclude that the typical dislocation in such a crystal would, in equilibrium, have a hollow core of the order of 1000 A. in diameter. This brings the unfortunate conclusion that these crystals, the ones in which we can most easily see the constituent parts, do not furnish satisfactory analogues of simpler crystals with regard to dislocations.

Let us now make an approximate allowance for the non-linear elastic behaviour. We shall assume that stress is related to strain by Hooke's law up to a strain of 0·1 and thereafter is constant (as in Figs. 1 (ii) and 2 (ii)). The strain-energy density is

$$\begin{cases} \mu b^2/8\pi^2 r^2 & (r \geqslant 5b/\pi); \\ \mu b/20\pi r - \mu/200 & (r \leqslant 5b/\pi). \end{cases} \qquad (3)$$

* The Burgers vector is the name we give to what Burgers (1939) called the 'strength' of a dislocation. This vector is parallel to the dislocation line in a 'screw' and normal to it in an 'edge' dislocation, these being only particular cases of the general situation. A simple account of the geometry and elastic fields of dislocations is given by Cottrell (1949).

Table 1. *Approximate rigidities and surface energies of solids*

Substance	Rigidity modulus μ (10^{11} erg cm.$^{-3}$)	Surface energy γ (erg cm.$^{-2}$)	γ/μ (10^{-6} cm.)	Reference
Copper	4·4	1400	0·32	Udin *et al.* (1949)
Sodium chloride	1·5	155	0·10	Rose (1936), Shuttleworth (1949)
Argon	0·106	42	0·40	Mackenzie & Mott (1950), Shuttleworth (1949)
Mica	8·0	4500 (in vacuo) 400 (in air)	0·56 0·05	Obreimoff (1930) Orowan (1933)

Wadsleyite (Mg_2SiO_4)

[010] dislocations: the largest lattice repeat (11.5 Å)

Peierls model of the edge [010](100) dislocation

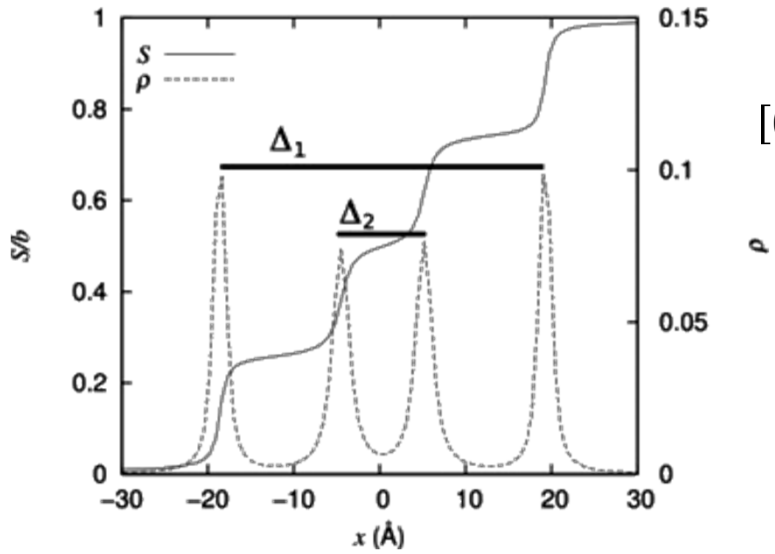

$$[010] \rightarrow \frac{1}{4}[010] + \frac{1}{4}[010] + \frac{1}{4}[010] + \frac{1}{4}[010]$$

Wadsleyite (Mg_2SiO_4)

[010] dislocations: the largest lattice repeat (11.5 Å)

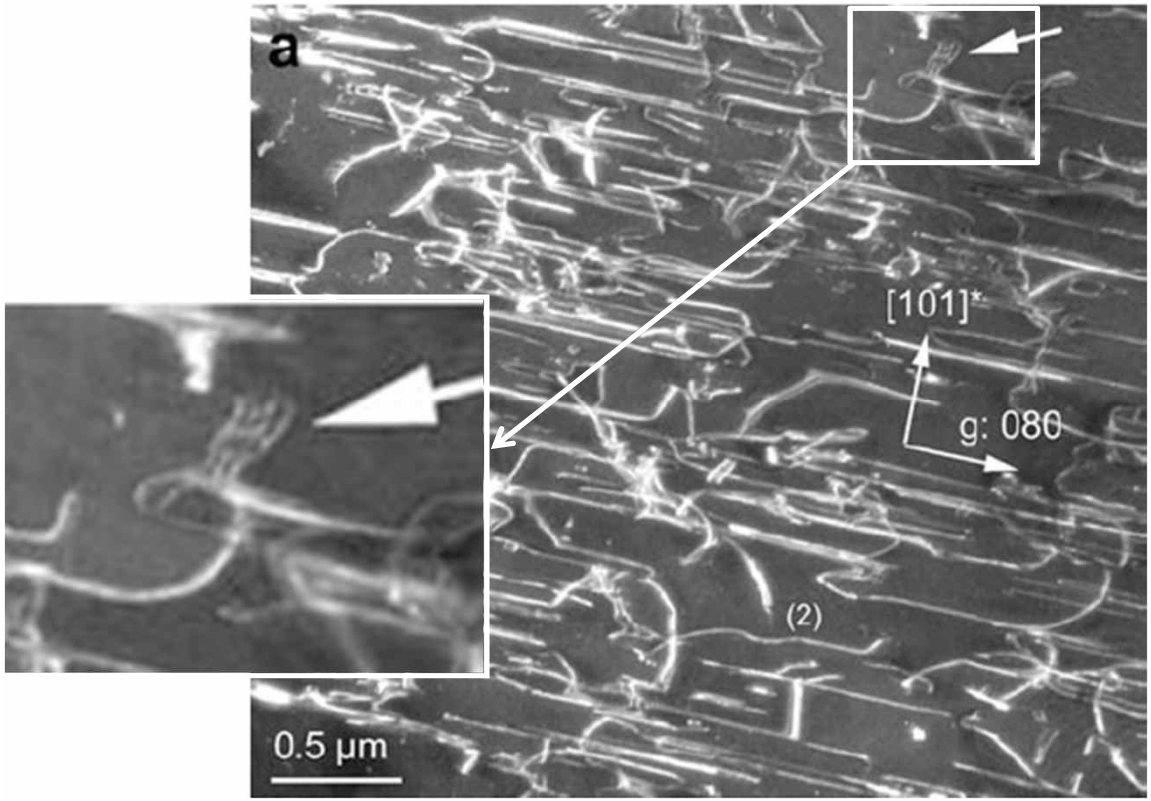

Wadsleyite deformed at 17 GPa - 1500°C

Wadsleyite (Mg_2SiO_4)

[010] dislocations: the largest lattice repeat (11.5 Å)

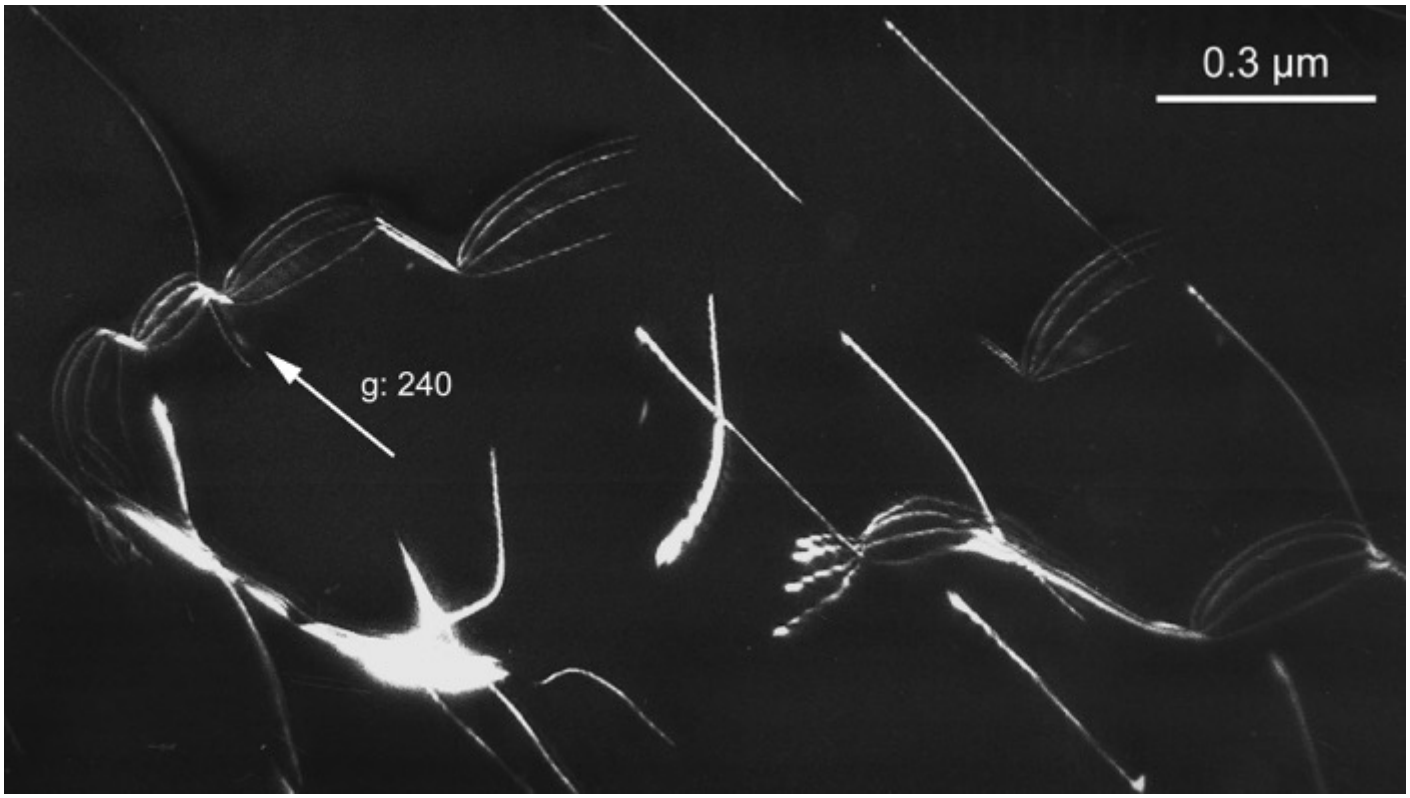

Wadsleyite (Mg_2SiO_4)

[010] dislocations: the largest lattice repeat (11.5 Å)

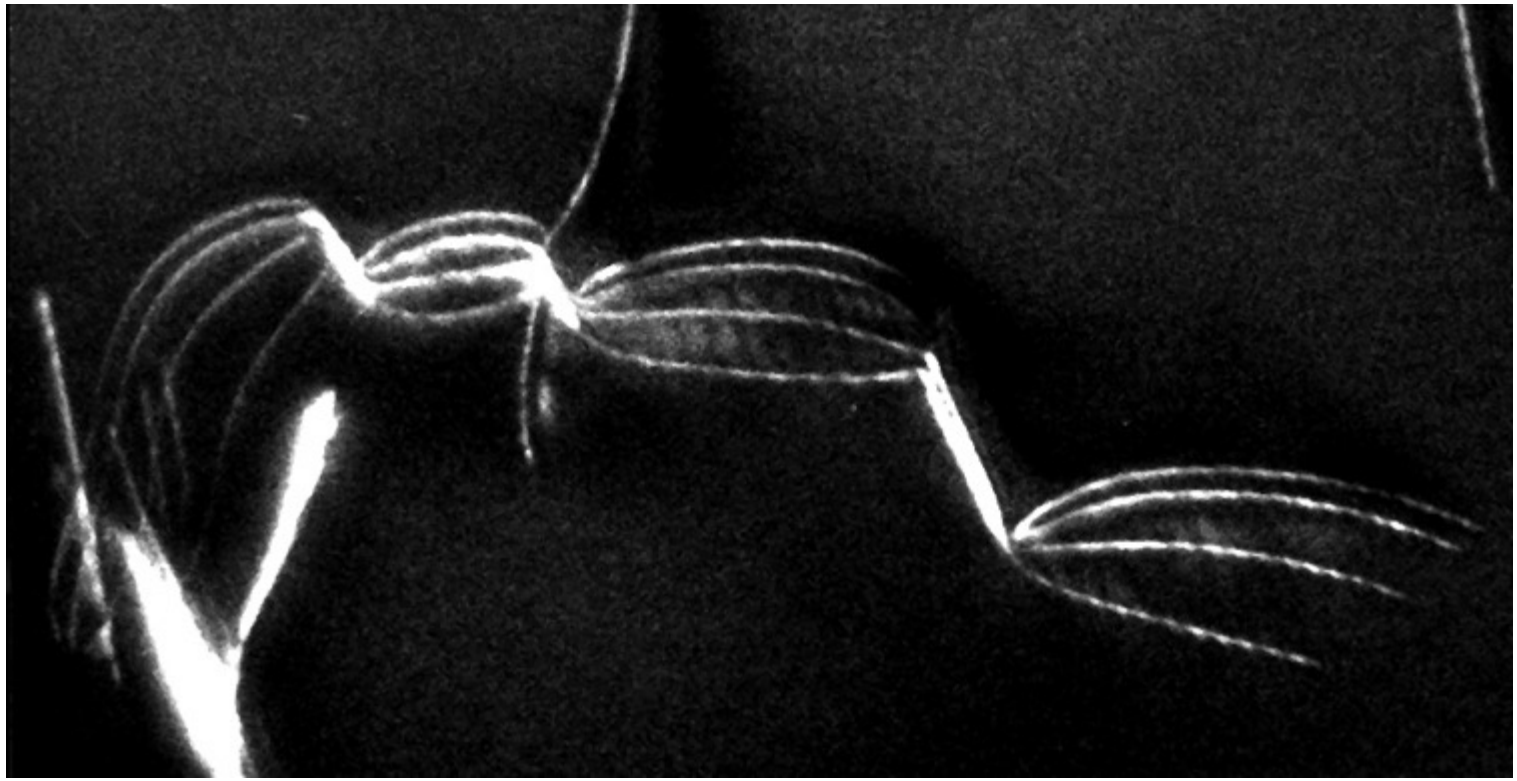

Garnets $X_3Y_2Z_3O_{12}$

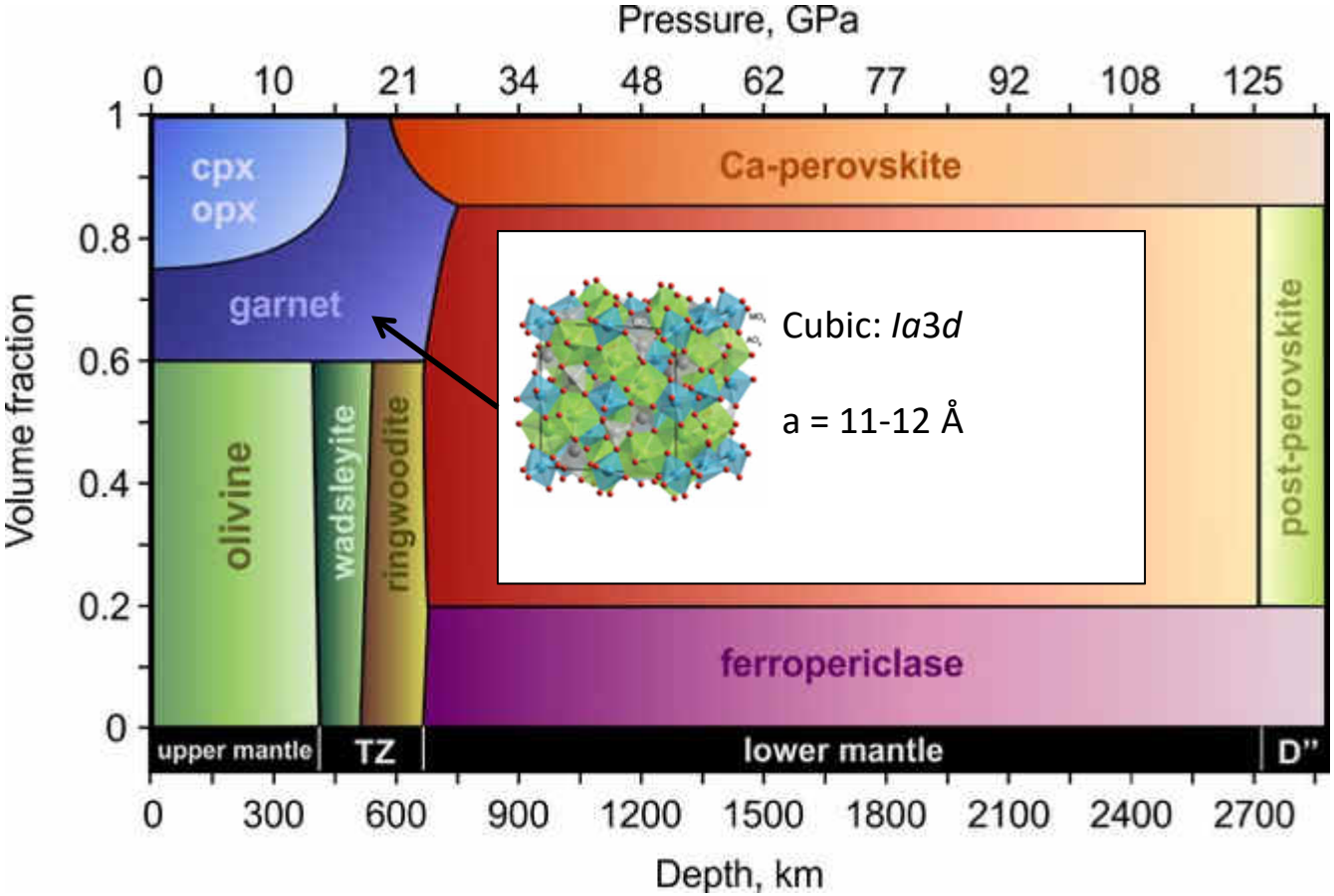

Garnets

Experimental deformation: 6.5 GPa, 900 °C

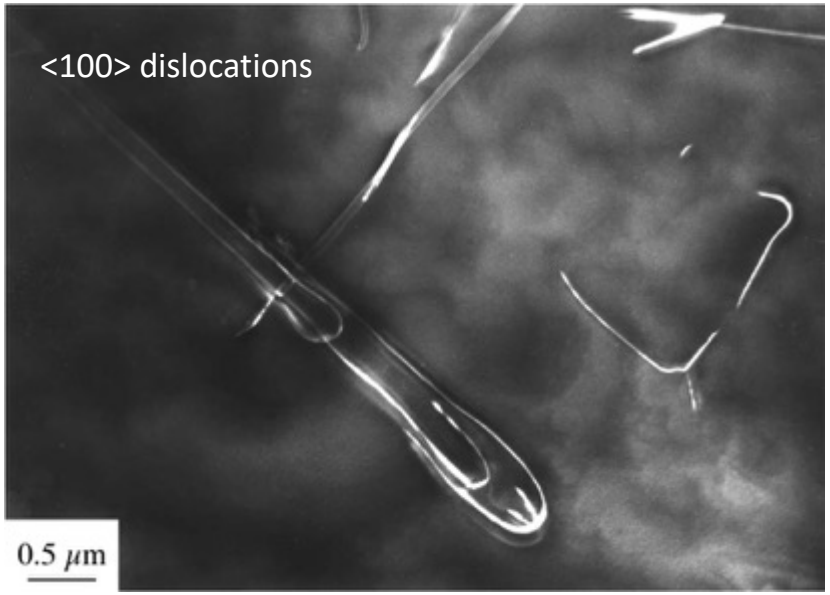

V. Voegelé et al. Physics of the Earth and Planetary Interiors 108 (1998) 305–318

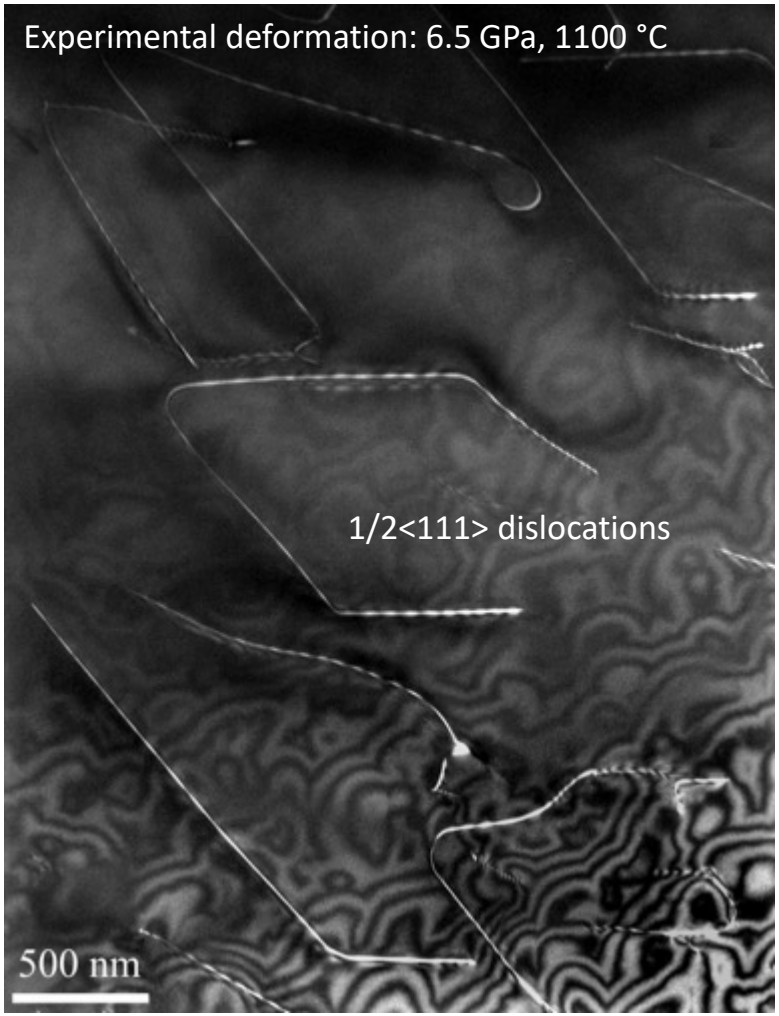

Garnets

Eclogites from the Alps

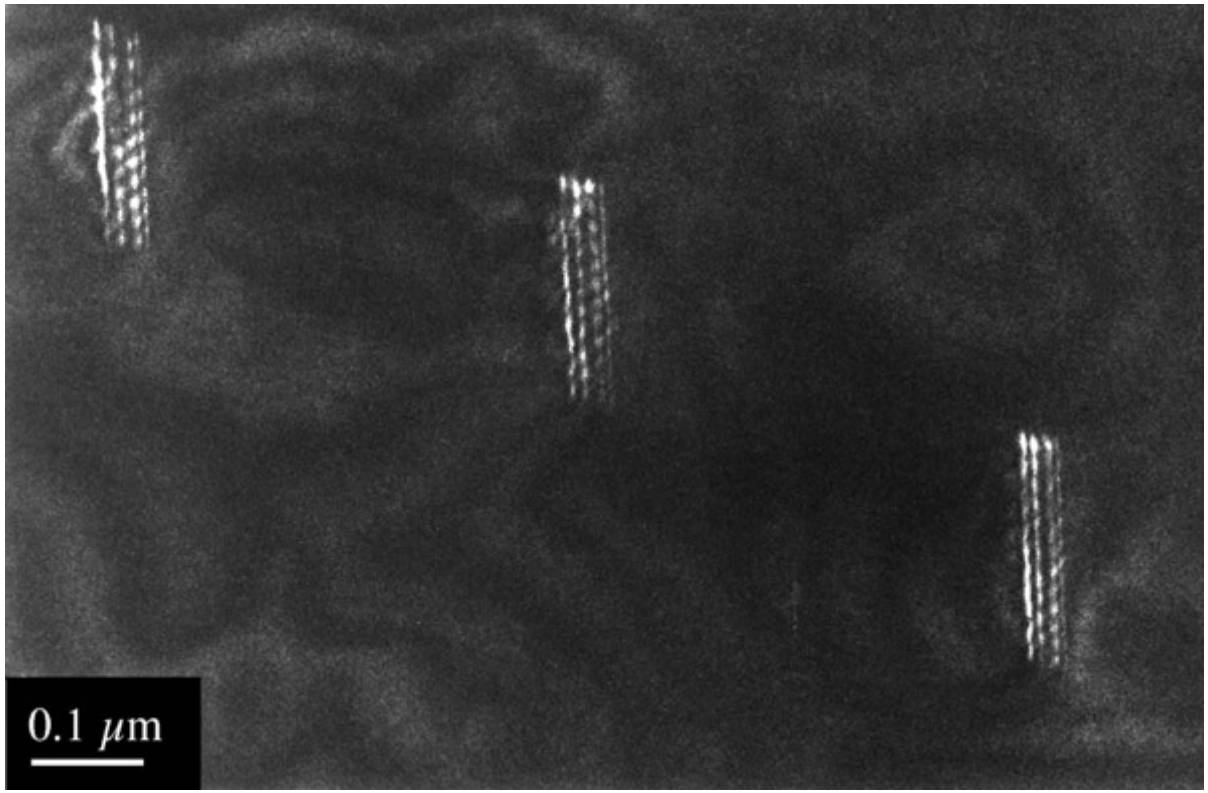

V. Voegelé et al. Physics of the Earth and Planetary Interiors 108 (1998) 319–338

Garnets

Eclogites from the Alps

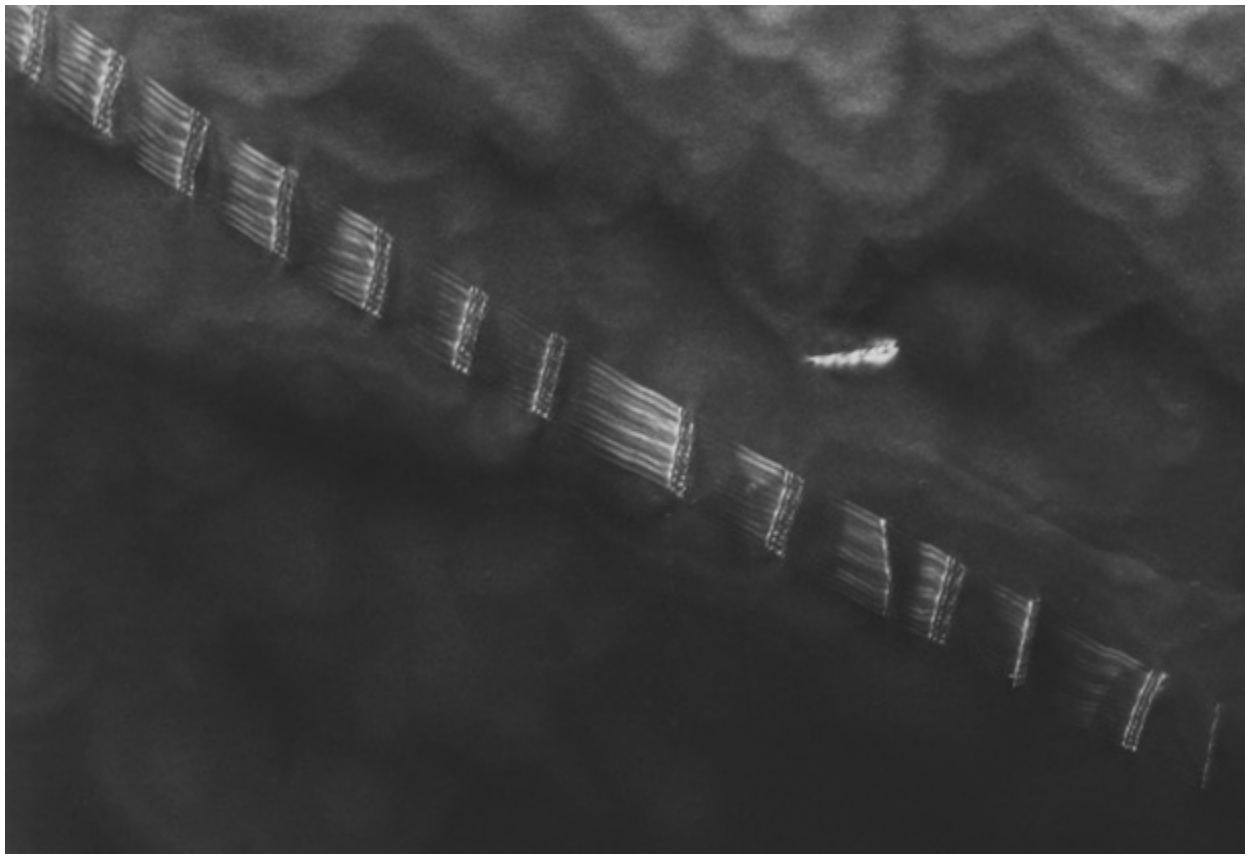

Garnets

Eclogites from the Alps

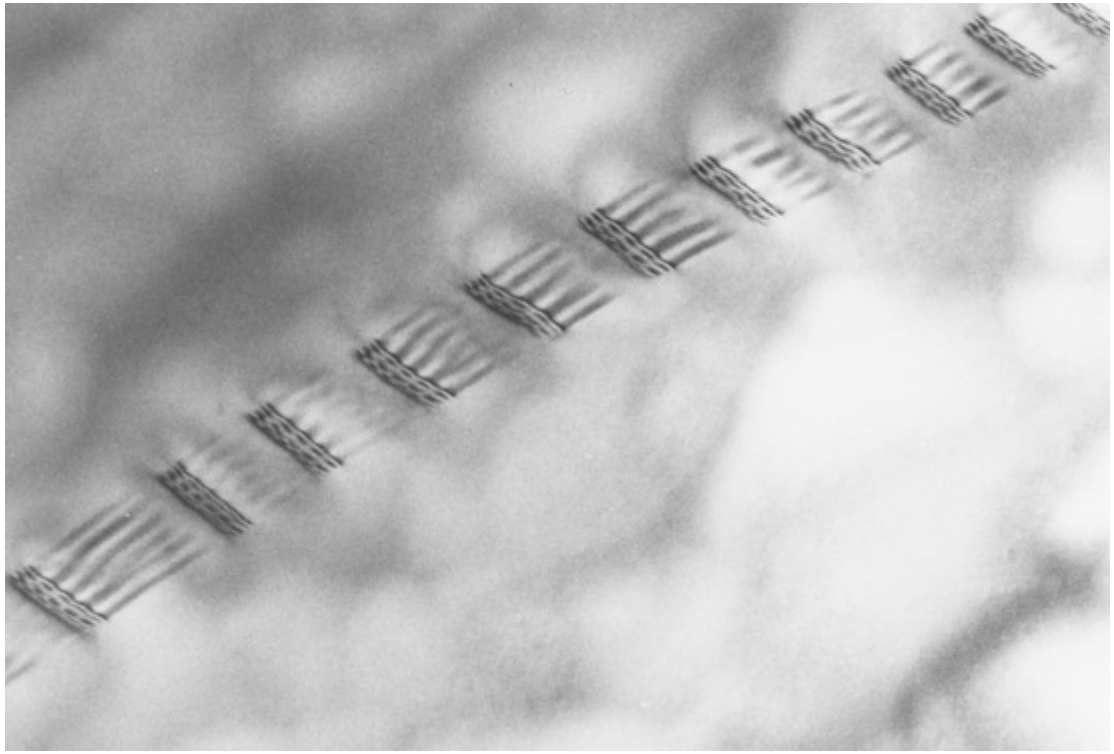

V. Voegelé et al. Physics of the Earth and Planetary Interiors 108 (1998) 319–338

The New York Times

Something Digs Intricate Tunnels in Garnets. Is It Alive?

The deep red gems have long been found marred with internal markings. Researchers propose a new explanation involving fungal microorganisms who have found a nice place to live.

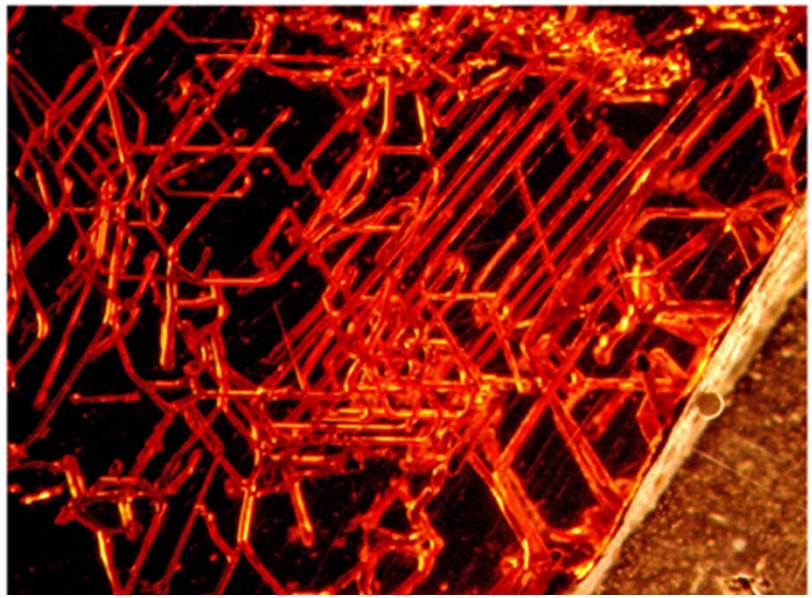

PLOS ONE

RESEARCH ARTICLE

Intricate tunnels in garnets from soils and river sediments in Thailand – Possible endolithic microborings

Magnus Ivarsson[1,2]*, Henrik Skogby[3], Bongkot Phichaikamjornwut[4], Stefan Bengtson[2], Sandra Siljeström[5], Prayote Dunchanum[6], Apichet Boonsoong[6], Minghwan Kruachanta[6], Federica Marone[7], Venela Belivanova[7], Sara Holmström[8]

1 University of Southern Denmark, Department of Biology and Nordic Center for Earth Evolution, Odense M, Denmark, 2 Swedish Museum of Natural History, Department of Palaeobiology, Stockholm, Sweden, 3 Swedish Museum of Natural History, Department of Geosciences, Stockholm, Sweden, 4 Gems and Jewelry Program, Faculty of Science, Srinakharinwirot University, Bangkok, Thailand, 5 RISE Research Institutes of Sweden, Bioscience and Materials/Chemistry and Materials, Stockholm, Sweden, 6 Department of Geological Sciences, Faculty of Science, Chiang Mai University, Chiang Mai, Thailand, 7 Swiss Light Source, Paul Scherrer Institute, Villigen, Switzerland, 8 Stockholm University, Department of Geological Sciences, Stockholm, Sweden

* magnus.ivarsson@biology.sdu.dk

OPEN ACCESS

Citation: Ivarsson M, Skogby H, Phichaikamjornwut B, Bengtson S, Siljeström S, Dunchanum P, et al. (2018) Intricate tunnels in garnets from soils and river sediments in Thailand – Possible endolithic microborings. PLoS ONE 13 (8): e0200951. https://doi.org/10.1371/journal.pone.0200951

Editor: Cassandra Marshall, Rutgers University, UNITED STATES

Received: August 30, 2017

Accepted: June 25, 2018

Published: August 8, 2018

Data Availability Statement: All relevant data are within the paper.

Funding: The authors acknowledge funding from the Swedish Research Council (Contracts No. 2007-4483 (SB), 2010-3829 (HS), 2012-4364 (MI), and 2013-4286 (SB), 2015-04126 (SS)), Danish National Research Foundation (DNRF53), and Paul Scherrer Institute (20100185 (MI) as well as Swedish National Space Board (Contract No. 85/10 (MI), 121/11 and 198/16 (SS)). The

Abstract

Garnets from disparate geographical environments and origins such as oxidized soils and river sediments in Thailand host intricate systems of microsized tunnels that significantly decrease the quality and value of the garnets as gems. The origin of such tunneling has previously been attributed to abiotic processes. Here we present physical and chemical remains of endolithic microorganisms within the tunnels and discuss a probable biological origin of the tunnels. Extensive investigations with synchrotron-radiation X-ray tomographic microscopy (SRXTM) reveal morphological indications of biogenicity that further support a euendolithic interpretation. We suggest that the production of the tunnels was initiated by a combination of abiotic and biological processes, and that at later stages biological processes came to dominate. In environments such as river sediments and oxidized soils garnets are among the few remaining sources of bio-available Fe^{2+}, thus it is likely that microbially mediated boring of the garnets has trophic reasons. Whatever the reason for garnet boring, the tunnel system represents a new endolithic habitat in a hard silicate mineral otherwise known to be resistant to abrasion and chemical attack.

Introduction

Endoliths are microorganisms living inside substrates, mostly rocks and minerals, but also shells, corals or wood [1,2]. Endolithic lineages have been developed among bacteria, fungi, algae, and several animal phyla, and they can either be chemolithoautotrophs (which utilize inorganically stored energy and carbon from inorganic sources like minerals), heterotrophs, or even photoautotrophs (like cyanobacteria) [1,3]. The usual advantage of entertaining an

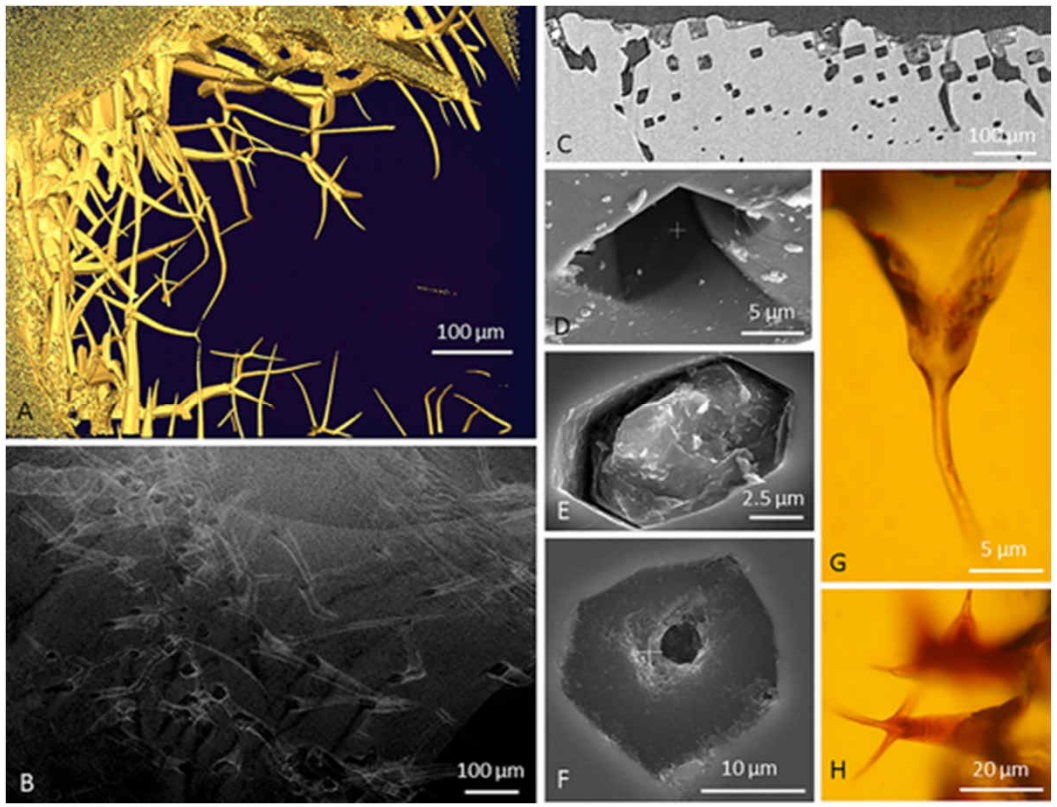

PLOS ONE

RESEARCH ARTICLE

Intricate tunnels in garnets from soils and river sediments in Thailand – Possible endolithic microborings

Magnus Ivarsson[1,2]*, Henrik Skogby[3], Bongkot Phichaikamjornwut[4], Stefan Bengtson[2], Sandra Siljeström[5], Prayote Dunchanum[6], Apichet Boonsoong[6], Minghwan Kruachanta[6], Federica Marone[7], Venela Belivanova[7], Sara Holmström[8]

1 University of Southern Denmark, Department of Biology and Nordic Center for Earth Evolution, Odense M, Denmark, 2 Swedish Museum of Natural History, Department of Palaeobiology, Stockholm, Sweden, 3 Swedish Museum of Natural History, Department of Geosciences, Stockholm, Sweden, 4 Gems and Jewelry Program, Faculty of Science, Srinakharinwirot University, Bangkok, Thailand, 5 RISE Research Institutes of Sweden, Bioscience and Materials/Chemistry and Materials, Stockholm, Sweden, 6 Department of Geological Sciences, Faculty of Science, Chiang Mai University, Chiang Mai, Thailand, 7 Swiss Light Source, Paul Scherrer Institute, Villigen, Switzerland, 8 Stockholm University, Department of Geological Sciences, Stockholm, Sweden

* magnus.ivarsson@biology.sdu.dk

OPEN ACCESS

Citation: Ivarsson M, Skogby H, Phichaikamjornwut B, Bengtson S, Siljeström S, Dunchanum P, et al. (2018) Intricate tunnels in garnets from soils and river sediments in Thailand – Possible endolithic microborings. PLoS ONE 13 (8): e0200351. https://doi.org/10.1371/journal.pone.0200351

Editor: Cassandra Marshall, Rutgers University, UNITED STATES

Received: August 30, 2017

Accepted: June 25, 2018

Published: August 8, 2018

Data Availability Statement: All relevant data are within the paper.

Funding: The authors acknowledge funding from the Swedish Research Council (Contracts No. 2007-4483 (SB), 2010-3829 (HS), 2012-4364 (MI), and 2013-4286 (SB), 2015-04126 (SS)), Danish National Research Foundation (DNRF53), and Paul Scherrer Institute (20100185 (MI) as well as Swedish National Space Board (Contract No. 85/10 (MI), 121/11 and 198/15 (SS)). The

Abstract

Garnets from disparate geographical environments and origins such as oxidized soils and river sediments in Thailand host intricate systems of microsized tunnels that significantly decrease the quality and value of the garnets as gems. The origin of such tunneling has previously been attributed to abiotic processes. Here we present physical and chemical remains of endolithic microorganisms within the tunnels and discuss a probable biological origin of the tunnels. Extensive investigations with synchrotron-radiation X-ray tomographic microscopy (SRXTM) reveal morphological indications of biogenicity that further support a euendolithic interpretation. We suggest that the production of the tunnels was initiated by a combination of abiotic and biological processes, and that at later stages biological processes came to dominate. In environments such as river sediments and oxidized soils garnets are among the few remaining sources of bio-available Fe^{2+}, thus it is likely that microbially mediated boring of the garnets has trophic reasons. Whatever the reason for garnet boring, the tunnel system represents a new endolithic habitat in a hard silicate mineral otherwise known to be resistant to abrasion and chemical attack.

Introduction

Endoliths are microorganisms living inside substrates, mostly rocks and minerals, but also shells, corals or wood [1,2]. Endolithic lineages have been developed among bacteria, fungi, algae, and several animal phyla, and they can either be chemolithoautotrophs (which utilize inorganically stored energy and carbon from inorganic sources like minerals), heterotrophs, or even photoautotrophs (like cyanobacteria) [3,3]. The usual advantage of entertaining an

Influence of crystallography

The hexagonal cross section of the tunnels, usually the marginal portions, is probably due to the cubic crystallinity of garnets. Chemical weathering of garnets would be expected to reflect the crystallinity and produce hexagonal etch marks according to the crystal structure. However, the propagation of the network of curvi linear, branching and anastomosing tunnels appears to be independent of crystallography. Even though their propagation is not random, considering anastomosis and relation to mineral surfaces, they occur independently of the mineral crystallinity. The exception is the linear arrangement of straight tunnels with a coordinated curvature. Such mutual kink of the tunnels suggests influence from the crystal medium.

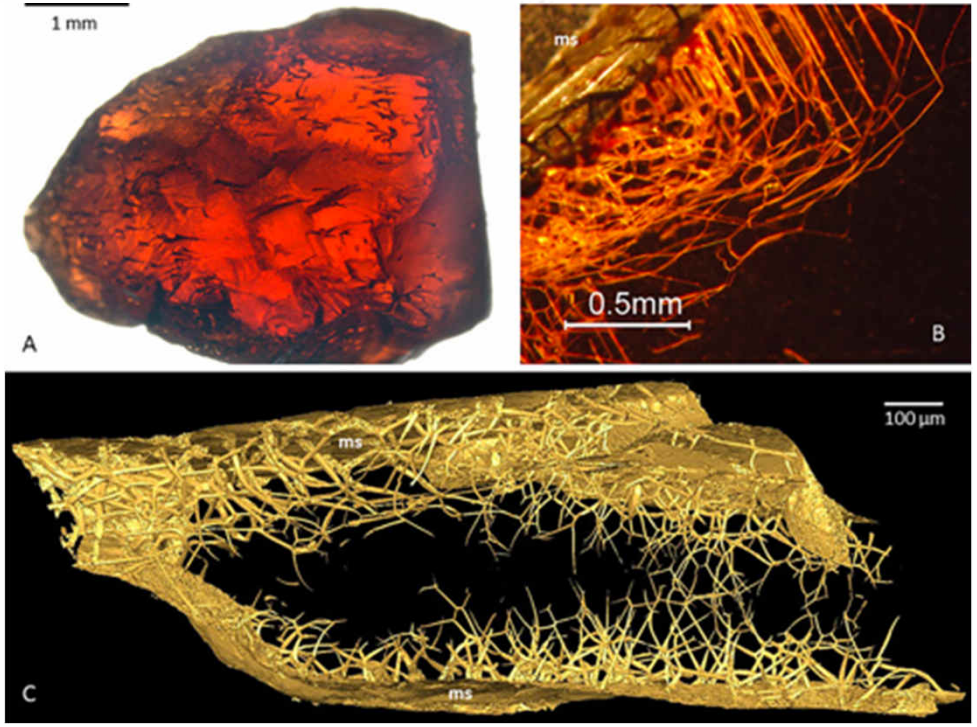

American Mineralogist, Volume 106, pages 1026–1029, 2021

Letter

On the formation of arrays of micro-tunnels in pyrope and almandine garnets

Jacques Rabier [1], Arthur H. Heuer [2], and Kevin J. Hemker [3,*]

[1]Département Physique et Mécanique des Matériaux, Institut Pprime, CNRS-Université de Poitiers, ISAE ENSMA, BP 30179, 86962 Futuroscope-Chasseneuil Cedex 05, France
[2]Department of Materials Science and Engineering, Case Western Reserve University, Cleveland, Ohio 44106, U.S.A.
[3]Departments of Mechanical Engineering, Materials Science and Engineering, Earth and Planetary Sciences, Johns Hopkins University, Baltimore, Maryland 21210, U.S.A.

Abstract

A recent paper devoted to unusual fine-scale tubular tunnels found in pyrope and almandine garnets suggested that the 5 to 100 µm diameter tunnels were produced by an endolithic organism that is able to chemically dissolve and penetrate the mineral, perhaps in search of nutrients. The hypothesized microbial boring of the garnets was based on the finding of endolithic remains in the tunnels, but boring alone does not adequately explain the linear, highly aligned or occasionally branched tunnels that have been imaged. We have prepared this short Letter, in the spirit of Occam's Razor, to highlight the very probable role that dislocations play in the creation of such tunnels by preferential etching of a dislocation-rich deformation microstructure. The geometrical features of the tunnels possess all the characteristics of classical dislocation substructures that have been observed in natural and synthetic garnets.

Keywords: Garnets, dislocations, etching, tunnels

Introduction

The intricate and beautiful X-ray computed tomographic images recently published by Ivarsson et al. (2018) contain clear evidence of highly aligned parallel tunnels that originate at the mineral surface and extend into the interior, see, for example, Figure 1. These tunnels form highly regular miniature palisades in some regions; in others, they exist as more chaotic branched networks with kinks and junctions with uniquely prescribed angles. The networks of curvilinear, branching, and anastomosing (interconnected) tunnels were interpreted as evidence that these tunnels are independent of crystallography, thus providing an indirect foundation for the authors' hypothesis of biological tunneling (Ivarsson et al. 2018). Unfortunately, this interpretation completely misses the striking geometric similarities between the tunnels in these tomographic images and published observations and understanding of dislocation microstructures in both natural and synthetic garnets [see, for example, Rabier (1995, 1979); Rabier et al. (1976a, 1981); Garem et al. (1982); Rabier and Garem (1984); Allen et al. (1987); Karato et al. (1995); Blumenthal and Phillips (1996); Voegelé et al. (1998a, 1998b)].

As is well known, dislocations are prominent in virtually all crystalline materials. Dislocation generation, multiplication, and motion are widely recognized as a common deformation response of crystalline materials to externally applied shear stresses and have been extensively observed and characterized in metals and alloys, minerals, ceramics, and semiconductors. The absence of dislocations in the pyrope and almandine garnets under discussion, if true, would be remarkable.

Here, we briefly review and discuss dislocations in garnets, tunnel formation due to abiogenic etching of dislocations in minerals, and the similarities between the geometry of dislocation substructures and the intricate tunnels and networks observed in these pyrope and almandine garnets (Ivarsson et al. 2018).

* E-mail: hemker@jhu.edu. Orcid 0000-0002-5008-2222

Dislocations in garnets

The relationship between dislocations and plasticity in garnets is well established. Synthetic garnets of technological interest such as $Y_3Al_5O_{12}$ (YAG, yttrium aluminum garnet), $Y_3Fe_5O_{12}$ (YIG, yttrium iron garnet), and $Gd_3Ga_5O_{12}$ (GGG, gadolinium gallium garnet) were first studied by Rabier and colleagues (Rabier et al. 1976a; Rabier 1979) and have exceptional plastic properties compared to other oxide crystals (Garem et al. 1982; Rabier and Garem 1984; Blumenthal and Phillips 1996). Likewise, the resistance to plastic deformation in natural garnets is significantly greater than that of most other minerals of the Earth's mantle (Karato et al. 1995; Voegelé et al. 1998a). This is related to the very large Burgers vectors of dislocations in garnets and to a "corrugated" oxygen sublattice, which promotes very high atomic-level friction stresses on moving dislocations.

The description of the garnet structure in terms of coordination polyhedra, so common in the mineralogical literature, has proven to be very useful in understanding dislocation properties in synthetic garnets (Rabier et al. 1976b). The garnet structure can be regarded as a body-centered cubic (bcc) lattice with a very large unit cell. The edge of the bcc unit cell is of order 1.2 nm, whereas most common minerals have considerably smaller unit cells. Thus, the magnitude of the smallest perfect unit Burgers vector, $\boldsymbol{b} = ½\langle 111 \rangle$, is about 1.0 nm. This results in a very large strain energy, proportional to Gb^2 per unit length of dislocation (G is the elastic shear modulus). The strain energy of a dislocation can be lowered by spreading of its core and by dissociation of the parent dislocation into partial dislocations that bound a planar stacking fault. The dissociated configuration is glissile as long as it remains on the glide plane, but it becomes sessile when reconfigured off of the glide plane (Garem et al. 1982; Blumenthal and Phillips 1996).

0003-004X/21/0006–1026$05.00/DOI: https://doi.org/10.2138/am-2021-7939

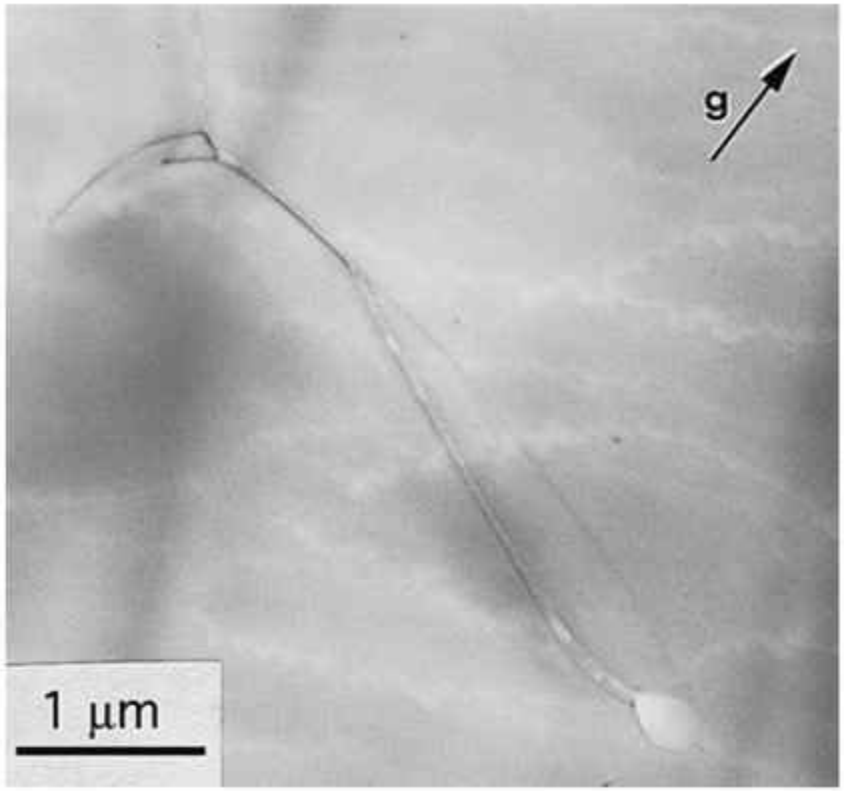

Fig. 17. Eclogite from Yakutia pipe. Hollow core. Bright field. *g*: 400.

V. Voegelé et al. Physics of the Earth and Planetary Interiors 108 (1998) 319–338

American Mineralogist, Volume 106, pages 1026–1029, 2021

Letter

On the formation of arrays of micro-tunnels in pyrope and almandine garnets

Jacques Rabier [1], Arthur H. Heuer [2], and Kevin J. Hemker [3,*]

[1]Département Physique et Mécanique des Matériaux, Institut Pprime, CNRS-Université de Poitiers, ISAE ENSMA, BP 30179, 86962 Futuroscope-Chasseneuil Cedex 05, France
[2]Department of Materials Science and Engineering, Case Western Reserve University, Cleveland, Ohio 44106, U.S.A.
[3]Departments of Mechanical Engineering, Materials Science and Engineering, Earth and Planetary Sciences, Johns Hopkins University, Baltimore, Maryland 21210, U.S.A.

Abstract

A recent paper devoted to unusual fine-scale tubular tunnels found in pyrope and almandine garnets suggested that the 5 to 100 µm diameter tunnels were produced by an endolithic organism that is able to chemically dissolve and penetrate the mineral, perhaps in search of nutrients. The hypothesized microbial boring of the garnets was based on the finding of endolithic remains in the tunnels, but boring alone does not adequately explain the linear, highly aligned or occasionally branched tunnels that have been imaged. We have prepared this short Letter, in the spirit of Occam's Razor, to highlight the very probable role that dislocations play in the creation of such tunnels by preferential etching of a dislocation-rich deformation microstructure. The geometrical features of the tunnels possess all the characteristics of classical dislocation substructures that have been observed in natural and synthetic garnets.

Keywords: Garnets, dislocations, etching, tunnels

Introduction

The intricate and beautiful X-ray computed tomographic images recently published by Ivarsson et al. (2018) contain clear evidence of highly aligned parallel tunnels that originate at the mineral surface and extend into the interior, see, for example, Figure 1. These tunnels form highly regular miniature palisades in some regions; in others, they exist as more chaotic branched networks with kinks and junctions with uniquely prescribed angles. The networks of curvilinear, branching, and anastomosing (interconnected) tunnels were interpreted as evidence that these tunnels are independent of crystallography, thus providing an indirect foundation for the authors' hypothesis of biological tunneling (Ivarsson et al. 2018). Unfortunately, this interpretation completely misses the striking geometric similarities between the tunnels in these tomographic images and published observations and understanding of dislocation microstructures in both natural and synthetic garnets [see, for example, Rabier (1995, 1979); Rabier et al. (1976a, 1981); Garem et al. (1982); Rabier and Garem (1984); Allen et al. (1987); Karato et al. (1995); Blumenthal and Phillips (1996); Voegelé et al. (1998a, 1998b)].

As is well known, dislocations are prominent in virtually all crystalline materials. Dislocation generation, multiplication, and motion are widely recognized as a common deformation response of crystalline materials to externally applied shear stresses and have been extensively observed and characterized in metals and alloys, minerals, ceramics, and semiconductors. The absence of dislocations in the pyrope and almandine garnets under discussion, if true, would be remarkable.

Here, we briefly review and discuss dislocations in garnets, tunnel formation due to abiogenic etching of dislocations in minerals, and the similarities between the geometry of dislocation substructures and the intricate tunnels and networks observed in these pyrope and almandine garnets (Ivarsson et al. 2018).

* E-mail: hemker@jhu.edu. Orcid 0000-0002-5008-2222

Dislocations in garnets

The relationship between dislocations and plasticity in garnets is well established. Synthetic garnets of technological interest such as $Y_3Al_5O_{12}$ (YAG, yttrium aluminum garnet), $Y_3Fe_5O_{12}$ (YIG, yttrium iron garnet), and $Gd_3Ga_5O_{12}$ (GGG, gadolinium gallium garnet) were first studied by Rabier and colleagues (Rabier et al. 1976a; Rabier 1979) and have exceptional plastic properties compared to other oxide crystals (Garem et al. 1982; Rabier and Garem 1984; Blumenthal and Phillips 1996). Likewise, the resistance to plastic deformation in natural garnets is significantly greater than that of most other minerals of the Earth's mantle (Karato et al. 1995; Voegelé et al. 1998a). This is related to the very large Burgers vectors of dislocations in garnets and to a "corrugated" oxygen sublattice, which promotes very high atomic-level friction stresses on moving dislocations.

The description of the garnet structure in terms of coordination polyhedra, so common in the mineralogical literature, has proven to be very useful in understanding dislocation properties in synthetic garnets (Rabier et al. 1976b). The garnet structure can be regarded as a body-centered cubic (bcc) lattice with a very large unit cell. The edge of the bcc unit cell is of order 1.2 nm, whereas most common minerals have considerably smaller unit cells. Thus, the magnitude of the smallest perfect unit Burgers vector, $\boldsymbol{b} = ½\langle 111 \rangle$, is about 1.0 nm. This results in a very large strain energy, proportional to Gb^2 per unit length of dislocation (G is the elastic shear modulus). The strain energy of a dislocation can be lowered by spreading of its core and by dissociation of the parent dislocation into partial dislocations that bound a planar stacking fault. The dissociated configuration is glissile as long as it remains on the glide plane, but it becomes sessile when reconfigured off of the glide plane (Garem et al. 1982; Blumenthal and Phillips 1996).

0003-004X/21/0006–1026$05.00/DOI: https://doi.org/10.2138/am-2021-7939

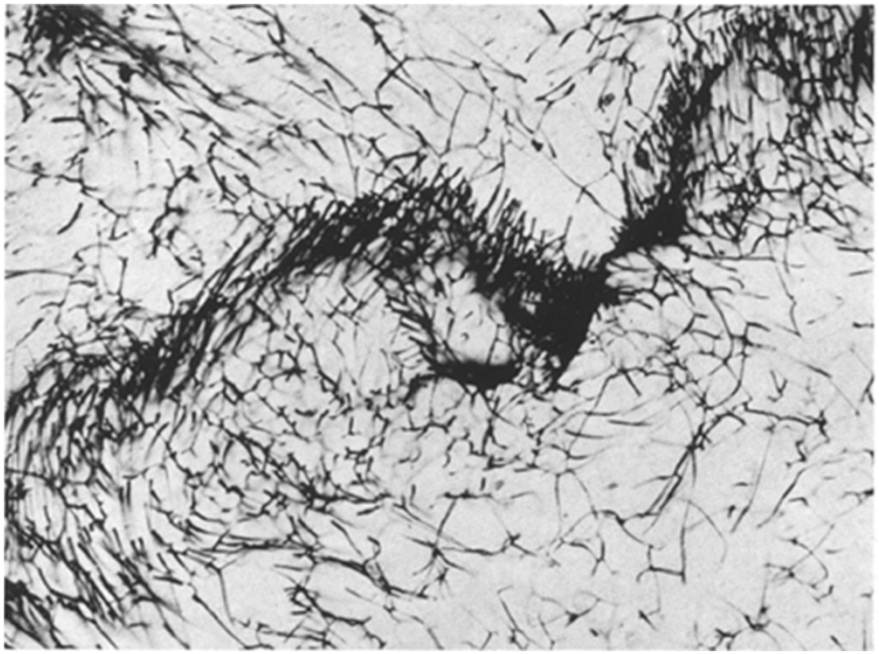

Carstens (1969) Contr. Mineral. and Petrol. 24, 368-353

Bridgmanite ($MgSiO_3$)

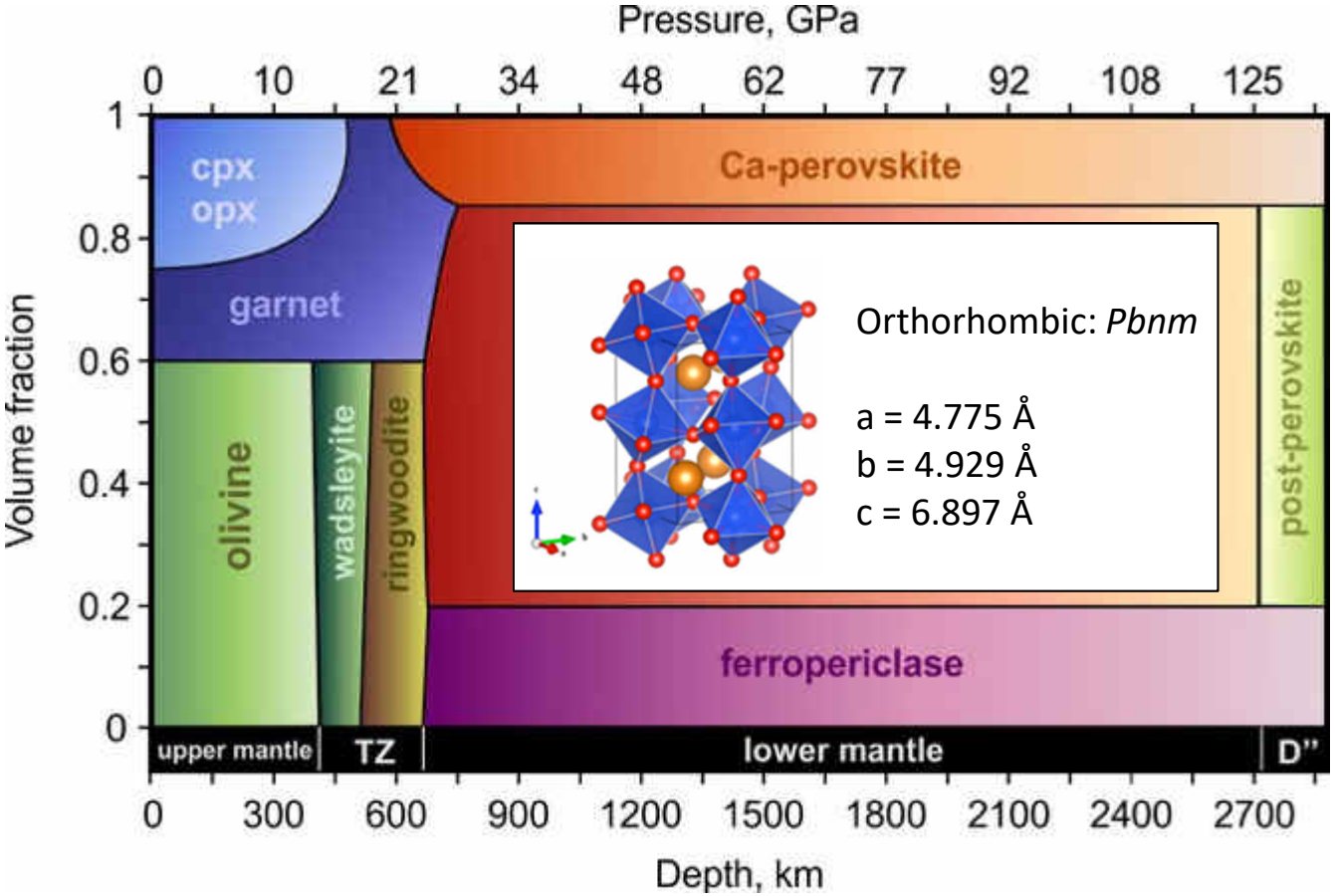

Modelling dislocations at the atomic scale

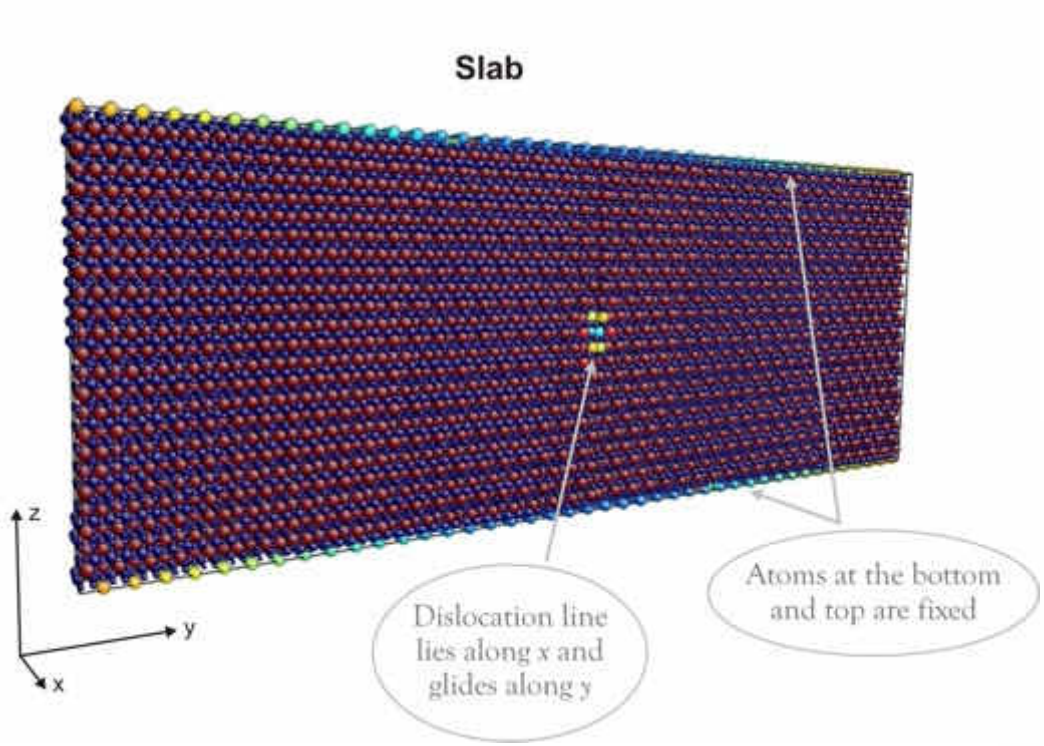

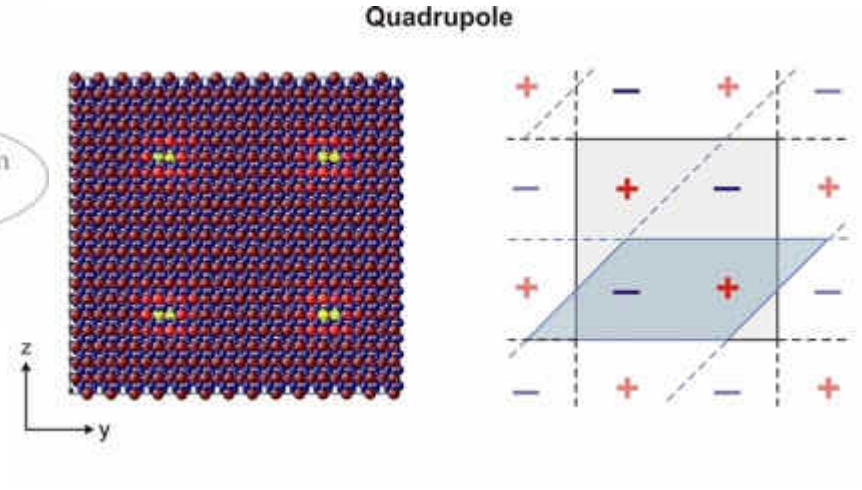

Modeling dislocations in bridgmanite at 30 GPa

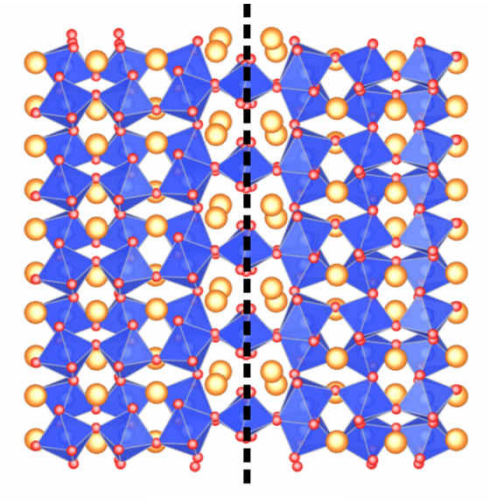

[100](010)

Screw dislocations

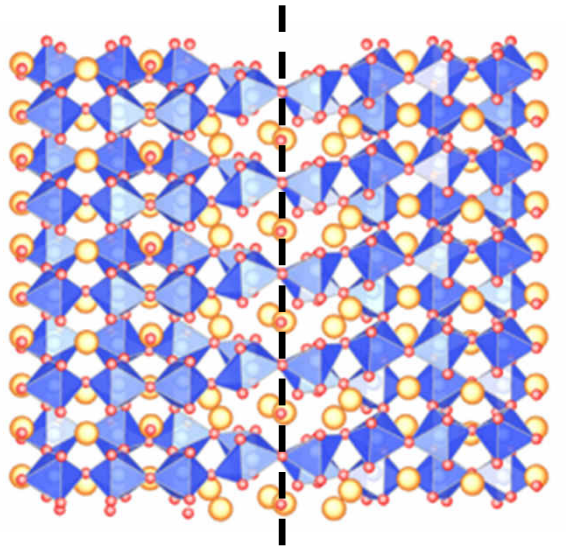

[010](100)

Hirel et al. (2014)

Modeling lattice friction

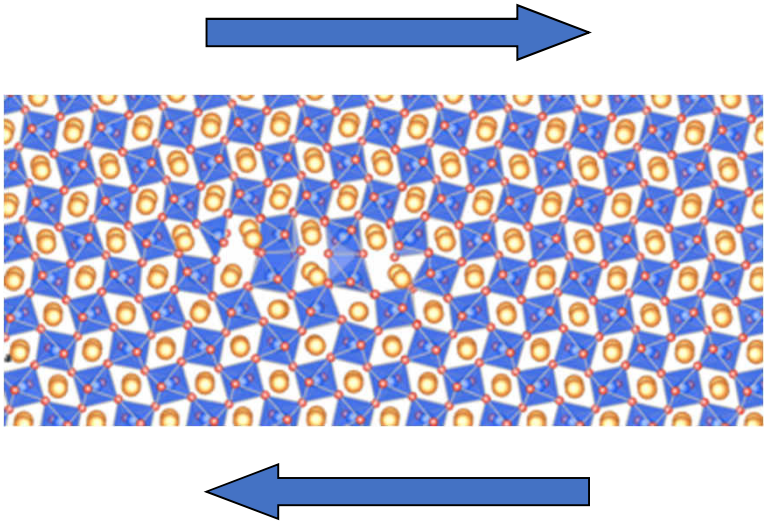

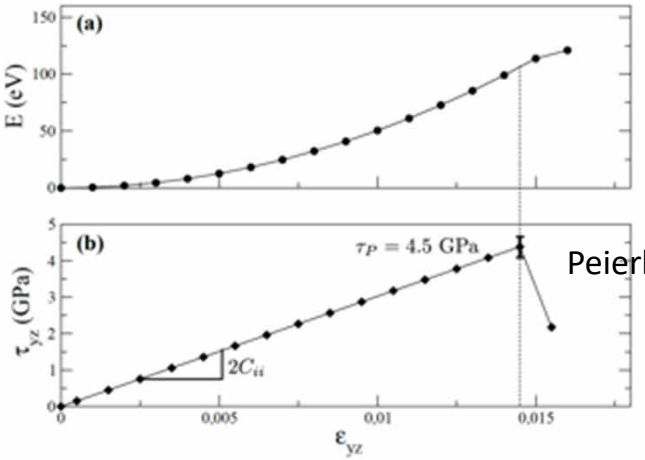

Peierls stress

Lattice friction in bridgmanite: influence of P

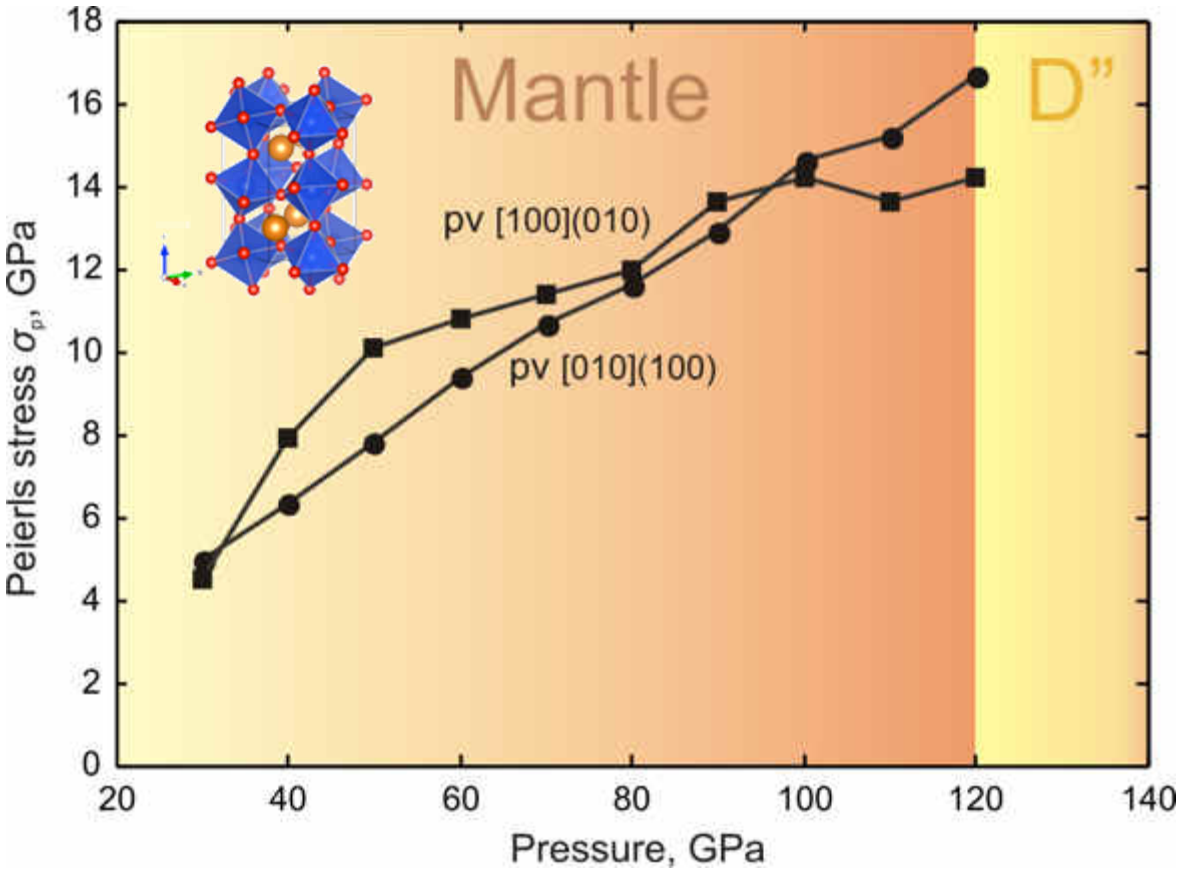

Hirel et al. Acta Mat 2014

Experiments under lower mantle conditions

GEOPHYSICS

Shear deformation of bridgmanite and magnesiowüstite aggregates at lower mantle conditions

Jennifer Girard, George Amulele,* Robert Farla,†
Anwar Mohiuddin, Shun-ichiro Karato‡

Rheological properties of the lower mantle have strong influence on the dynamics and evolution of Earth. By using the improved methods of quantitative deformation experiments at high pressures and temperatures, we deformed a mixture of bridgmanite and magnesiowüstite under the shallow lower mantle conditions. We conducted experiments up to about 100% strain at a strain rate of about 3×10^{-5} second^{-1}. We found that bridgmanite is substantially stronger than magnesiowüstite and that magnesiowüstite largely accommodates the strain. Our results suggest that strain weakening and resultant shear localization likely occur in the lower mantle. This would explain the preservation of long-lived geochemical reservoirs and the lack of seismic anisotropy in the majority of the lower mantle except the boundary layers.

The large, rocky lower mantle is mostly composed of $(Mg,Fe)SiO_3$ bridgmanite (~70%) and $(Mg,Fe)O$ magnesiowüstite (~20%) (and a few percent of calcium perovskite $CaSiO_3$) (1). Many of Earth's geochemical and geophysical questions depend strongly on the rheological properties of materials in this region. For instance, geochemical observations suggest that the lower mantle hosts a large amount of incompatible elements working as a reservoir of these elements (2, 3). The degree of preservation of these reservoirs is controlled by the nature of mixing or stirring of materials (4, 5), which strongly depends on the rheological properties of materials in this region. However, very little is currently known about the rheological properties of materials in the lower mantle because of the difficulties in quantitative experimental studies of deformation under the conditions of the lower mantle.

The main difficulties include the controlled generation of stress (or strain rate) and reliable measurements of stress and strain under the high-pressure and -temperature conditions [e.g., (6)]. Consequently, previous studies on plastic deformation of lower mantle minerals were either performed at high pressures and low temperatures (7–10), at high pressures and high temperatures without stress-strain rate control (11), or on analog materials at low pressures (12–14). Applying low-temperature experiments to Earth's interior is difficult because rheological properties are highly sensitive to temperature. Also the mechanisms by which deformation occurs are sensitive to temperature and strain rate, creating extrapolation issues for both low-temperature and poorly controlled strain-rate (stress) measurements [e.g., (15)]. Furthermore, microstructural evolution often leads to strain-dependent rheological behavior, which is particularly important for a sample containing two materials with a large strength contrast (16). The lower mantle approximates a two-phase mixture (bridgmanite and magnesiowüstite) with presumably a large strength contrast [e.g., (13, 17, 18)], and therefore large strain (>30%) experiments are essential to

Department of Geology and Geophysics, Yale University, New Haven, CT, USA.
*Present address: Department of Earth and Planetary Sciences, Macquarie University, Sydney, NSW, Australia. †Present address: Bayerisches Geoinstitut, Universität Bayreuth, Bayreuth, Germany. ‡Corresponding author. E-mail: shun-ichiro.karato@yale.edu

Girard et al. (2016) Science

27 GPa
2130 K

Rotational Drickamer apparatus

Yamazaki & Karato (2001)

SEM on deformed sample

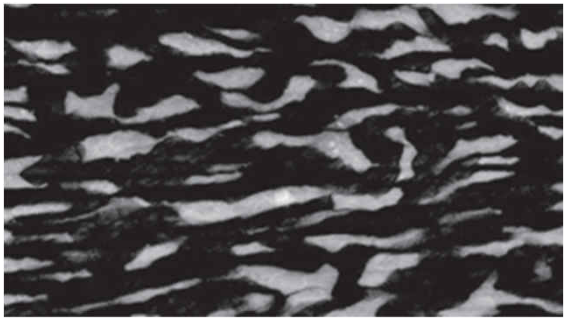

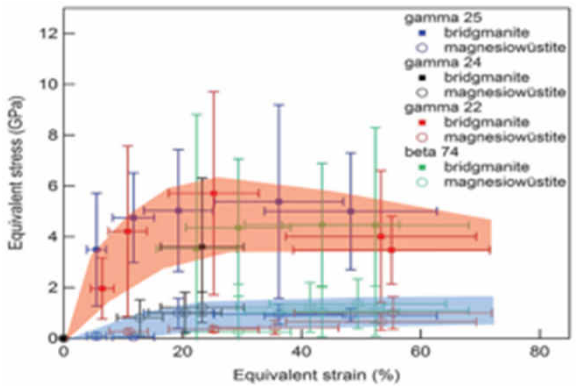

Synchrotron: rheological data

Dislocations in perovskites

Edge dislocations

$MgSiO_3$ $[110]_{pc}$

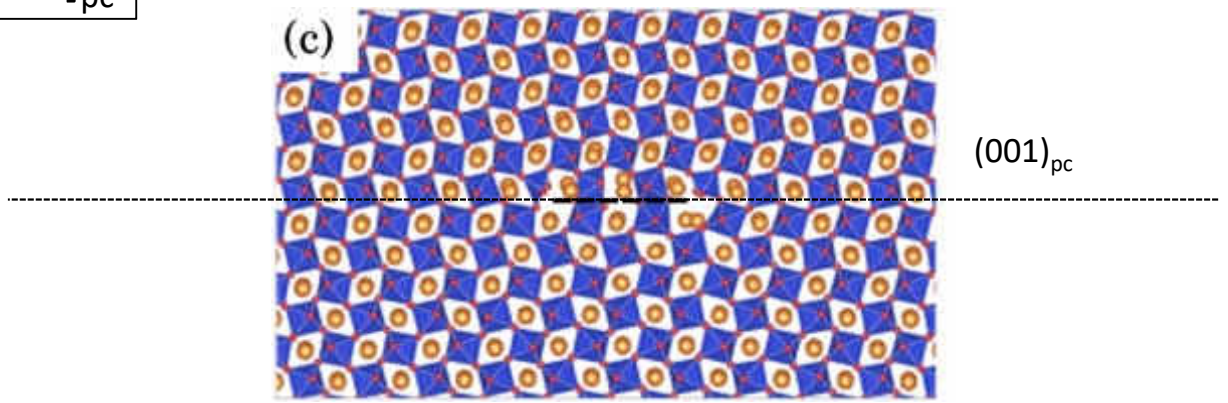

Hirel et al. Scripta Mat (2016)

Dislocations in perovskites

Edge dislocations

$SrTiO_3$ [110]

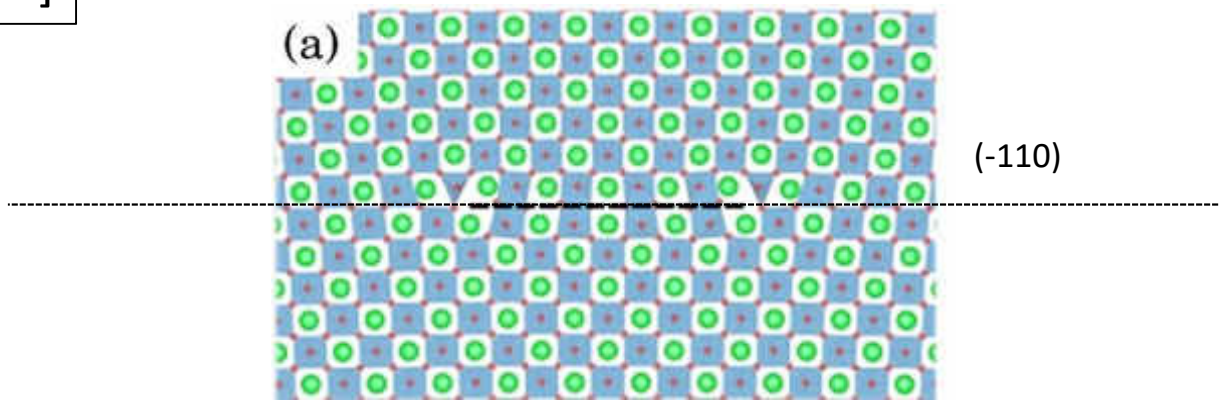

Hirel et al. Scripta Mat (2016)

journal

J. Am. Ceram. Soc., 84 [5] 1161–63 (2001)

Surprising Results of a Study on the Plasticity in Strontium Titanate

Dieter Brunner, Shahram Taeri-Baghbadrani, Wilfried Sigle, and Manfred Rühle*

Max-Planck-Institut für Metallforschung, D-70174 Stuttgart, Germany

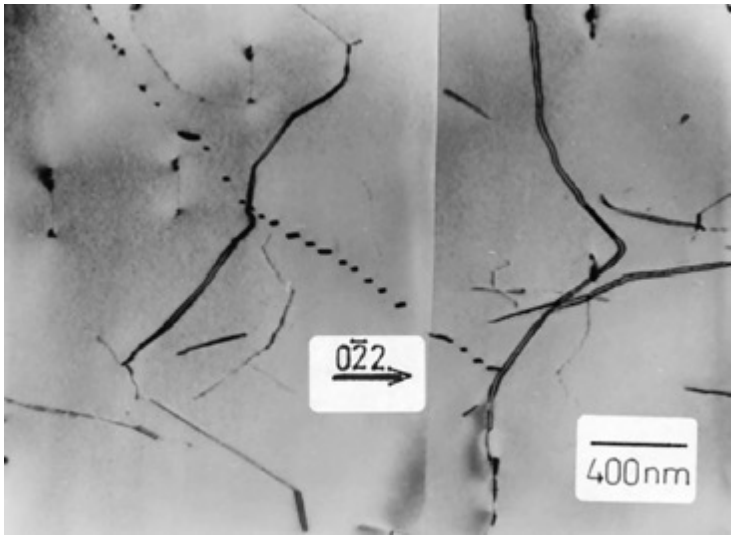

journal

J. Am. Ceram. Soc., 84 [5] 1161–63 (2001)

Surprising Results of a Study on the Plasticity in Strontium Titanate

Dieter Brunner, Shahram Taeri-Baghbadrani, Wilfried Sigle, and Manfred Rühle*

Max-Planck-Institut für Metallforschung, D-70174 Stuttgart, Germany

$SrTiO_3$ <110> slip

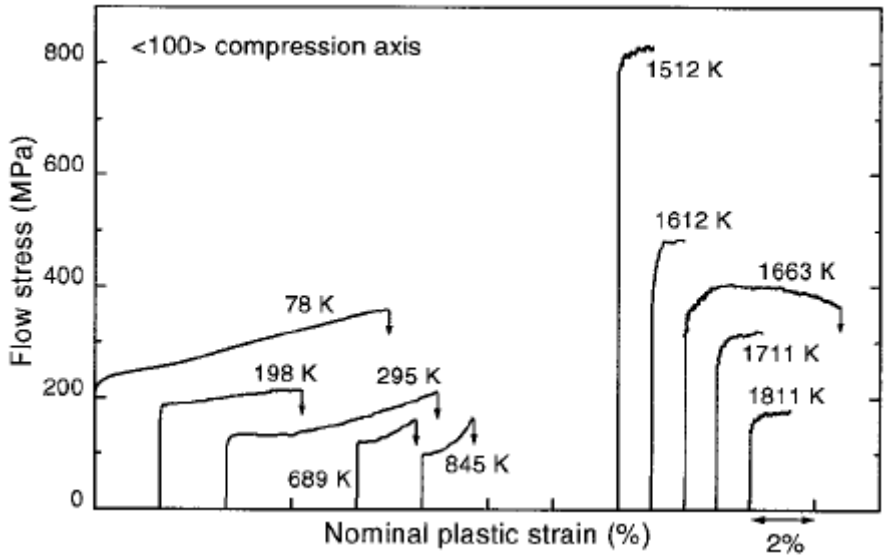

journal

J. Am. Ceram. Soc., 84 [5] 1161–63 (2001)

Surprising Results of a Study on the Plasticity in Strontium Titanate

Dieter Brunner, Shahram Taeri-Baghbadrani, Wilfried Sigle, and Manfred Rühle*

Max-Planck-Institut für Metallforschung, D-70174 Stuttgart, Germany

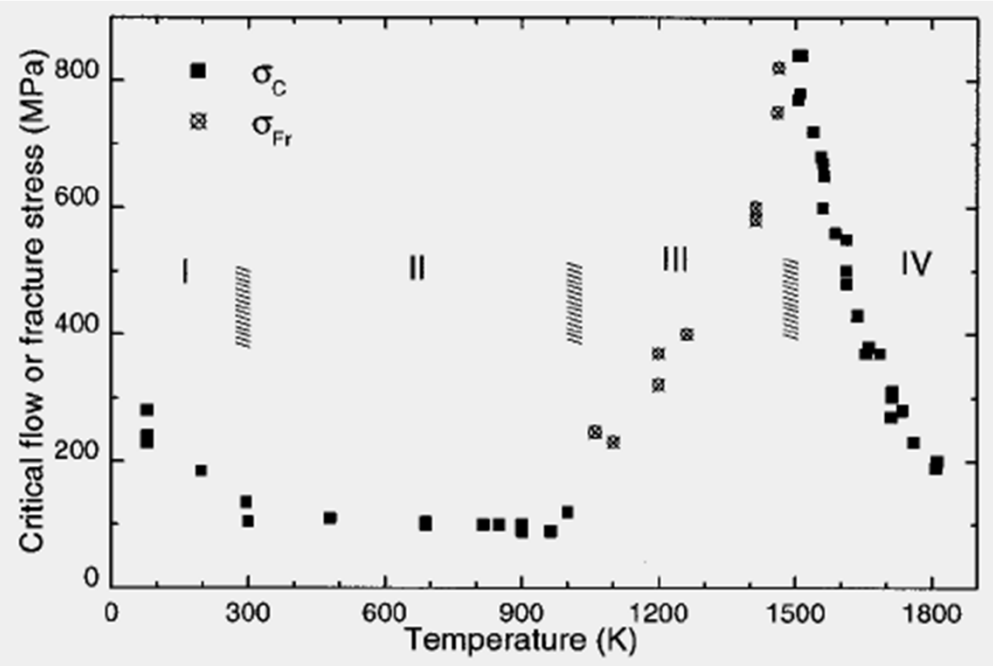

$SrTiO_3$ high temperature: climb dissociation

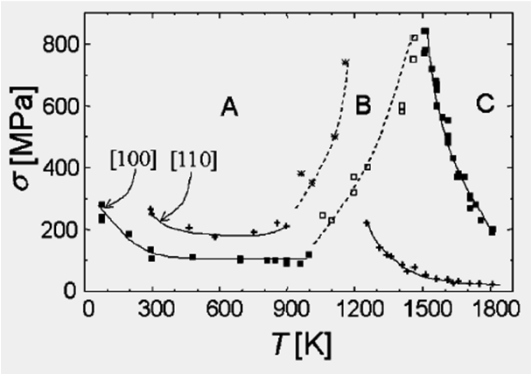

Brunner et al. (2001)
Gumbsch et al. (2001)

Edge dislocations

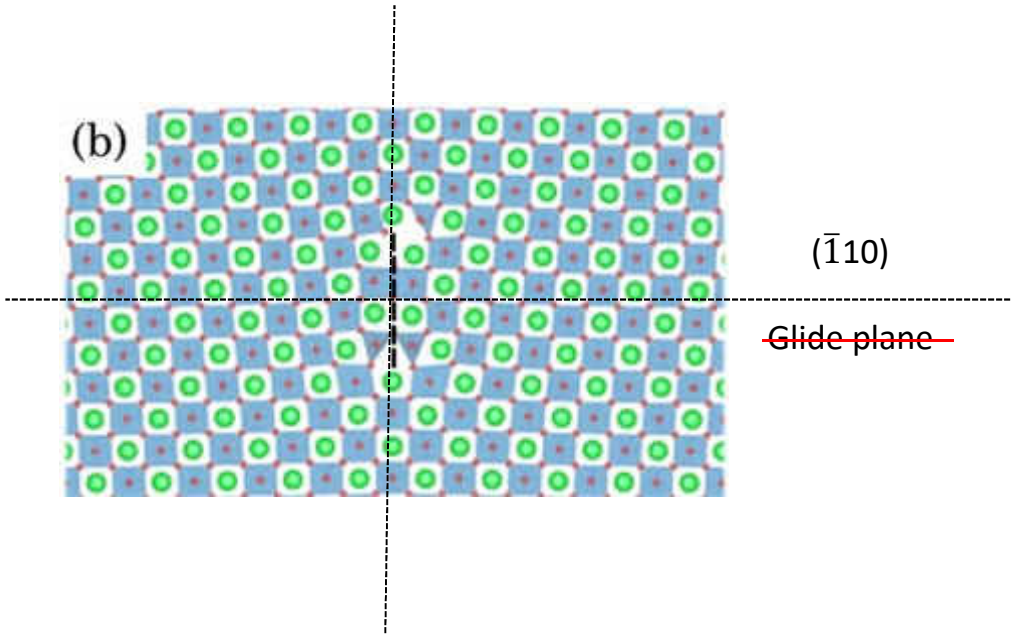

Hirel et al. Scripta Mat (2016)

$MgSiO_3$ high temperature: climb dissociation

$MgSiO_3$ $[110]_{pc}$

Edge dislocations

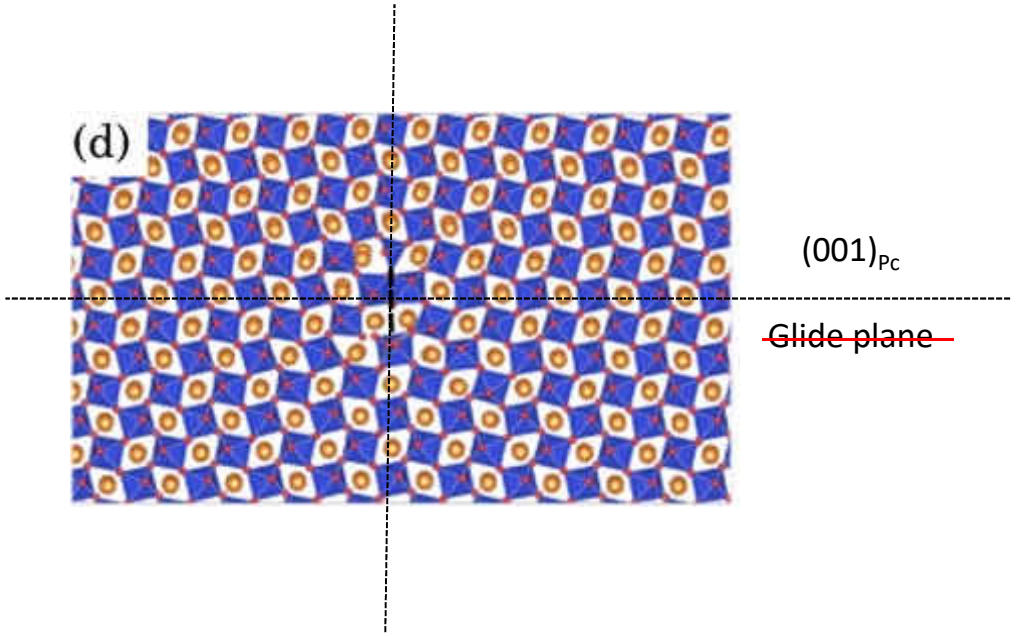

Hirel et al. Scripta Mat (2016)

Climb dissociation in perovskite

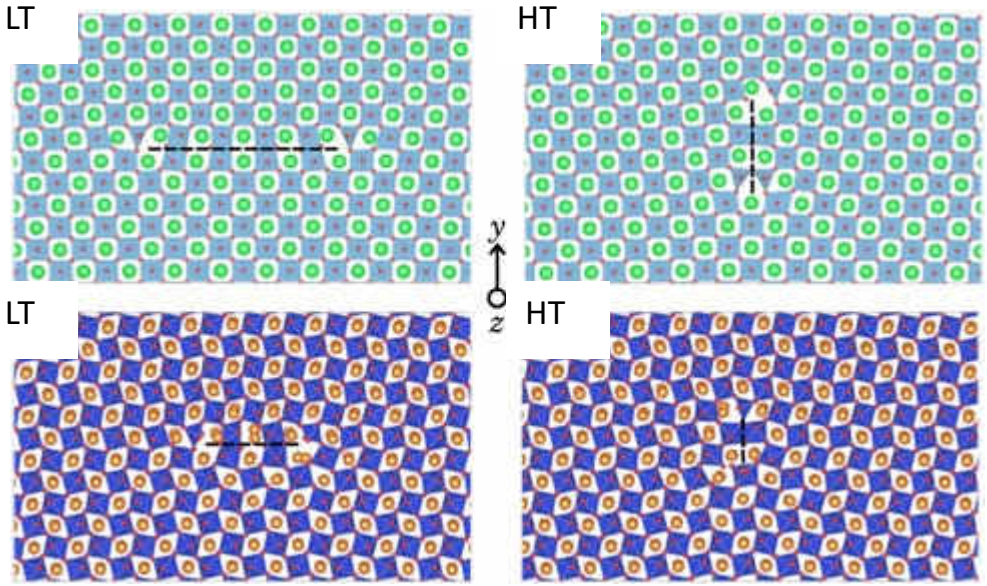

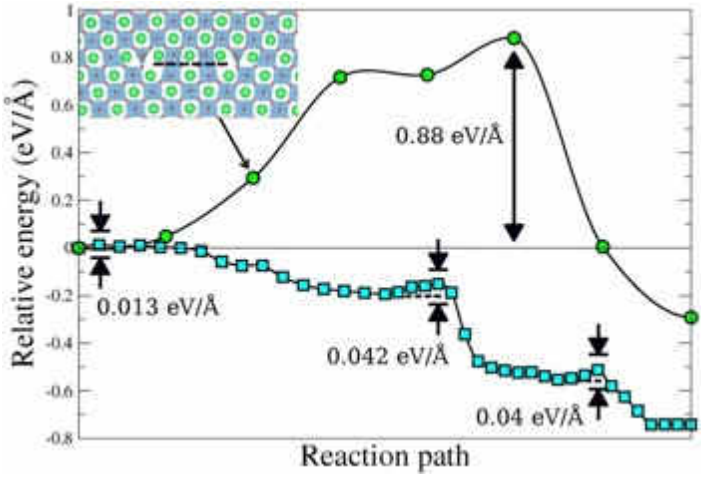

Hirel et al. (2016)

Lattice friction in $MgSiO_3$ bridgmanite

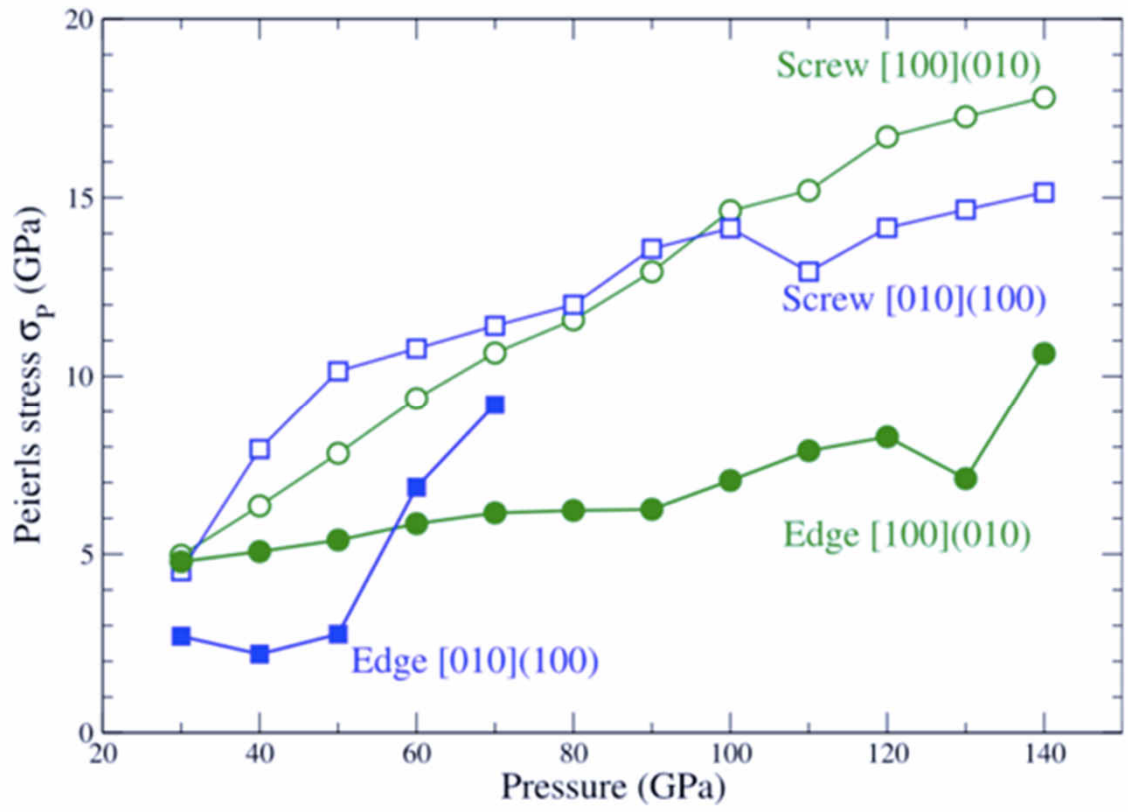

Hirel et al. Acta Mat 2014

Post-perovskite ($MgSiO_3$)

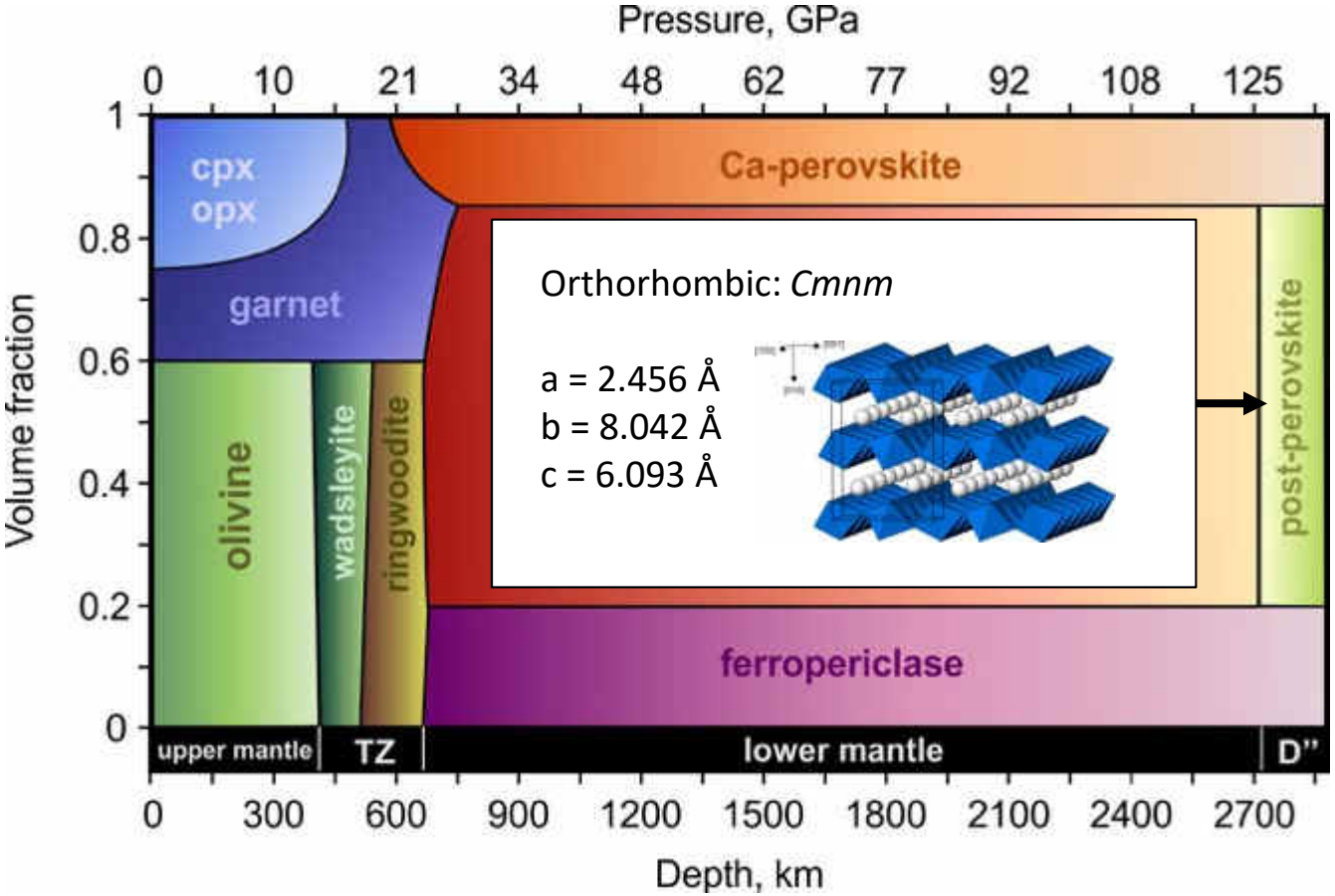

Post-perovskite ($MgSiO_3$)

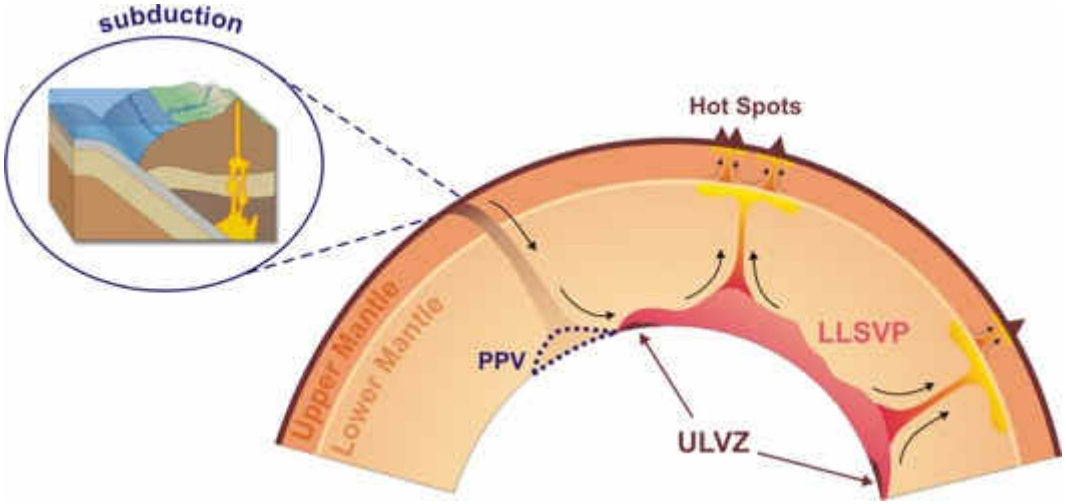

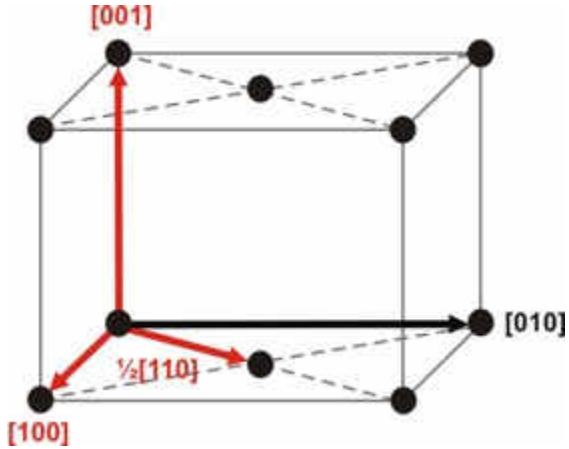

Possible Burgers vectors

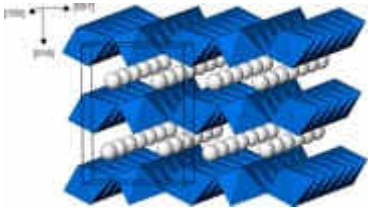

Post-perovskite ($MgSiO_3$)

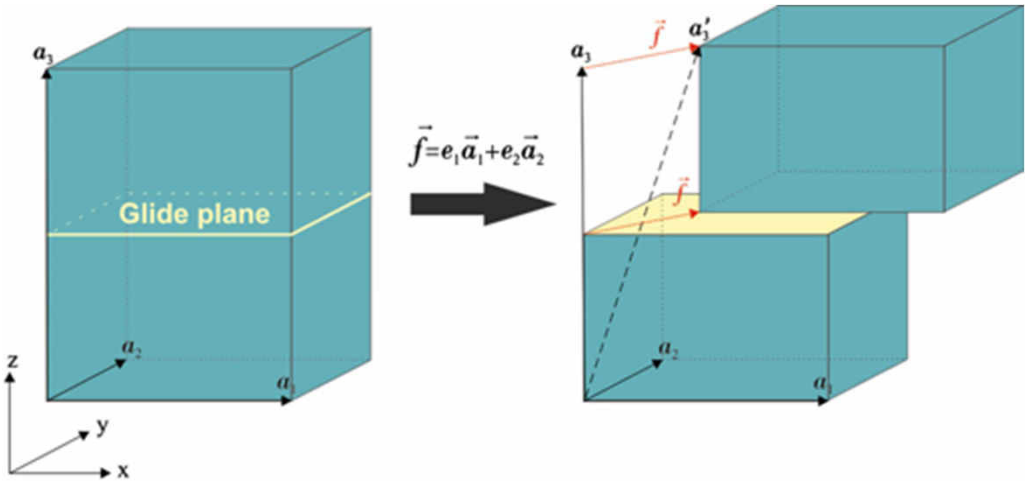

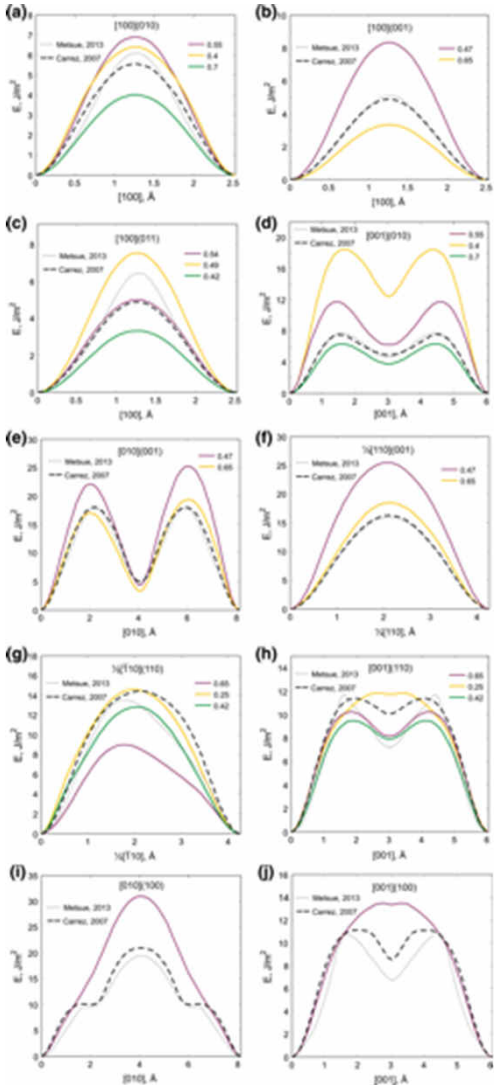

Post-perovskite ($MgSiO_3$)

[100] glide: the shortest lattice repeat (2.456 Å)

Screw dislocation

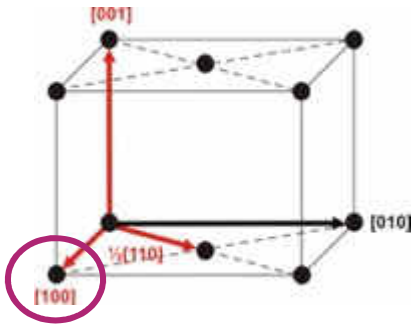

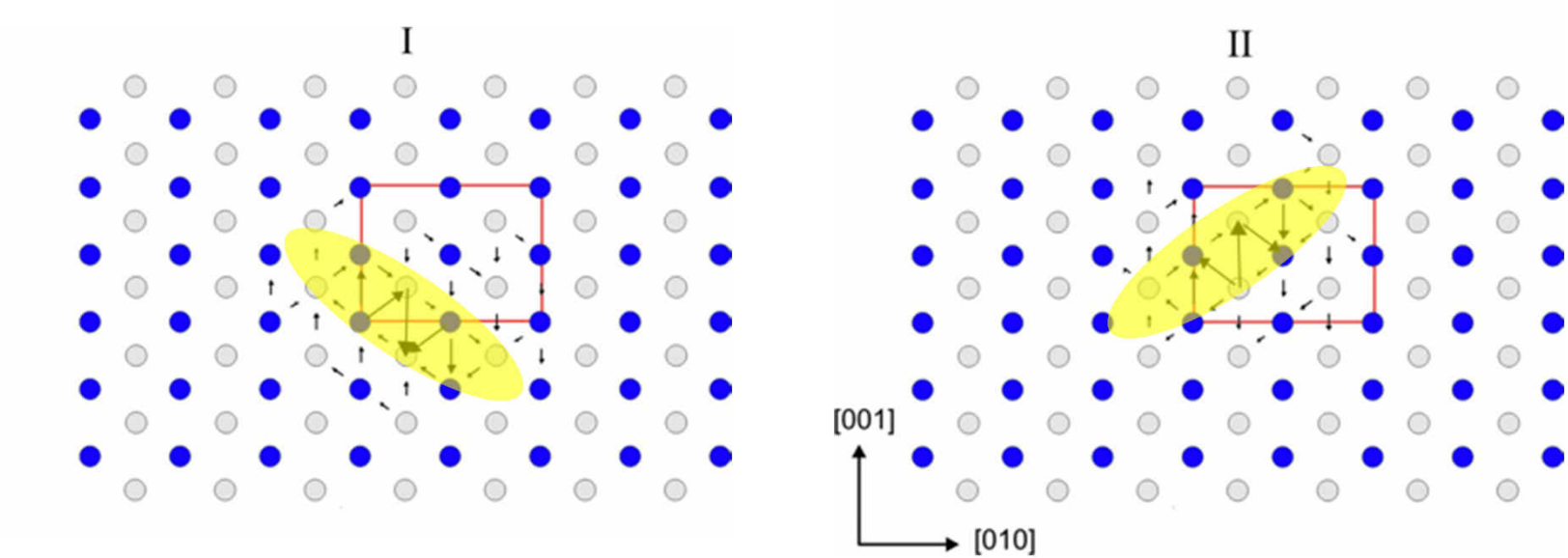

Post-perovskite ($MgSiO_3$)

[100] glide: the shortest lattice repeat (2.456 Å)

Screw dislocation

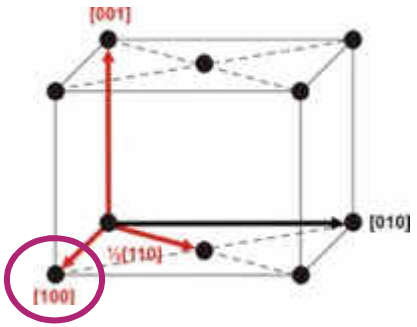

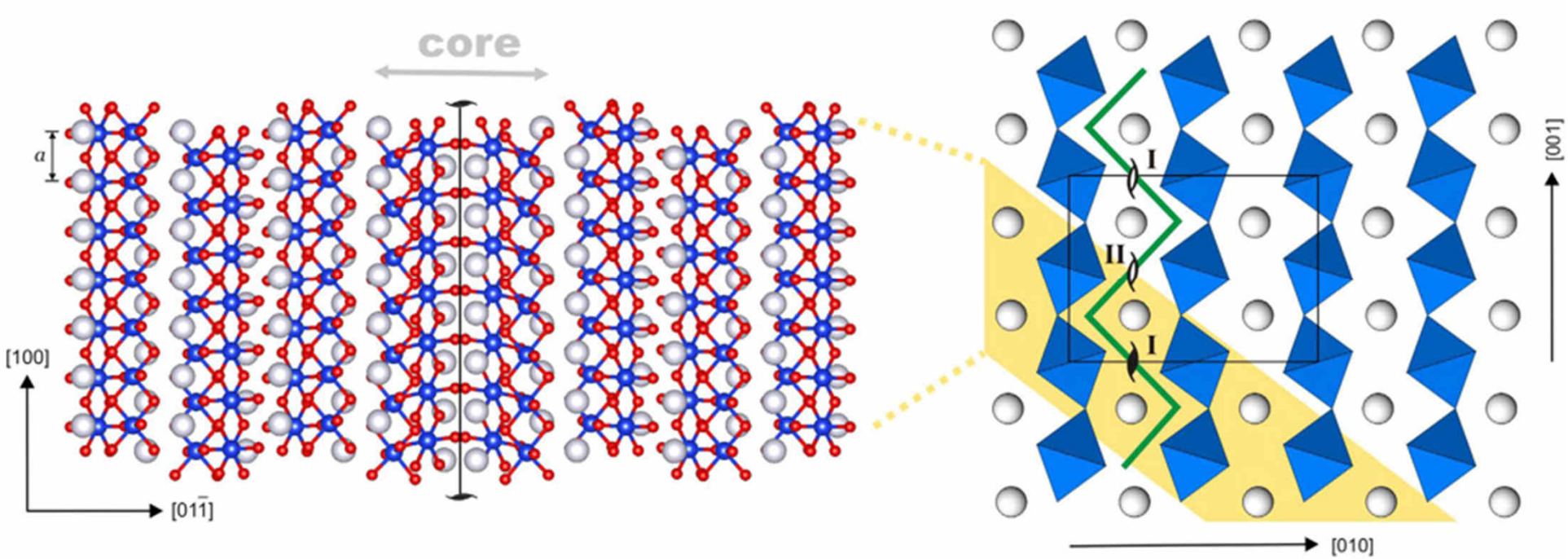

Post-perovskite ($MgSiO_3$)

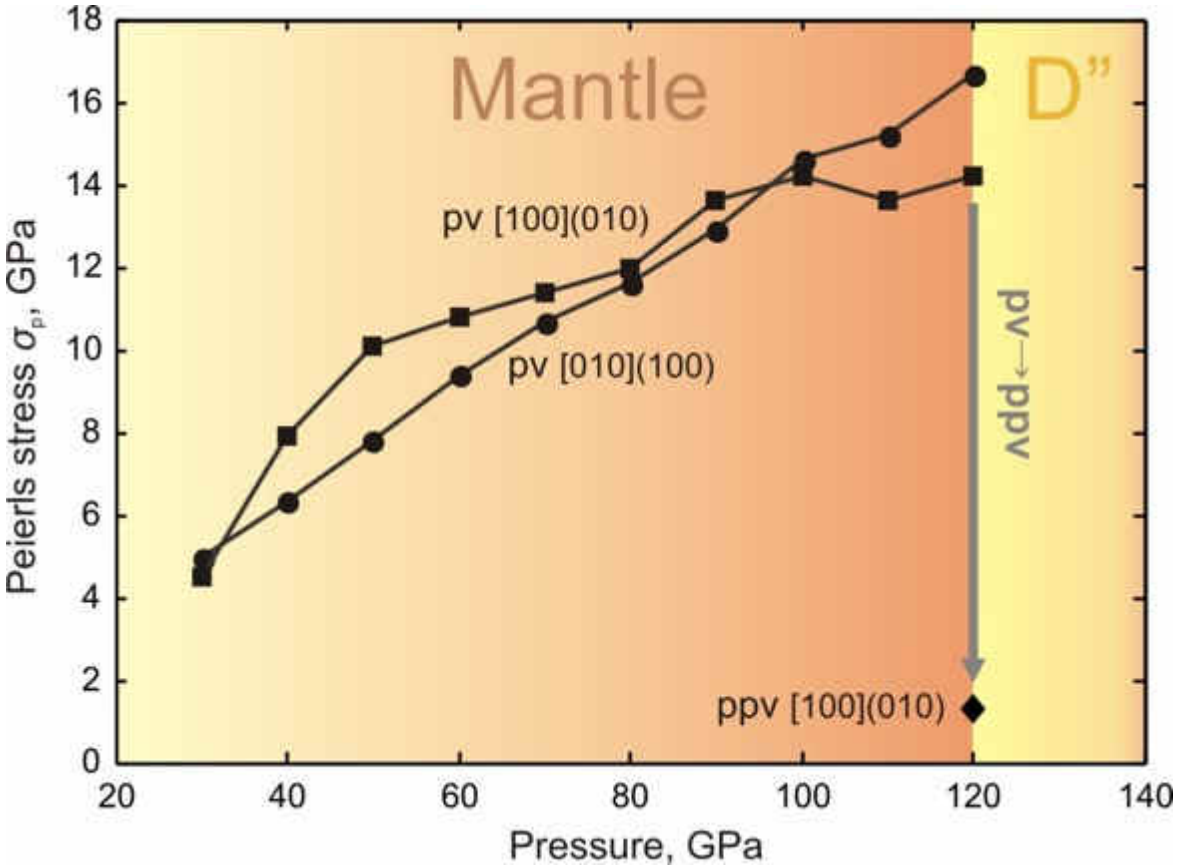

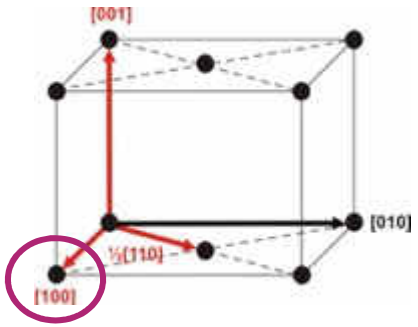

Post-perovskite ($MgSiO_3$)

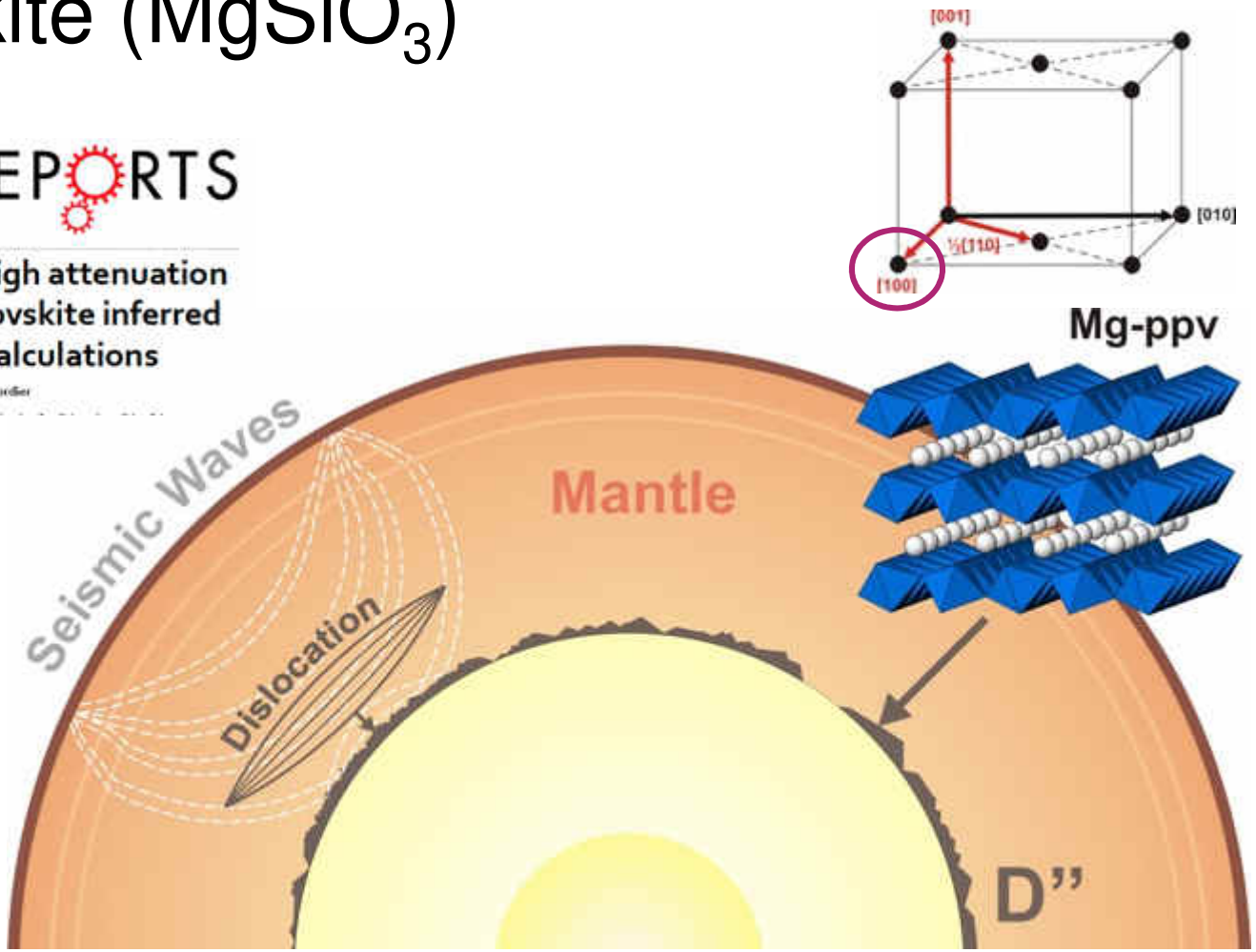

Post-perovskite ($MgSiO_3$)

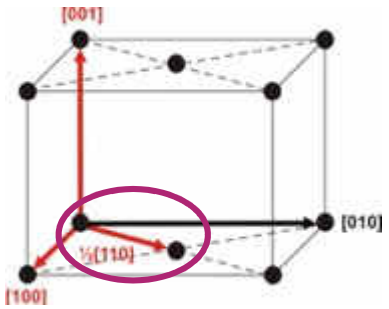

$\frac{1}{2}[110]$ glide: the 2nd shortest lattice repeat (4.2 Å)

$\frac{1}{2}[110](1\bar{1}0)$ edge dislocation

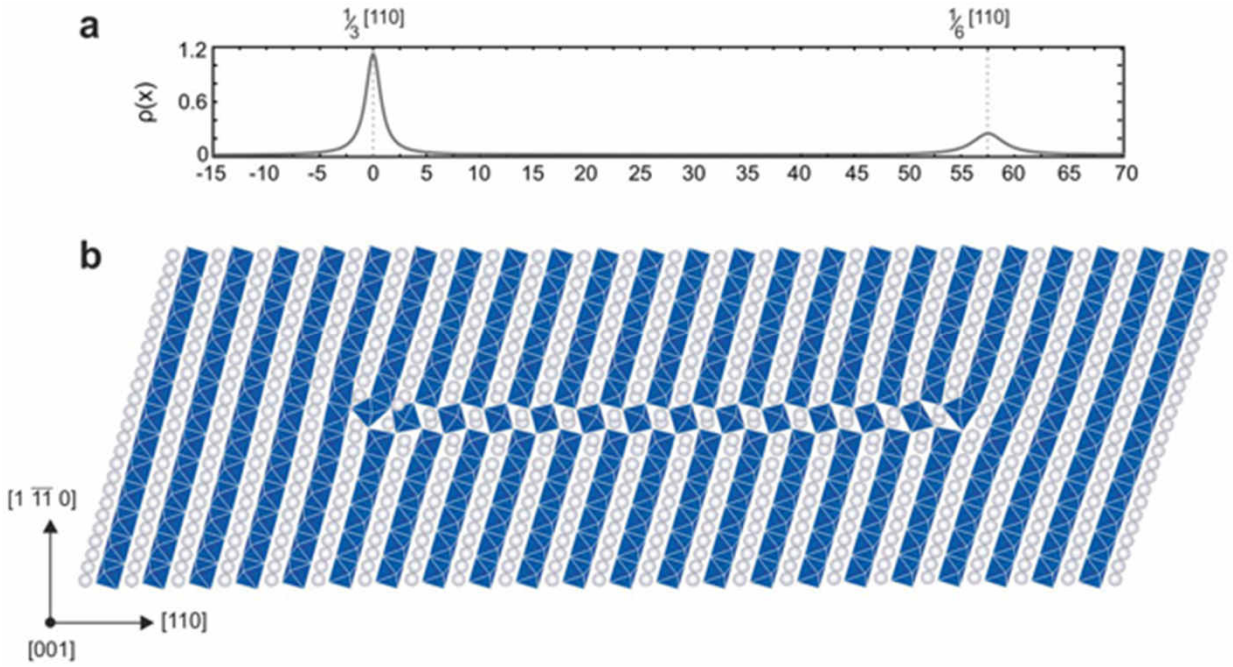

Post-perovskite ($MgSiO_3$)

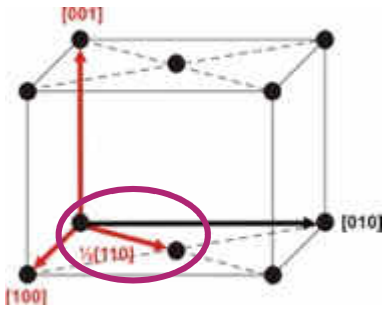

$\frac{1}{2}[110]$ glide: the 2nd shortest lattice repeat (4.2 Å)

$\frac{1}{6}[110](1\bar{1}0)$ edge dislocation

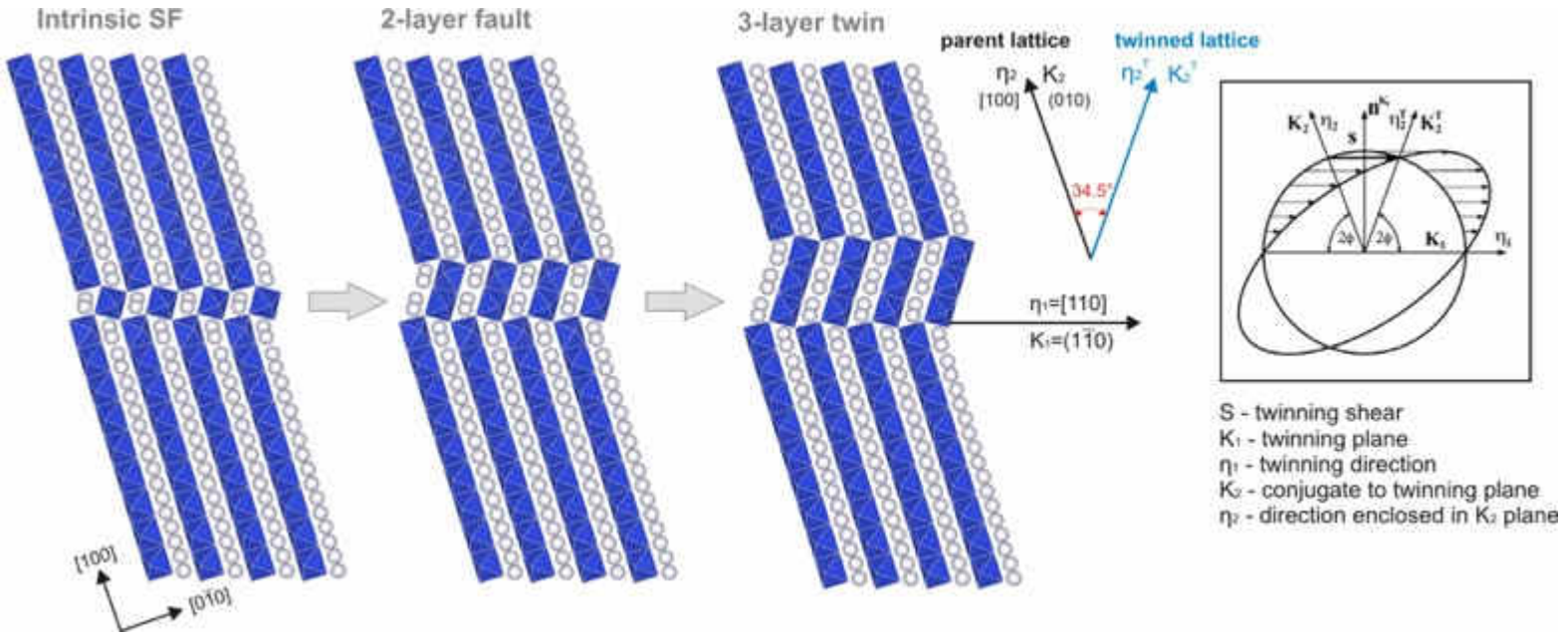

Post-perovskite ($MgSiO_3$)

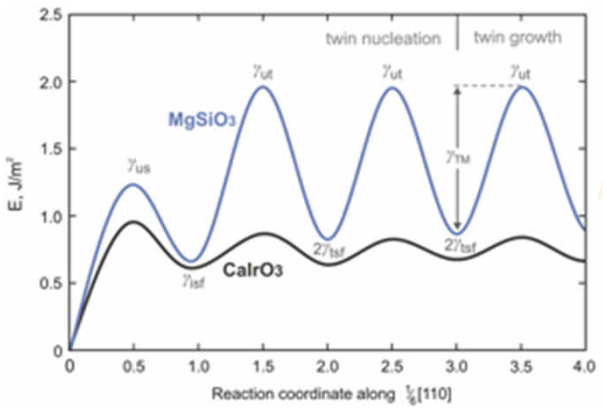

SCIENTIFIC REPORTS

OPEN

Prediction of Mechanical Twinning in Magnesium Silicate Post-Perovskite

Philippe Carrez, Alexandra M. Goryaeva & Patrick Cordier

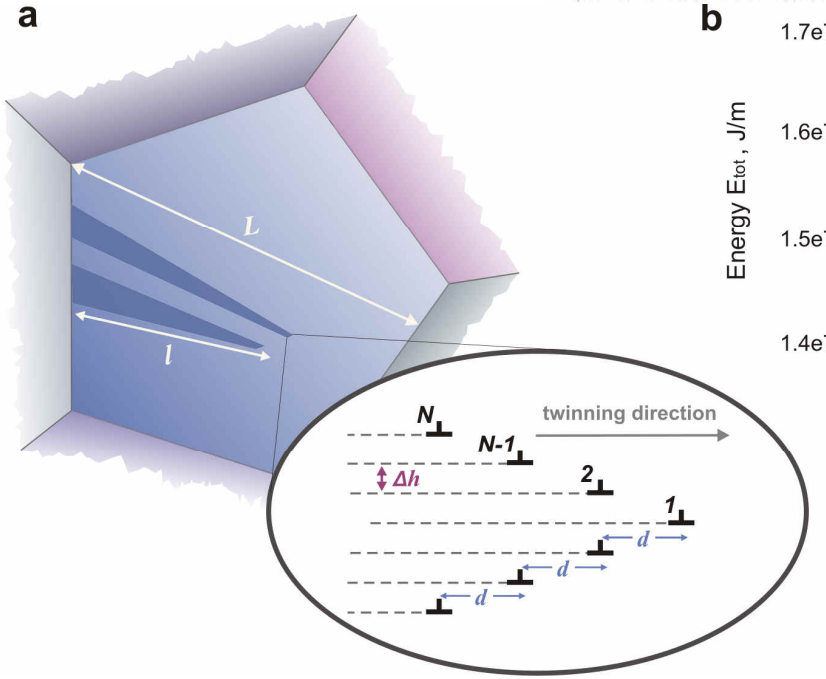

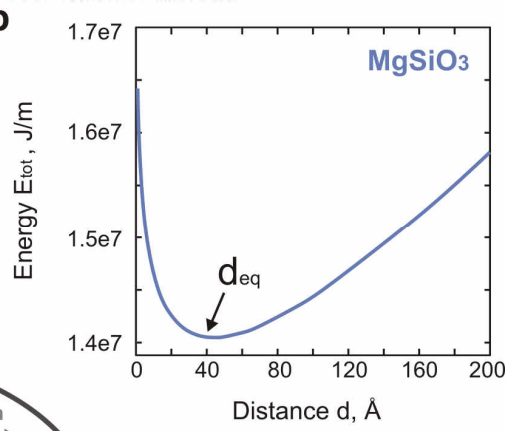

Notes and thoughts

- Dislocations are two-fold
  - Far-field: elasticity
  - Near field: atomic configurations

- The dislocation cores control the mobility
- In materials with complex crystal chemistry (and sometimes low symmetries) dislocation cores can exhibit various configurations
- Great progress have been made on the modeling side
- Observations are needed

THANK YOU

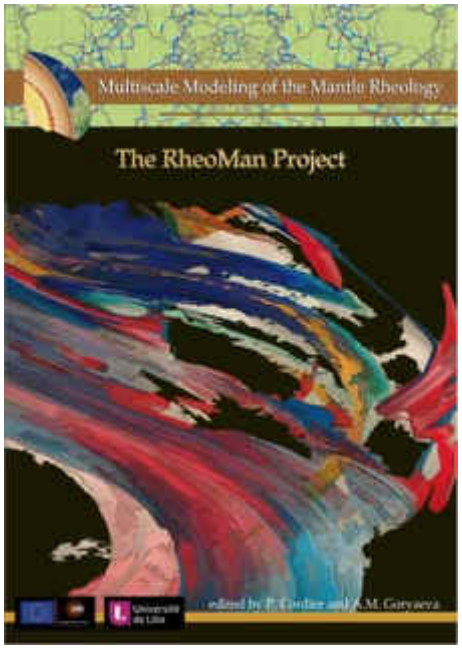

Ebook Rheoman

Free download at www.rheoman.eu

Follow us on http://timeman.univ-lille.fr/